1990

Characteristic discharge and suspended-sediment relationships in two glacier-fed rivers in the Karakoram

Richard E.J. Kelly
Wilfrid Laurier University

NOTICE

The quality of this microform is heavily dependent upon the quality of the original thesis submitted for microfilming. Every effort has been made to ensure the highest quality of reproduction possible.

If pages are missing, contact the university which granted the degree.

Some pages may have indistinct print especially if the original pages were typed with a poor typewriter ribbon or if the university sent us an inferior photocopy.

Reproduction in full or in part of this microform is governed by the Canadian Copyright Act, R.S.C. 1970, c. C-30, and subsequent amendments.

AVIS

La qualité de cette microforme dépend grandement de la qualité de la thèse soumise au microfilmage. Nous avons tout fait pour assurer une qualité supérieure de reproduction.

S'il manque des pages, veuillez communiquer avec l'université qui a conféré le grade.

La qualité d'impression de certaines pages peut laisser à désirer, surtout si les pages originales ont été dactylographiées à l'aide d'un ruban usé ou si l'université nous a fait parvenir une photocopie de qualité inférieure.

La reproduction, même partielle, de cette microforme est soumise à la Loi canadienne sur le droit d'auteur, SRC 1970, c. C-30, et ses amendements subséquents

ISBN 0-315-58134-4

CHARACTERISTIC DISCHARGE AND SUSPENDED-SEDIMENT RELATIONSHIPS IN TWO GLACIER-FED RIVERS IN THE KARAKORAM

By

Richard E.J. Kelly

B.A., University of Manchester, 1988

THESIS

Submitted to the Department of Geography
in partial fulfilment of the requirements
for the Master of Arts Degree
Wilfrid Laurier University
1990

Abstract

The purpose of this thesis is to investigate relationships between meltwater flow and production and flushing of suspended-sediment beneath two alpine glaciers. During the ablation seasons of 1987 and 1988, discrete, hourly measurements were taken of discharge, stage, suspended-sediment concentration and electrical conductivity in two rivers draining catchments of the Bualtar and Batura Glaciers in the Karakoram, N. Pakistan. The discharge time series of the Bualtar River reveals that flow varies over a daily period of three to four weeks, at a diurnal level and over one to four hours. Over all three time scales, electrical conductivity is inversely proportional to discharge suggesting that at high flows, outwash water is derived from surface melt while at low discharges, water originates from subglacial and englacial stores. Variations in suspended-sediment concentration are proportional to discharge at a daily time scale but become less well defined at diurnal and shorter periods. In the Batura River, stage measurements show that diurnal flow variations are superimposed on a longer-term rising limb and have fluctuations over periods of one to four similar to those observed in the Bualtar River in 1987. Conductivity in the Batura River is inversely proportional to discharge. The suspended-sediment concentration record at both sites demonstrates that timing of maximum and minimum sediment flushing over diurnal and shorter periods is not constant with respect to associated flow variations.

Investigation of empirical linear regression relationships between flow and sediment transport in both rivers shows that changing hysteresis relationships between variables does not permit adequate prediction of suspended-sediment from discharge. Hence, further development of a deterministic model of subglacial erosion, designed by Keeley (1986), is undertaken in order to account for processes of sediment supply and removal at the glacier bed which regression analysis cannot model.

Model prediction of variations in suspended-sediment transport in the Bualtar River at the daily level are good suggesting that rates of removal of subglacially eroded bedrock and sediment are directly proportional to discharge variations in arterial conduits. However, short, hourly fluctuations are not simulated well by the model. At this level, sediment accessibility to changing conduit networks within the glacier is more important than subglacial erosion. At a diurnal scale, model performance is variable demonstrating that varying sediment loads in outwash channels are the result of more complex processes of sediment supply and removal than the model accounts for.

Acknowledgements

I would like to express my appreciation to Dr. Gordon Young, Dr. Houston Saunderson and Dr. Mike English for their guidance throughout the course of this dissertation. In addition I would like to thank Dr. Peter Johnson for his invaluable input as the outside reader. I would especially like to thank Dr. David Collins at the University of Manchester for his continual enthusiastic input to the study and for valuable discussion.

In the U.K. I would like to thank members of the University of Manchester Alpine Glacier Project (UMAGP) who helped with data collection and laboratory work over the two field seasons. In addition, special gratitude goes to Graeme Boyce whose ideas on the model were very thought-provoking.

In Canada, thanks go to all currently associated with the "Ice Garage" at Wilfrid Laurier University including Chris, Paul, Bob, Pete and Ali. I would particularly like to thank Chris who proved to be a steadfast sounding board from which to bounce ideas. Also, many thanks go to The Wiz for directing resources my way over the last couple of years. Some of the figures were drafted by Elizabeth Macey to whom I am grateful.

Moral support over the final months was provided by many people in both Canada and U.K. I would especially like to thank Sasha, and Nancy and David Butz who were particularly helpful when things became fraught.

This study is part of a preliminary research project undertaken by UMAGP in conjunction with the Snow and Ice Hydrology Project at Wilfrid Laurier University.

Table of Contents

ABSTRACT i
ACKNOWLEDGEMENTS ii
LIST OF FIGURES iv
LIST OF TABLES viii

CHAPTER 1 INTRODUCTION 1

Preamble 1
Objectives 9

CHAPTER 2 THEORETICAL CONSIDERATIONS 11

Introduction 11
Glacier Hydrology 12
The Role of Meltwaters in Glaciers 12
Water Sources: Storage and Release 15
Supra- and Englacial Water Routing 20
Configurations of Water Routing Near the Bed 28
Development of the Drainage Network 36
Sediment Delivery to Meltwaters 40
Weathering at the Bed 41
Integration of Sediments with Meltwaters 46
Discharge-Suspended-sediment Relationships 48
Modelling Subglacial Erosion 51
Non-regression-based Empirical Models 51
Process-orientated Modelling 53

CHAPTER 3 STUDY REGION AND FIELD DATA COLLECTION SITES 55

Regional Context 55
Introduction 55
Climate and Weather 57
Glaciers 59
Hydrology 59
Glacier Erosion Systems 61
Specific Locations of Sites 66
Bualtar Glacier 66
Batura Glacier 70

CHAPTER 4 FIELD DATA COLLECTION TECHNIQUES 73

Bualtar Glacier, 1987 73
Discharge 73
Suspended-sediment Concentration 77
Electrical Conductivity 80
Batura Glacier, 1988 81
Stage 81
Suspended-sediment Concentration 82
Electrical Conductivity 83

CHAPTER 5 INTERPRETATION OF RESULTS 84

Bualtar 1987 84
Discharge 84
Electrical Conductivity 89
Suspended-sediment 95
Discharge-Suspended-sediment Relationships I 105
Summary of Bualtar Results 110
Batura 1988 111
Stage 111
Electrical Conductivity 114
Suspended-sediment 117
Stage-Suspended-sediment Relationships II 123
Summary of Batura Results 126
Data Errors 127
Discussion of Results 129

CHAPTER 6 DEVELOPMENT OF A MODEL OF SUB-GLACIAL EROSION 134

Introduction 134
Model Design 135
Description of the Model and Assumptions 135
Model Parameters 139
Data Set Requirements 142
Programme Description 142
Results of Modelling 147
Bualtar River 148
Batura River 153
Summary of Subglacial Modelling Results 157

CHAPTER 7 DISCUSSION AND CONCLUSION 159

Comparison between Empirical and Causal Model Results . . 159
Discussion 163
Summary and Conclusion 167

BIBLIOGRAPHY 172

APPENDIX I . . . . . A.i
APPENDIX II . . . . . A.iii
APPENDIX III . . . . . A.iv

List of Figures

FIGURE

2.1	Basal slip of glacier ice over bedrock	14
2.2	Schematic diagram of water routing through a glacier	21
2.3	Equipotential surfaces and flow directions	26
2.4	Linked-cavity drainage network	32
2.5	Control of surface topography of channels at the bed	37
3.1	The Karakoram and surrounding mountain systems	56
3.2	The Hunza Valley	64
3.3	The Central Hunza Valley	65
3.4	The Bualtar and Barpu Glacier system	67
3.5	The Batura Glacier	71
5.1	Bualtar River discharge, 1987	85
5.2	Daily average, minimum and maximum discharge in the Bualtar River, 1987	87
5.3	Electrical conductivity in the Bualtar River, 1987	90
5.4	Index of solute load in the Bualtar River, 1987	94
5.5	Suspended-sediment concentration in the Bualtar River, 1987	96
5.6	Daily average, minimum and maximum suspended-sediment concentration in the Bualtar River, 1987	98
5.7	Suspended-sediment load in the Bualtar River, 1987	103
5.8	Sequentially plotted discharge and suspended-sediment data from the Bualtar River, 1987	108
5.9	Water stage in the Batura River, 1988	112
5.10	Daily average, minimum and maximum stage in the Batura River, 1988	113
5.11	Electrical conductivity in the Batura River, 1988	115
5.12	Suspended-sediment concentration in the Batura River, 1988	118
5.13	Daily average, minimum and maximum suspended-sediment concentration in the Batura River, 1988	119
5.14	Index of suspended-sediment load in the Batura River, 1988	121
5.15	Sequentially plotted stage and suspended-sediment data from the Batura River, 1988	125
6.1	Schematic flow diagram of a model of subglacial erosion	144
6.2	Predicted and measured suspended-sediment load in the Bualtar River, 1987	149

6.3 Scatter-plot of predicted and observed suspended load in the Bualtar River, 1987 151
6.4 Predicted and observed index of suspended-sediment load in the Batura River, 1988 154
6.5 Scatter-plot of predicted and observed indices of suspended-sediment load in the Batura River, 1988 156

7.1 Plot of residuals from subglacial modelling and regression analysis for Bualtar data, 1987 161
7.2 Plot of residuals from subglacial modelling and regression analysis for Batura data, 1988 162

A.1 Scatter-plot of all paired discharge and suspended-sediment concentration for Bualtar River . . . . . A.i
A.2 Scatter-plot of all paired log-transformed discharge and suspended-sediment concentration for Bualtar River . . . . . A.i

List of Tables

TABLE

A.1 Linear regression statistics for log-transformed discharge and suspended-sediment concentration data in the Bualtar River, 1987 . . . . . A.ii

A.2 Linear regression statistics form log-transformed stage and suspended-sediment concentration data in the Batura River, 1988 . . . . . Aiii

Chapter One

Introduction

1.1 Preamble

Glacial runoff is an important resource in many parts of the world. Not only does meltwater supply local rural and urban areas with water for domestic, agricultural and industrial purposes, but it is also harnessed for provision of hydro-electric power to industrialised and industrialising countries (Meier and Roots, 1982). Furthermore, its temporal characteristics give an indication of geomorphological processes at work within the glacial environment in addition to climatological controls influencing the region.

Glaciers also reveal evidence of former climatic controls in a glacierised area from snow stratigraphy records in the accumulation zone (Mayewski *et al*, 1984). Such evidence may be a trait of larger scale global climatic trends, (Wood, 1988). Thus, in the present debate on global climatic change, along with deep ocean sediments, glaciers are a potential key to reconstructing previous global climatic trends and consequent predictions of future conditions.

Climate exerts a direct control on water release from or water storage in a glacierised mountain watershed. Therefore, glaciers have an important regulatory effect on the regimes of rivers which are fed by glacial runoff (Tangborn, 1984). During both

winter and summer, precipitation in the mountains is often greater than over adjacent lowlands as a result of orographic effects (Barry, 1981). A large proportion of precipitation falls in the form of snow since temperatures are cooler at high altitudes than at low elevations. This snowfall is a direct input into the glacier system. In the summer-time, mountain temperatures are warmer than in winter facilitating melting of snow and glacier ice, the output from the glacier system. The timing and magnitude of meltwater flow over summer ablation seasons depends upon the volume and areal extent of winter snow accumulation and on climatic conditions at the start of the melt season. In dry, warm years there might be comparatively less winter snow cover than in cool, wet years. Hence, early season glacier snow- and ice-melt is enhanced augmenting flow in arterial rivers by releasing water from glacierised catchments. However, in cool, wet years, winter snow accumulations may be greater both areally and volumetrically at the start of the summer. Since snow has a high albedo it reflects incoming solar radiation energy and suppresses glacier ice-melt. Consequently, water remains stored within the glacier until later in the melt season.

For some countries the presence of glaciers in large catchments provides water for major agricultural and industrial activities which might otherwise remain marginal. This is especially the case for developing countries where two contrasting climatic regimes may dominate; for example, a cool, moist mountain climate and dry semi-arid lowland region. If the natural resource base is weak, a heavy dependence upon water supply is paramount. In this case, during the summer, lowland regions away from the mountains may experience hot, dry weather which initiates drought conditions. However, if rivers have a glacial source component, increased glacier melting and runoff in late summer can provide relief for agricultural and industrial operations thus

alleviating the threat of drought. During the winter, although there is very little snow and ice-melt from glacierised sub-basins, rainfall in the lowlands may furnish demand with an adequate supply of water.

Thus, the timing and magnitude of water storage release may have critical implications for the development of economic activities. In countries where hydroelectric power generation is dominant (e.g. Switzerland and Norway), an understanding of the characteristics of water release from a glacierised catchment is crucial for efficient resource management. For example, calculation of potential maximum outwash flows is necessary to establish reservoir dimensions. Although glaciers reduce streamflow variability over successive years, sudden flood events can cause short term flooding in the lower reaches of glacier-fed rivers. Rainfall events over all elevation ranges in glacierised basins can cause flooding downstream since the delivery time of runoff through a glacier system is very quick (Rudolph, 1962). Unlike normal vegetated slope surfaces, rainfall on a glacier surface does not easily infiltrate through ice. Water flows over the surface or washes into channels and becomes routed through the subglacial system. However, these events only occur during the later part of ablation seasons when the transient snowline has migrated up-glacier exposing underlying ice (Østrem, 1972). Another formidable cause of short term downstream flooding is the release of ice dammed waters from within the glacial environment (Jökulhlaups), (for example, Mathews, 1973). Even though the magnitude of flood events can be calculated (e.g. Clague and Mathews, 1973, Clarke, 1982) the timing of these inundations may be difficult to predict. If superimposed on seasonally high summer flows, the results can be devastating (Hewitt, 1982).

Not only do larger-scale agricultural operations benefit from a glacial river regime, but smaller mountain settlements may also rely totally on meltwater for irrigation of agricultural lands (Butz, 1989). Although mountain regions are generally cooler and wetter than lowland areas, in some regions of the world (for example, The Karakoram Range of Pakistan), zones within the mountains may be arid. Valley bottoms particularly may receive less precipitation than higher altitude zones because orographic snow- or rainfall only falls at higher elevations. Lack of water in areas characterised by steep slopes, poorly developed soil horizons and short growing seasons can prevent the natural vegetation of slopes. However, by diverting glacier meltwater for irrigation, settlements can cultivate land which would otherwise remain unproductive (Whiteman, 1985).

In addition to being stores of water, glaciers are also powerful erosional tools on the landscape. Glaciers slide across and creep by plastic deformation along their beds shattering and scouring the bedrock in the process. Avalanched sediments may be incorporated into glaciers from surrounding valley sides as slopes are undercut. This combined debris source is subsequently entrained down valley either by inclusion into ice, or by fluvial transportation. Eventually, the sediment is ejected from the glacier in seasonal meltwater streams. Thus, from many glaciers of the world, meltwaters are highly charged with vast amounts of sediment of greatly varying size (Caine, 1974). These sediments can create problems for hydroelectric installations downstream and unless sediment load is accounted for in their design, the working lives of reservoirs and power turbines may be drastically reduced (for example, the Warsak dam on the Kabul River in N.W. Pakistan has had its working life drastically reduced due to siltation of the reservoir). Although these sediments may cause problems for agriculture

and industry, an understanding of characteristics of temporally changing sediment yields and solute loads can provide an important insight into conditions in the glacial environment. The purpose of this paper is to establish a greater understanding of the relationship between glacial erosion at the bed, as indicated by evacuated sediment loads, and the fluvioglacial environment. This approach is only one way of examining part of the glacial environment. Thus, before exploring part of the glacier sedimentary system it is necessary to briefly discuss two other concepts which are important in understanding the glacial environment.

Firstly, the need to understand the glacial system is one which can be approached using a hydrological method (e.g. Kasser, 1967, 1973; Tangborn *et al*, 1975). The seasonally changing storage component of water (ΔS) within a glacierised catchment can be conceptually expressed by the equation:

$$\Delta S=P-R-E \qquad (1.1)$$

where P is precipitation, R is runoff and E is evaporation (Röthlisberger and Lang, 1987). This equation is known as the water balance of a glacierised area and is directly related to the mass balance (b):

$$b=c-a \qquad (1.2)$$

where c is accumulation and a is ablation (assuming the changing volume of stored water is negligible). Here b is equal to ΔS and so the use of the water balance equation is called the hydrological method (Röthlisberger and Lang, 1987). If climatic

conditions are stable, yearly balances approach equilibrium. However, the adjustment of a glacier to changing climatic controls, and hence changing mass balance, continues for many years (Jóhannesson *et al*, 1989). Therefore, even though the current year's net balance is zero, glaciers retreat and advance in response to balance changes from previous years' changes (Paterson, 1981). The time taken for different glaciers to adjust to changing climatic conditions varies depending on the physical dimensions of the ice mass; smaller glaciers generally respond more quickly than larger ones.

Secondly, proglacial meltwater characteristics also reflect changing climatic and meteorologic controls affecting glacierised basins. Variations in discharge from a glacier are intimately related to changes in global radiation which is the main source of energy (Lang, 1973). Global radiation increases during the summer raising flow levels in glacier-fed channels, and decreases during winter reducing discharge levels. Superimposed on these base-flows are periodic flow variations ranging from a few days to a couple of weeks and relating to spells of warm and cool weather. Over a shorter time-scale still, diurnal hydrographs are a result of daily ice-surface warming and cooling. However, diurnal peak global radiation precedes daily flow maxima by several hours as a result of the time taken during routing of meltwaters through the glacier. Sudden changes in meltwater-routing over shorter time periods of tens of minutes can be manifest in the hydrograph by sudden pulses or drops in discharge (Emmenegger and Spreafico, 1979).

Thus, the influence of climate on the glacier system and the way in which water storage and release mechanisms respond to changing climate are the most important influences on long-term variations of characteristics in the fluvioglacial environment.

Bearing these two influences in mind, shorter, within-season variations in meltwater characteristics can be examined to infer processes operating in the glacier environment.

Suspended-sediment characteristics in meltwaters can be used to indicate routing of water through glaciers (Collins, 1989). Available energy for entrainment of sediments in a stream increases with increased flow (Morisawa, 1968). However, although closely related to discharge on an annual and seasonal basis, over diurnal and shorter periods, transport and concentration of fluvioglacial sediments are not as well correlated with flow. The reason for this discrepancy is because supply of eroded sediment at the bed and within the ice mass changes as sources become exhausted and replenished as basal drainage networks alter their positions and tap new deposits (Collins, 1988). Furthermore, meltwater routing changes also affect acquisition of solute loads by meltwaters from englacial and subglacial environments thus modifying water quality characteristics in glacier-fed streams (Raiswell, 1984). Therefore, by monitoring and analysing meltwater quality characteristics, it is possible to gain an understanding of hydrological and glaciological processes acting within the glacial environment.

The relationship between discharge and suspended-sediment concentration is important for indicating erosion processes beneath glaciers and can be investigated using various techniques. Stochastic time-series analysis empirically defines related trends from previous periods (Gurnell and Fenn, 1984a). Although it can be a successful method for the simulation of suspended-sediment transport, a heavy dependence is placed on statistics in previous records to establish time series and prediction does not take into account physical processes. Linear and multiple regression analysis is another useful tool for describing the relationship between discharge and suspended-sediment concentration (Bogen, 1980; Østrem, 1975). However, regression

analysis is a purely statistical approach and is unable to predict suspended-sediment concentration over successive short timescales. Routing of water and sediment supply changes within the glacier over diurnal periods and cannot be accounted for by a statistical regression analysis alone. Perhaps the best method for examining the relationship between glacial discharge and sediment transport is a process-orientated modelling approach. Prediction of future sediment transport regimes, based on knowledge of physical traits in the fluvioglacial environment, is only possible when sedimentary processes acting within the glacier system and the relationship between flow and suspended-sediment concentration in meltwaters are understood. However, a fully deterministic model of the fluvioglacial environment is un-practical because uncertainties about the nature of subglacial and englacial environments persist. Hence, a partially stochastic and partially process-orientated (deterministic) method provides a useful design for water quality simulation (Shaw, 1984). The present study attempts to implement such a hybrid method.

For design and implementation of a stochastic/process-orientated model which simulates and forecasts suspended-sediment transport in glacial environments using discharge data, collection and examination of meltwater quality data is necessary. Thus, discrete field measurements of discharge, suspended-sediment concentration and solute load need to be taken during the melt season if not over the whole year. It may then be possible to make inferences about the subglacial and englacial environment and attempt to model geomorphic process acting therein.

1.2 Objectives

The objectives of the research are four-fold in nature. The first reflects a need to investigate fluvioglacial characteristics of meltwaters draining two glaciers in the Karakoram in order to establish varying magnitudes of characteristics in their glacier-fed streams. The second deals with the nature of empirical relationships between sediment transport and discharge in measured streams. The third objective is to use an alternative causal model of subglacial erosion to describe the relationship between flow and sediment transfer. Finally, comparison between the deterministic and statistical approaches will assess the relative merits of each method. Thus, the thesis objectives are:

1. to measure variability of water flow, suspended-sediment concentration and electrical conductivity in meltwaters draining Bualtar and Batura Glaciers during 1987 and 1988 ablation seasons respectively and infer hydrological processes acting beneath each glacier;

2. to examine empirical relationships between flow and suspended-sediment transport from Bualtar and Batura Glaciers in order to establish the effectiveness of statistical techniques for predicting suspended-sediment flushing from these glaciers;

3. to implement and improve a model of subglacial erosion devised by Keeley (1986) which conceptualises the glacier system in terms of erosion at the bed and subsequent sediment removal by subglacial meltwaters draining the glacier;

4. to compare the effectiveness of a causal modelling approach with that of an empirical strategy.

Chapter Two

Theoretical Considerations

2.1 Introduction

In order to model erosional processes beneath a glacier, it is necessary to account for the changing nature of water, sediment and chemical discharges from within a glacier system. Different components in the outwash record of each variable reflect different sources and types of routing taken through the glacier. Hence, an understanding of the forces creating such temporally changing proglacial characteristics is necessary to develop the rationale behind a subglacial erosion model.

Erosion can be defined as not only the breakdown of an in situ parent material but also the transportation away from source of its weathered product (Chorley *et al*, 1984). In the glacial context, water provides a major mechanism for removing glacially weathered products from bedrock within and beneath the ice. Ice conveys sediment at a very slow rate (debris can remain entrained in ice for 10^2-10^3 years) so that glaciers behave as large sediment stores (Drewry, 1987). However, meltwaters within the glacier system are able to remove great volumes of weathered sediments from the englacial and subglacial environment over considerably shorter periods of time. Thus, it's temporally changing nature of flow (in both physical states) and ability to weather and

flush sediments and solutes from within are of paramount importance for erosional processes.

2.2 Glacier Hydrology

2.2.1 The role of meltwater in glaciers

Liquid water is of major importance for the movement of both temperate alpine and "cold" glaciers. Glaciers move by creeping over and sliding across their beds (Paterson, 1981). For "cold-based" glaciers, where temperatures at depth do not allow the presence of great volumes of liquid water, general movement is by creep flow as a result of internal deformation of ice. With higher ice temperatures, and hence increased liquid water content, it has been shown that creep rate increases (Duval, 1979; Paterson, 1981). For example, a change in water content in ice from 0.1% to 1% produces an increase in creep rate of an order of magnitude (Duval, 1979). Therefore, warmer, temperate glaciers experience greater creep rates than cold-based glaciers since they contain comparatively more water due to ice being at pressure-melting point. This is especially the case during the summer season when meltwater is also derived from other parts of the glacier. Furthermore temperate glaciers move across their bed by basal sliding and regelation (Fowler, 1987; Kamb, 1970; Weertman, 1979). Both processes are intimately related since they usually occur concurrently.

At the base of a temperate glacier, ice may be at its pressure-melting point at many places along the bed. Consequently, a meltwater layer between the sole of a

temperate glacier and its underlying bed is able to progressively submerge small bedrock protruberances which act as frictional agents against glacier motion. This results in a lowering of basal shear stress allowing sliding velocities to increase (Weertman, 1964). Eventually, total submergence of small bed protruberances leads to the formation of a thin film of water at the ice-rock interface (Hallet, 1979b). It has been shown that larger discharges of water in the subglacial environment can produce increased sliding velocities (Hodge, 1976). However, it should be noted that although increased water discharge at the base can enhance basal sliding, water pressure is a more important factor. Maximum sliding occurs when subglacial water pressures are at their greatest and not necessarily when water volumes beneath the bed are at their maxima (Iken *et al*, 1983).

Basal sliding is inextricably linked with the process of regelation (or pressure melting and refreezing). Where ice is in contact with the bed, on the up-glacier side of bed protruberances, overburden pressure is greater than on the lee side causing the ice to melt. The excess water seeps to the lower side of the "bump" where pressure is less, and refreezes to form a layer of regelation ice (Figure 2.1), (Sugden and John, 1984). Hence, a sinuous base rock has its roughness tempered facilitating increased glacier sliding. The efficiency of regelation sliding depends not only on the availability of water but also on the size of protruberances. Nye (1973a) proposed that for obstacles protruding more than 0.1m into the overlying ice, regelation slip is at its least efficient. During the ablation season, for bumps that are larger than this critical size, water may collect on the lee side forming water-filled cavities. The reason for this is that not all pressure-melted water from the upstream side is refrozen but remains in liquid form

Figure 2.1 Basal slip of glacier ice over bedrock of rough topography and subsequent formation of regelation ice layer. (Adapted from Kamb, 1964).

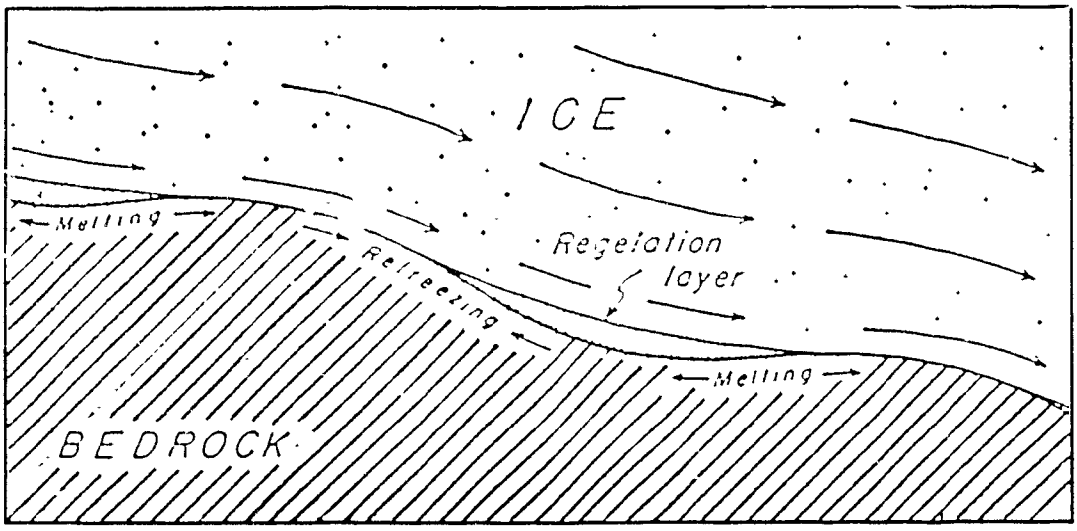

within a cavity. Such cavities are situated below the obstacle where the ice has become separated from its bed due to plastic flow (Walder and Hallet, 1979).

Meltwater is not only an important regulator of glacier flow but it is also instrumental in basal erosion processes. Water directly abrades and crushes bedrock forming potholes and channels as a direct result of intense water pressure causing considerable mechanical erosion (Nye, 1973b). Where unconsolidated sediments are deposited from direct glacial erosion processes, high water pressures decrease sediment shear strength. This results in deformation and removal of basal sediments (Drewry, 1987). Sediments from within the ice are also entrained by meltwater flowing through the glacier. The lower glacier sole is characteristically rich in sediments and water at the bed has opportunity to incorporate them into its body. Debris entrainment into channels and conduits at the bed is by direct particle removal into suspension and bedload, and through solution of sediments and bedrock. Thin films of water at the bed also dissolve basal sediments. Evidence of this process is from calcite deposits beneath some glaciers (Hallet, 1979b). Eventually sediments are flushed from the glacial system and deposited downstream. Hence, records of sediment and solute loads in glacier-fed streams may be used as indicators of glacial and fluvioglacial erosion processes.

2.2.2 Water Sources: Storage and Release

Water in the glacial environment is derived from four sources; melt of surface snow and ice, meltwater produced by internal deformation within the ice, geothermal heat from underlying crustal regions, and liquid precipitation events.

Surface melt during the spring and summer ablation season provides the most important source with volumes usually being several orders of magnitude greater than other sources (Shreve, 1972). In winter, precipitation falls as snow in the upper and often in the lower regions of the glacier. During spring, this snow is the first major water supply in the ablation season. As the sun's angle of incidence increases during summer, net radiation, comprised of incoming direct and reflected solar radiation, produces sensible and latent heat energy for melting of snow and gradually reduces its areal coverage. In the lower ablation regions, the snow layer above glacier ice is thinner than in the accumulation areas since winter snowfall is less here due to higher temperatures at lower elevations. It should be noted that snow accumulation distributions within both accumulation and ablation zones are not constant because local topographical effects produce irregularities in snow depth (Türcan, 1975). Generally, however, as the snow melts, the areal extent of exposed ice progressively increases as the snowpack melts up-glacier. This can be shown through observation of the snowline migration to the equilibrium line over the summer. It is possible, as Young (1980) showed, to simulate the elevation of the transient snowline at Peyto glacier using winter snow accumulation and summer air temperature data. As the melt season proceeds, glacial meltwater flows increase because exposed areal extent of ice increases. Glacier ice has a lower albedo than snow (Bezinge, 1987). Consequently, the capacity of ice to absorb incoming and reflected solar energy is greater than snow because ice absorbs more solar radiation than snow. This is why snowfall events in the lower glacier region in later summer suppress glacier runoff (Collins,1977).

The storage of water and release of surface meltwater from a glacier environment is, therefore, in direct response to local climatic conditions. On an annual

timescale, winter and summer snowfall contribute to the water storage at the glacier surface. If winter snowfalls are great, summer ice meltwater flows may be delayed until snow coverage is reduced even though a compensatory effect may be provided by the annually larger contribution of snowmelt to outwash (Krimmel and Tangborn, 1974). In this case, the rise of the transient snowline is slow. If winter snow accumulations are smaller, summer runoff begins soon after the onset of spring melt. Furthermore, long, hot, dry summers produce greater discharge maxima than short, cool, wet summers because the latter experiences less direct solar radiation as a result of increased cloud cover.

On a shorter timescale of one to three weeks, local mountain weather systems also influence glacier melting at the surface. Cloudy, wet weather retards ice melt as a result of reduced net radiation while warm periods enhance melting and augment water supply to glacier-fed streams. Finally, in the summer months, release of surface water occurs on a diurnal scale. During the day, incoming solar radiation provides energy for the melting of surface ice. At night time, melting is suppressed due to the relative lack of net radiation. Hence, supply of surface water to the proglacial channel is cyclic; high flows during the day and low flows during night. However, the delivery of diurnally melted surface waters from glacial systems to proglacial rivers is not instantaneous. A lag time exists between maximum input radiation (at solar noon) and peak flows in the proglacial channel and is caused by the time taken for routing of meltwater from the surface, through the glacier and out at the portal. For different glaciers, the lag varies depending on glacier shape and aspect. Over the melt season the lag time decreases as the englacial and subglacial drainage network becomes more efficient. Furthermore, during the ablation season, the position of solar noon changes

due to the earth's precession around the sun. Thus, for northern hemisphere glaciers, at the beginning of the summer season solar noon, and hence maximum potential solar radiation input, is earlier in the day than later in the season. Consequently, diurnally early peak flows in spring gradually become later peak flows at the end of summer.

In winter, the low angle of incidence of the sun in the northern hemisphere emits comparatively low energy radiation. Also, snowfall precipitation prevents ice melt by forming a snow layer on the glacier surface. Therefore, during winter, temperatures are cooler and surface ice melt is minimal. These shorter cycles are progressively superimposed on longer seasonal trends.

Theakstone (1988) examined annual, seasonal and diurnal variations in glacier flow from Austre Okstindbreen, Okstinden in Norway by investigating fluctuations in isotopic $\delta^{18}O$ concentrations. Variations in the isotope record were related to changing relative contributions from new snow melt, old snow and glacier ice melt and water derived from storage within the glacier.

Another source of water release in a glacier system is from the way in which glacier ice moves. Glacier motion involves two types of movement, creep and slide both of which are a response to gravity forces which facilitate the spreading of ice under its own weight. Creep flow is the way in which glaciers move as a result of ice deformation. In glaciers, gravitational forces continually produce strains greater than the critical limit under which ice deformation prevails. In addition, glacier ice contains sediment impurities and its polycrystalline structure is imperfect. Both factors lower the critical stress point at which plastic flow is dominant in glacier ice. Hence, glaciers move under plastic deformation or Glen's Flow Law (Glen, 1955). In the process of

creep flow, mechanical heat is produced as a result of strain in the ice. This heat is enough to cause melting of the ice through the profile.

The second method of glacier motion is by sliding. Weertman (1957) recognised two types of glacier sliding, enhanced deformation and regelation. Localised enhanced creep around bed obstacles is a mechanism by which ice melts in a similar way to general creep movement. Stresses are supplied by bed protrusions which force ice to flow around them. This is in addition to stresses produced by the ice overburden force alone. Velocity around an obstacle increases with increasing sized protrusions. However, this sliding method is not between bed and ice. Instead it occurs near the glacier sole where ice is below pressure-melting point. Water is liberated from ice as a result of mechanical heat dissipation. For regelation sliding, as noted above, ice on the upstream side of protrusions has a different applied pressure than on the downstream side. Hence, regelation pressure-melting of ice provides water to the drainage system. If, however, protruberances are greater than one metre in size, then regelation does not take place and enhanced creep occurs (Weertman, 1957).

Water release in response to glacier movement is seasonal in characteristic. Creep flow is probably the only alpine glacier movement type during winter when ablation is at a minimum and water volumes at the bed are insufficient to initiate sliding. Sliding at the bed often only happens during summer when there is sufficient meltwater to reduce friction from bed topography. Generally, the annual contribution of meltwater from the motion of glaciers is of the order 0.01m to 0.02m (Drewry, 1987) although faster moving glaciers have greater melt rates.

The third source of water release from a glacier is from the geothermal melting of basal ice. Although the flux of heat varies depending on local geological conditions

(Stacey, 1977), an average annual melt rate of 6mm of ice from the base of a glacier at pressure-melting point has been suggested (Paterson, 1981). Water derived from geothermal heating of ice has less variability since it continues constantly throughout the year.

Groundwater flow provides another source of water to the glacier system. Snowmelt and storm runoff from surrounding valley sides may enter the glacier mass from small, valley side streams or from beneath the glacier via groundwater flows. The regime of such input flows varies depending on source. Groundwater flows are often the only source of water from the glacial environment during winter time when there is no snow or ice melt. Snowmelt from the peripheral areas around glaciers can provide water all year round although it is most marked during the spring event.

The final source of water is from liquid precipitation during storm events. Rainfall can make an important contribution to glacial runoff (Richards, 1984) although compared with glacier melt, it is usually minimal.

2.2.3 Supraglacial and Englacial Water Routing through Glaciers

There are various ways in which liquid water moves through a glacier. A useful way to investigate routing is to examine water movement through the accumulation and ablation zones since atmospheric conditions, which strongly influence routing, are different in both these regions (Figure 2.2).

In the accumulation zone, much of the surface is covered by snow. Since snow is a porous medium, surface channels do not exist. Therefore, meltwater slowly

Figure 2.2 Schematic diagram of water routing through a temperate glacier. (From Collins, 1988).

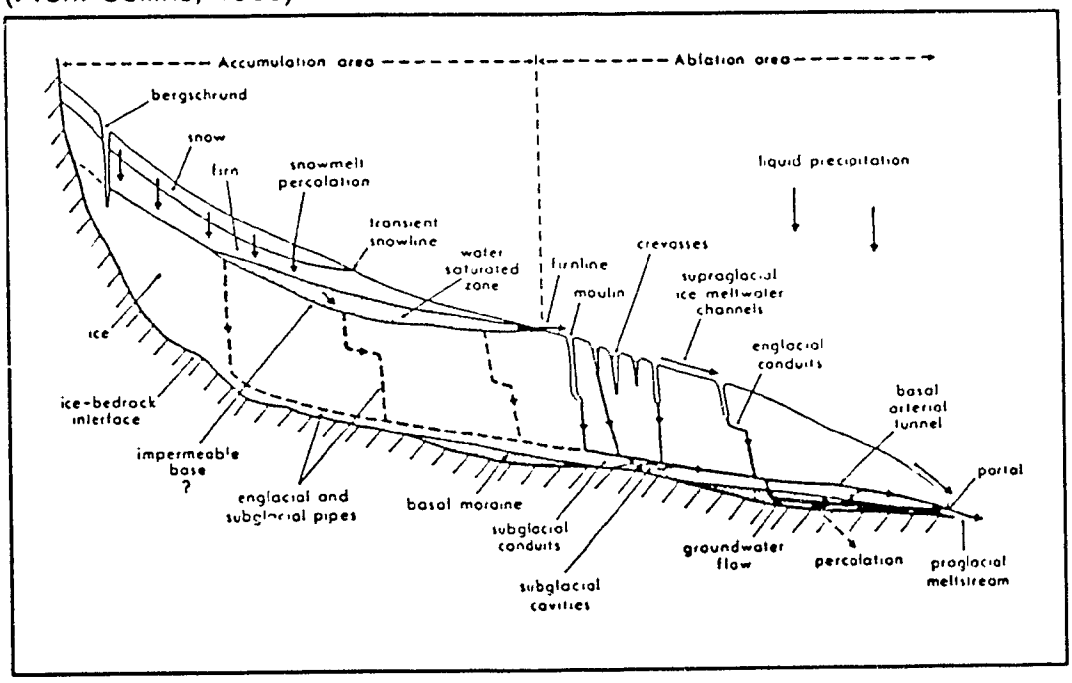

percolates under gravity through the snow to the firn layer beneath. The rate of flow can be investigated by applying Darcy's Law (Colbeck, 1973) which relates the vertical water flux to the slope of the snow surface, capillary pressure gradient through the snow, permeability of snow and water viscosity. With increasing depth, snow becomes transformed into firn; the intermediate phase during snow transition to ice. Water continues to percolate through the firn layer until it reaches the firn-ice interface where firn becomes relatively impermeable ice as the pores within the firn are sealed. Over this section of the vertical profile, percolation may become channelised as greater volumes of water flow with increasing depth. However, at the firn-ice transition, saturation caused by the impermeability of ice below does not permit water to continue percolation into the ice at the same, relatively high rate. Hence, a saturated water zone exists within the firn area. This region of the glacier acts as a water store (Fountain, 1989) the surface level of which can be likened to a water table and in this context, varies depending on the season. In spring, the level rises and in winter it falls as the availability of meltwater changes (Lang *et al*, 1977). The store extends from the firnline beneath the snow layer into the accumulation zone. Although the slope of water table approximates the glacier surface slope, it is not parallel (Lang *et al*, 1977). Thus, the distance from snow surface to water table increases with distance up the glacier. Furthermore, variations in thickness are related to proximity of sinks such as crevasses which drain the stored water. The store debouches onto the glacier surface at the firnline supplying water to supraglacial channels.

Beneath the firn water store, water is able to percolate very slowly through ice. The reason for this is that ice is not perfectly impervious due to interstitial veins between ice crystals (Nye and Frank, 1973; Raymond and Harrison, 1975). The flow

of water through intergrannular veins is proportional to the fractional volume occupied by the water. The deformability of ice allows these intersections to grow and shrink in response to changing water pressure and dissipation of heat generated at the walls by friction. As the water descends further into the glacier, water from intergrannular flow exploits ice cracks and fissures allowing larger quantities of water to develop a system of pipes and conduits in the englacial environment. The water contained in these conduits is above freezing and a continual water supply allows larger passages to "gradually increase in size at the expense of the smaller ones" (Shreve, 1972, p206). Thus, there is an arborescent network of conduits in the ice extending upstream within the glacier. In the accumulation area, these conduits are usually in the form of englacial and subglacial pipes and do not impinge on the bedrock beneath. This is different from subglacial conduits existing within the ablation zone which may flow at the ice-bedrock interface.

In the ablation zone, there are three principal and interconnected routes which meltwater can take through the glacier. Firstly, since the ablation region is not covered with snow for the whole year, open channel flow can develop at glacier surfaces which are devoid of snow. With increased melting during the summer, more water drains over the snow-free glacier ice. Mechanical heat energy dissipated by friction with the channel wetted perimeter, facilitates enlargement of the cross-sectional area. Thus, during particularly warm years, surface channels become relatively large. These conduits may eventually reach the glacier snout where they coalesce with main proglacial streams. However, on their way to the glacier terminus, there may be many crevasses and moulins at the surface into whic' streams are likely to descend. Crevasses form in response to glacial motion and underlying bed topography. Where a glacier

undergoes a sudden steepening of gradient, for example, as a result of a step in the bed profile, the increased stress at the surface causes fracturing in the ice since the tensile strength is exceeded. This kind of transverse crevasse is common in many glaciers. Water sink holes in the surface (moulins) form along these structural lines or fractures in the glacier. Moulins may develop when cracks temporarily open. However, capture of water may occur if stresses at the surface produce crevasses up-glacier. Their dimensions range from being tens of centimetres in diameter to metres across. The larger the diameter, the more likely the chance that they have existed for several years.

The propagation of moulins into englacial environments has been examined by Holmlund (1988). If glacier ice is below its pressure-melting point and hence impermeable, apart from intergranular flow, the only way for surface meltwater to enter the englacial system is to descend into crevasses. If crevasses are not too deep, water fills the fracture and may overflow. However, deeper crevasses may connect with englacial and subglacial conduits when ice reaches its pressure-melting point at depth. Hence, moulins form the beginning of the arborescent network described by Shreve (1972). Although glacier motion sometimes carries moulins into zones of compression, heat energy carried within and viscous energy from meltwaters may keep the moulins open.

If moulins descend to great depths, water may debouch into subglacial conduits. However, it is more likely that water from moulins will feed englacial paths before joining subglacial routeways. This is the second part of the route taken by meltwater through the glacier. The propagation of water-carrying englacial paths is controlled by the excess pressure in water compared with that in the ice, and secondly, by the stress field within the ice (Röthlisberger and Lang, 1987). Increased excess pressure with

depth causes the crack to spread downwards. At lower depths the conduit dips in the downstream glacier direction since water will flow perpendicular to the equipotential surfaces as defined by Shreve (1972):

$$\Phi=\Phi_0+\rho_w gZ+\rho_i g(H-Z)+p(\dot{r}) \qquad (2.1)$$

where Φ is the potential, ρ_w and ρ_i are the densities of water and ice respectively, g is the acceleration due to gravity, H and Z are elevations above sea level of the glacier surface and of a point on the bed or within the glacier respectively, $\dot{r}$ is the rate of closure of conduit by plastic flow of ice and $p(\dot{r})$ is contribution to the pressure that is a function of $\dot{r}$. The first term to the right of the equation is a reference potential for the glacier, the second is the potential energy of water due to its height above sea level, the third is an expression of the pressure in water due to overlying ice and the last part is the pressure difference between water and ice that results in opening or closure of tunnels by the plastic deformation of ice. If the equation is differentiated with respect to distance from the snout, assuming $p(\dot{r})$ is much smaller than the other expressions and setting the equation to zero, it can be shown that the equipotential surfaces in a glacier are inclined upwards in a direction opposite to the slope of the glacier with an angle of approximately eleven times the slope of the glacier surface (Figure 2.3). Hence, englacial conduits will flow downwards but with a strong horizontal component. An example of this phenomenon is illustrated by Iken (1974; cited in Röthlisberger and Lang, 1987). However, as Hooke (1984) notes, if channels reach a diameter of 3 to 4mm, the mechanical energy dissipated by falling water will be enough to melt the downglacier side of the conduit faster than the sides close by

Figure 2.3 Profile of the long axis of a glacier showing equipotential surfaces and theoretical flow directions of englacial water routing. (Adapted from Hooke, 1989).

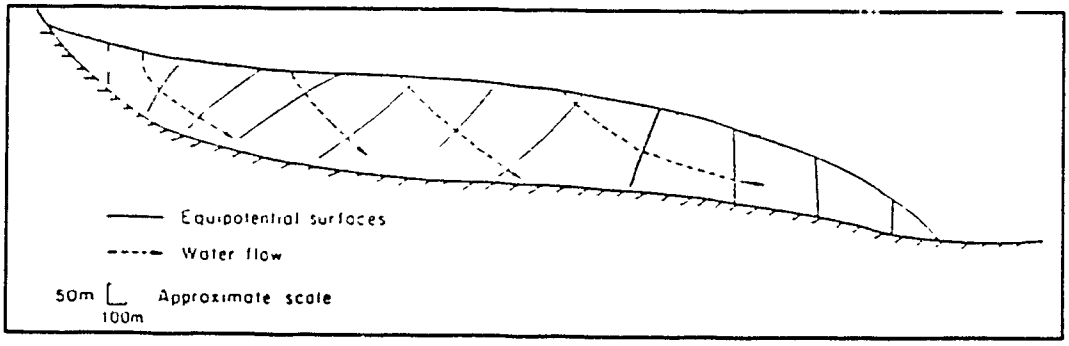

ice creep deformation. With increased diameter of pipe, the melt rate at the sides would increase. Assuming a constant supply of water, the growth of conduit diameter would be self perpetuating. Thus, the vertical component of an englacial pipe flow increases. Furthermore, differential movement of ice through the vertical profile will produce steepening of the englacial pipe since ice flows faster at the surface than at depth. However, as Hooke (1989) notes, if constrictions at depth produce backwater effects, oversteepening of conduits will not occur.

Storage of water in cavities within the englacial environment is a common occurrence. Paterson and Savage (1970) found considerable evidence for the presence of such cavities because a radar echo sounding technique used to investigate subglacial bed topography received strong echoes from such stores. These echoes distort the incoming signal from pure glacial ice. In addition, ice at melting point absorbs more radio waves than ice which is at temperatures below pressure-melting.

It should be noted that englacial conduit routing of water in the ablation zone is a more important method of meltwater transport in the englacial environment than seepage through ice. However, interstitial water flow still continues in this region.

Having reached the bed through englacial conduits or by discrete intergranular flow, water is transported along or near the bed. There are three main ways in which water moves along the bed; sheet flow (for example, Weertman, 1972), conduit flow (for example, Nye, 1973; Röthlisberger, 1972) and through linked cavity systems (Lliboutry, 1968; Walder and Hallet, 1979). When water reaches the bed, assuming an impermeable basement, it flows out under the pressure gradient. At any point along its course, the gradient can be expressed in a more tangible manner than the fluid potential equation (equation 2.1):

$$P_g=\rho_i g(\tan\alpha_s-\tan\beta)\cos\beta \quad (2.2)$$

where P_g is the pressure gradient, ρ_i is the density of ice, α_s is the surface slope of ice, β is the bed slope and g the acceleration due to gravity (Drewry, 1987). For small angle of surface and bed slopes:

$$P_g=\rho_i g\alpha_s+(\rho_w-\rho_i)g\beta \quad (2.3)$$

where ρ_w is the density of water. The pressure gradient is a function of the ice overburden pressure. The type of basal flow is important not only in terms of the time taken for water to leave the glacier but also for the mechanisms of glacier sliding and basal erosion.

2.2.4 Configurations of Water Routing at or near the Bed

Sheet Flow

It has been argued that water flow at the bed of a glacier overlying an impermeable basement will runoff in the form of a thin film less than 4mm thick (Weertman, 1972). The principle behind this idea is that if basal water pressure (P_w) is equal to ice overburden pressure (P_i) then meltwater flows in a film at the base. The direction of flow is perpendicular to the surface slope (equation 2.3) which is ten times more effective in influencing flow than local bed topography (Weertman, 1972).

However, it is apparent that some bed slope angles exceed those at the surface and take control of flow direction. The implication of this observation is that the direction of sheet flow will not always be determined by surface slopes. Film thickness also varies over the glacier bed because as ice slides past bumps, pressure on the up-stream side melts the ice (regelation) and forces the water to areas of low pressure. Thus, water will not always flow predominantly parallel to the long axis of the glacier but collect between protruberances.Quantification of this phenomenon can be achieved using equation 2.3 if $\beta \neq 0$, α_y(surface slope across the glacier)=0 and β_y(basement slope across the glacier)$\neq$0. If the glacier cross-profile is convex or concave upwards, water flows towards the margins or the centre respectively. If the surface is horizontal, water flow will be dictated by bed topography.

The stability of water moving in sheet flows has been investigated by Walder (1982). It was suggested that sheet flow is "quasi-stable" for films up to 4mm thick overlying gently undulating and rough basements, and with moderate to high glacier velocities. However, with increased sheet thickness and pressure gradient, films become unstable. Nevertheless, the presence of a film of water at the base of a glacier reduces the frictional coefficient between ice and bed and facilitates sliding.

Evidence for the existence of subglacial water films has been provided by dye-tracing experiments. Theoretically, water films move relatively slowly at the base so the time taken for meltwater entering the subglacial drainage system to leave the glacier should be great. This was observed by Stenborg (1970) at Störglaciaren when injected dye gave a poor trace at the outlet.Further evidence for the existence of water films has been examined by Walder and Hallet (1979) at recently deglaciated bedrock sections of the Blackfoot Glacier, Montana. Calcite precipitates were thought to be

formed in the presence of a thin layer of water over 80% of the ice rock interface. Since flow in these films is slow, there is enough time for the deposition from solution of calcite which would not occur in fast flowing channels and conduits at the bed.

Linked Cavities

Water flow in thin films, however, cannot account for the large volumes of water expelled at the glacier terminus for most alpine glaciers during the ablation season. Also, instability of water stores greater than 4mm in thickness is not compensated for by sheet flow. The presence of water-filled cavities at the bed accounts for discrepencies in sheet flow theory. A pre-requisite for such phenomena is that the bed is not flat but consists of protruberances and undulations. When ice flows past protruberances, water melted by pressure on the stoss side accumulates on the lee side. If ice flows over the bump at fast enough speed, the ice becomes separated from the bed because its rate of deformation due to overburden pressure is not sufficient to remain in contact with the basement (Kamb 1987). The ice will rejoin the bed downglacier. Therefore, melt water occupies the cavity and if water pressures are great enough, the cavity begins to grow in size. This pressurised water may find its way to adjacent lee areas where the ice has not separated from its bed and cause detachment at these places (Hooke, 1989).

Where the ice rejoins its bed or on the stoss side of the next bump downstream, pressure may be enough to prevent water in the filled cavity from flowing beneath the ice at this point (Walder, 1986). This acts as a constriction to the cavity and increases the potential gradient needed to drive water flow thus raising water pressures. It has been suggested (Hooke, 1989) that if pressures build up sufficiently, water may be

squeezed beneath the ice in a thin film producing sheet flow. However, this is not a plausible situation because water will tend to avoid regions of high cryostatic pressure (Walder, 1986).

The lateral spreading of pressurised water in cavities links different cavities together forming an integrated drainage network (Figure 2.4). As before, flow should be perpendicular to equipotential surfaces (equation 2.1) but such a network produces long, winding routes which avoid centres of high ice overburden pressure. This can be shown using dye-tracing techniques. Iken and Bindschadler (1986) interpreted multiple dye concentration peaks in glacial outwash as the result of water routing through a complex subglacial drainage system, with various branches and/or storage spaces. The links between cavities may be in the form of N and R channels (see Conduits below). Also, there may be more than one entrance and exit to cavities in addition to "dead-end" areas that act as sites for water storage (Walder and Hallet, 1979).

A linked cavity configuration has an important influence on the sliding velocities of glaciers (Bindschadler, 1983). The geometry of linkages in the cavity network is a crucial factor since the size and extent of these connections depends on basal shear stresses, bed roughness and water pressures at the bed (Kamb, 1987). The connection between cavitation and sliding has been described by Iken (1981). Maximum sliding rates are thought to coincide with maximum growth rates. However, others have argued that greatest sliding rates occur with maximum extent of cavity development over the bed. It is possible that both theories are mutually inclusive because high water pressures, as a result of large meltwater volumes descending to the bed, facilitate both scenarios and are vital for the initiation of accelerated glacial sliding (Iken and Bindschadler, 1986; Kamb *et al*, 1985).

Figure 2.4 Plan view of a conceptualised linked cavity drainage network at the bed. Direction of glacier sliding is shown by the large arrow with water flow course indicated by small arrows. Hatched lines show where ice becomes separated from the bed and plain lines indicate sites of recontact.
(Adapted from Kamb,1968).

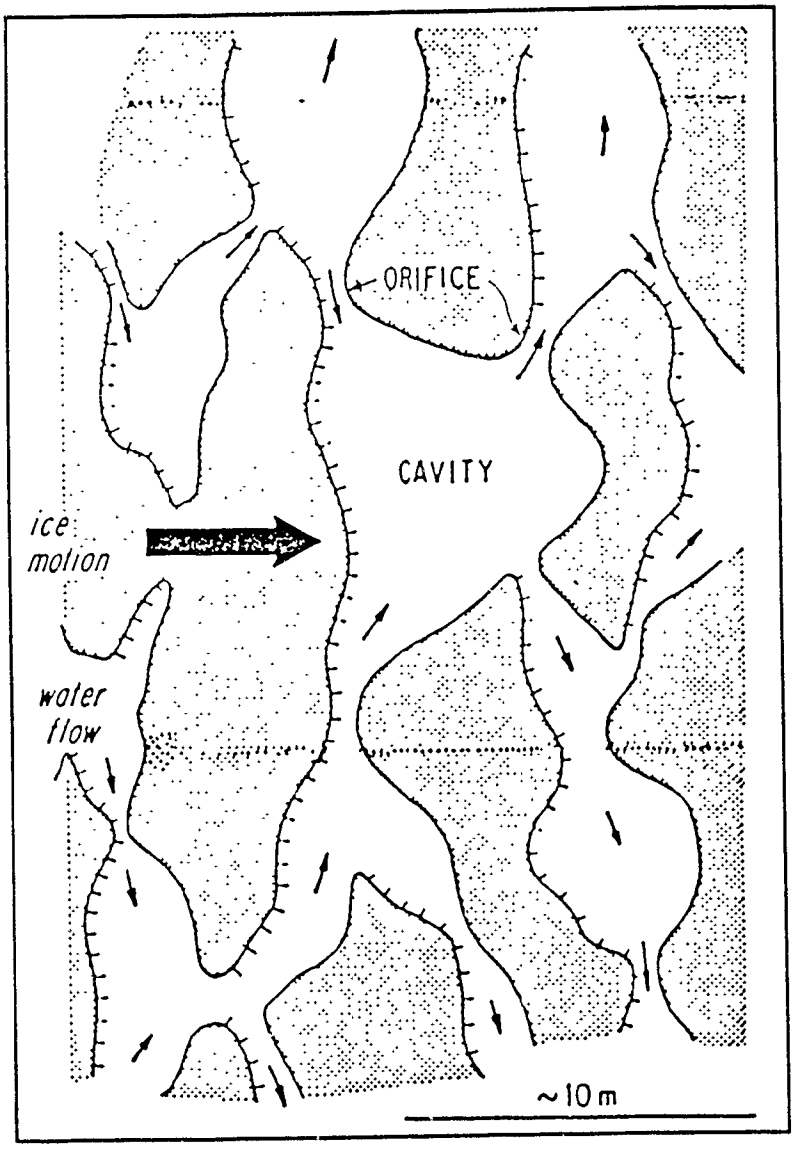

Conduits and Channels

Finally, the third method by which water is transported at or near the glacier bed is through discrete conduits. If water pressures are less than the ice overburden pressure, water will flow into pre-existing channels. Nye (1976), Röthlisberger (1972) and Weertman (1972) have identified two types of channel flow: Röthlisberger channels ('R' channels) and Nye channels. The former proposes that water flows at the bed but incises upwards into the ice and the latter that channels carve downwards into bedrock.

Röthlisberger (1972) shows that for a conduit to remain open and not change in size, the ice overburden pressure will equal melting of conduit walls by water friction with the ice. This is where the theory diverges from Shreve's (1972) idea that water pressure in conduits equals the cryostatic pressure. For R-channels, tunnel melting is caused by heat generated from turbulent flow of water. This is counteracted by pressure from overlying ice forcing tunnel closure. If a channel is in steady state, the closure rate is the same as the melt rate hence, the channel remains open. However, if overburden pressure is greater than the melt rate, the conduit will close. Conversely, if the melt rate exceeds the overlying ice pressure, the conduit will grow in cross-sectional area. Quantification of the relationship between closure and opening can be modelled mathematically. Cryostatic pressure can be expressed using an adapted Glen's flow law of ice for the closure rate. The tunnel melt rate can be directly related to water discharge in the tunnel, the pressure gradient (equation 2.2), and is inversely proportional to the tunnel circumference and latent heat of fusion of ice.

Observations show that some R-channels are situated along the central axes of glaciers (for example, Drewry, 1987). A focusing mechanism directing water melted from the base of a glacier to the channel exists in many glaciers because over most

of the bed, cryostatic pressure is greater than water pressure. However, at a critical distance away from the channel (100 times the channel radius), this focusing mechanism for ice melt at the glacier sole is inoperative because pressure forces water in any direction which is not necessarily related to the conduit location (Weertman, 1972). Hence, it is probable that water in the R-channel is derived mostly from moulins and englacial conduits.

Water pressure increases in an R-channel as meltwater production at the surface increases. If the channel becomes full, then turbulent water melts the conduit sides thus increasing the channel dimensions. Also, if the increased pressure becomes greater than the cryostatic pressure, channel enlargement occurs by creep deformation. When water supply does not continue to increase, then pressure will drop since flow is not being constricted. However, this process may take a long time. A more immediate effect is that with increasing pressures, water becomes forced out beneath the glacier possibly in a thin film (Weertman, 1972). This has important implications for sediment capture in meltwater channels (Collins, 1989).

The relationship between water pressure and discharge in R-channels is more complicated than suggested. Pressure may increase as flow decreases and vice versa. Over annual timescales, water pressure and discharge are out of phase; high winter pressures have low discharges while high summer flows have relatively low pressures. However, on a diurnal scale, channel dimensions do not immediately respond to changing water pressures so pressure and flow are in phase (Röthlisberger, 1972; Röthlisberger and Lang, 1987). What is certain is that raised water pressures at the bed increase the "bed separation index" (Bindschadler, 1983) between ice and subglacial rock and so influence sliding velocities (Iken, 1981).

The second type of subglacial water channel was proposed by Nye (1973b). In this case, water incises the bedrock below to form more permanent conduits than R-channels although their durability depends on erosive power of the glacier on bedrock and the bedrock type. For Nye channels to exist, a subglacial meltwater channel must flow at the same position for a long time for water to erode the basement rock. Assuming this is the case, theoretically, Nye channels will parallel the direction of ice flow and must be greater in depth than the amplitude of undulations in the ice which control sliding. The reason for this is that otherwise, pressure-melted ice which refreezes on the downstream side of undulations (<4mm in amplitude) will expel any water in the channel.

Evidence for Nye channels has been found by Walder and Hallet (1979) on the recently deglaciated limestone underlying the Blackfoot Glacier in Montana, U.S.A.. The channels were 25-50mm deep, 100-200mm wide, 2-5m in length, 5m apart and parallel to the former direction of ice flow. The suggestion made was that these channels were formed when the glacier surface was undergoing significant melting such that large volumes of meltwater were being discharged at the base (Drewry, 1987).

It should be noted that the difference between Nye and Röthlisberger channels is of secondary importance when applying conduit theory because the b ' ınce between closure of channel from cryostatic pressure and the melting of sides or roof by turbulent heating of ice holds unconditionally (Röthlisberger and Lang, 1987).

A central issue in examining both types of subglacial channels is their location at the glacier bed. Shreve's (1972) gravity potential theory (equation 2.1) suggests that water will flow downslope to the lowest point. However, meltwater tends to take existing paths rather than melting new routes. Thus, the formation of the first channel

is critical. Hooke (1984) proposed a model which suggested that water in R-channels flows diagonally down glacier from glacier margins to the centreline. The rationale behind this theory is that water flows downslope along the line of maximum gradient and general glacier flow tends to orientate the channel parallel to the direction of movement. However, this idea assumes a perfectly smooth bed and does not take into account bed roughness, bumps, furrows, hollows and gullies (Röthlisberger and Lang, 1987). Thus, a theory has been proposed which does not require knowledge of the bed topography. By examining the piezometric level (the height liquid water would rise in a borehole due to cryostatic pressure) which is usually 10/11^{ths} of the ice thickness, it has been suggested that water will move from high to low regions of overburden pressure (Weertman, 1972), (figure 2.5). Hence, the way in which water flows down glacier depends upon the configuration of surface slopes.

2.2.5 Development of the Drainage Network

The glacier drainage system comprises of all of the above routing paths. Shreve (1972, p205) describes the whole drainage network of a glacier consisting of "a supraglacial part much like an ordinary river system in a karst region, an englacial part comprised of tree-like systems of passages penetrating the ice from bed to surface, and a subglacial part consisting of tunnels in the ice carrying water and sediment along the glacier bed". This is a good first approximation to reality. However, the configuration of the network changes throughout the year (Collins, 1988).

Figure 2.5 Control of surface topography on the direction of channels at the bed. The figure shows a glacier plan with corresponding profiles at I, II and III. Water equivalent lines are represented by the dashed lines with the dotted lines running through the lowest point of water equivalence. Arrows trend from high to low piezometric pressure and indicate theoretical direction of water flow.
(From Röthlisberger and Lang, 1987).

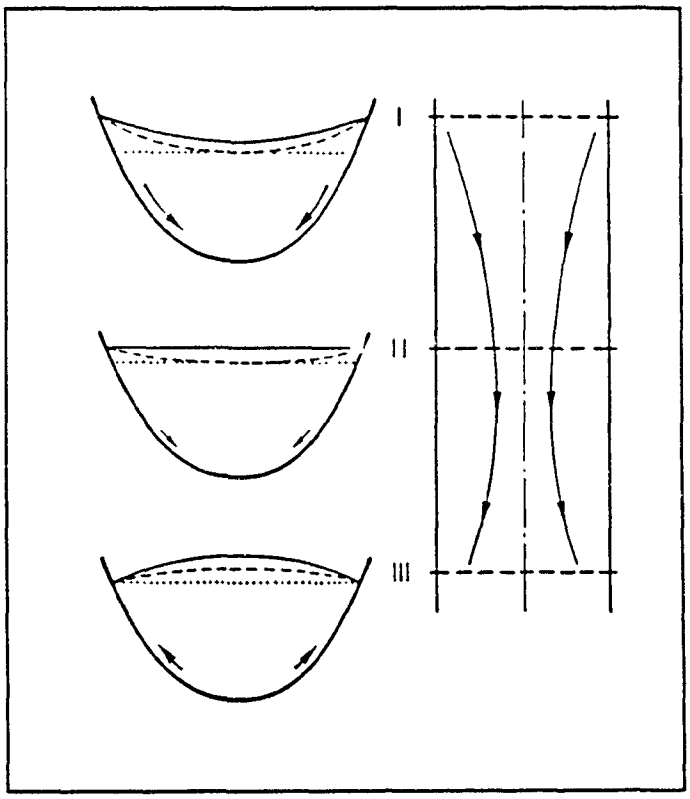

In winter, surface melting ceases so ice overburden pressure closes most subglacial channels and cavities. With the onset of the spring thaw, surface snow- and ice melt reaching the bed is unable to escape at the snout since the subglacial drainage network is undeveloped. Water pressure builds up in remnant conduits and cavities from the previous year and water becomes spread out over the bed. Cavities in the lee of protruberances at the bed increase in size with this influx of water at high pressure and basal slippage of ice increases. With increased volumes of highly pressurised water at the bed, connection of cavities occurs and a linked cavity network evolves. The linked cavity network eventually connects with the main channel drainage system and subsequently becomes simplified since melting is enhanced where there is more water flow (Röthlisberger and Lang, 1987). Also, the conduit system should become less complex over the summer because the pressure differential between large and small channels causes the larger conduits to grow at the expense of the smaller ones (Röthlisberger, 1972). However, not all of the cavity-stored water is immediately drained into the rapidly developing conduit system. Some will remain in isolated pockets until later in the melt season.

Before integration with the main conduit system, the cavity network is a major water store. This has implications for the motion of glaciers. However, the pressure of subglacial water and the stage of development of cavity system are more important than the absolute volume of water stored at the bed (Iken *et al*, 1983). Pressurised water storage at the bed and separation of ice from its basement by cavitation has been attributed to cause the uplift of the Unteraargletscher as observed originally by Flotron (1973). It has also been suggested that this is the trigger for rapid 1982-1983 surging

of the Variegated Glacier, Alaska although in this case the drainage network transformed from conduit system to a linked cavity system (Kamb, 1987).

Instability of channel location at the bed is another characteristic of the subglacial drainage system. Although most glacial meltwater portals infrequently change their position at the terminus, the migration of subglacial R-channel conduits over the bed of the Gornergletscher has been noted by Collins (1979a). Reorganisation of subglacial channels may cause sudden injections of sediment into flow producing high magnitude variations in the suspended-sediment record at the outlet. Another example is the sudden release of pockets of water from many glaciers and ice-dammed lakes from a few glaciers. The former are easily monitored over the melt season while it is more difficult to monitor the latter, more irregular phenomena as their timing varies over the melt season and from one glacier to the next.

Current research in glacial hydrology and erosion processes at the bed seeks to synthesise existing knowledge about the routing of meltwaters through glaciers by developing models which will not only describe the relationships between supraglacial, englacial and subglacial routing but also simulate their changing associations over successive ablation seasons. In order to achieve this goal, discharge hydrograph records do not supply all the information required. Thus further indicators of temporally changing conditions in the subglacial environment are needed to reinforce runoff data. Two useful tracers have been used, sediment and solute loads, both of which reflect changing water routings in a glacier system.

2.3 Sediment Delivery to Meltwaters

In glacierised catchments, sediment is continuously produced at the base and margins of glaciers by glacial erosion processes. During the ablation season, when large volumes of meltwater reach the bed, weathered sediments become entrained into flows and are expelled at the snout in glacier-fed streams. The sediment characteristics of such proglacial streams give an indication not only of the routing of water through the glacier, but also the magnitude of subglacial erosion of bedrock. In some glacierised regions of the world, where relief surrounding the glaciers is steep, sediment is also deposited onto the surface as a result of subaerial and slope erosion mechanisms. This sediment becomes incorporated into the body of glacier ice and can be important in suppressing flow rates of the glacier (Drewry, 1987). Alternatively, very large avalanche deposits at the surface may locally increase glacier flow producing a "pseudo-surge" phenomenon (Hewitt, 1988). Although these surges probably locally increase erosion rates at the bed by enhancing sliding and flushing weathered sediment (Humphrey *et al*, 1986), in comparison with the annual total sediment budget from subglacial erosion, the contribution to proglacial sediment concentrations is usually rather smaller. Hence, the mechanisms of glacier erosion and the availability of sediment at the bed are important when examining flow and sediment records at the snout.

2.3.1 Weathering at the Bed

Erosion processes within the glacier environment can be classified into three groups: failure of bedrock, subglacial wear and activity on basement rock by water. However, there is no unifying theory which accounts for all methods probably because for the most part, observation of the subglacial environment is impossible. Where it has been possible to directly observe from adduction galleries the magnitude of subglacial erosion processes beneath alpine glaciers (for example, Bogen, 1989, at Jostedalsbre in Norway), the inferences are not always applicable during other times of the year or to other glaciers which have different basal characteristics, bed topographies and underlying geologies. Observations have to be made in winter when flows are minimal allowing access to the bed. At this time, erosion from glacier sliding is also at its least powerful. During summer, however, sliding increases and it is expected that erosion rates increase. Hence, to a certain extent, current theories about the nature and magnitude of subglacial erosion have to remain speculative although work by Boulton (1979) and Hallet (1979a, 1981) have made important contributions to its development.

Failure of bedrock consists of fracture of fresh rock by crushing from the overlying ice and evacuation of loosened rock into ice or water (Drewry, 1987). The loading of ice on a bedrock substratum can sometimes be sufficient to weaken the rock and make it available to removal by the glacier. Clasts within the ice are also an important crushing agent and repeated transport of debris-laden ice over a section of bedrock will progressively weaken the underlying basement. The susceptibility of bedrock to crushing depends on its physical character such as the presence of pre-existing joints and cracks, and also the nature of the applied stress from the glacier.

In this last case, the relative slopes of bedrock and surface topography will be important. Evidence of high stresses at the base comes from the existence of features such as chattermarks and gouges on recently uncovered glacier beds.

Once the bedrock structure has become weakened, it is prone to evacuation from its basement by water and ice action. General entrainment of debris into ice and water is accomplished by various methods although evacuation strictly applies to three methods of removal of fractured rock by the glacier system. Firstly, Röthlisberger and Iken (1981) suggested that evacuation of weakened and loosened bedrock fragments can be achieved by high pressure subglacial water quickly opening subglacial cavities and subsequently exposing bedrock to a heat-pump effect (Robin, 1976). This "Robin" effect produces cold patches where pressure melting occurs. These cold regions of ice have increased adhesion to the rock and with continuous ice flow, the patches remove the bedrock to which they are stuck. A secondary effect of the Robin effect is that with a local reduction in ice temperatures at these patches, the ice becomes harder and so further assists the fracturing of the bedrock. The next type of debris evacuation occurs in cavities in the lee of bed protruberances. The "hydraulic jack" effect produced by sudden increases in water pressure at the base causes fractured rock in the step precipices to break away from its parent rock as a result of increased glacier flow (Röthlisberger and Iken, 1981). The fragments then fall into the cavity and are entrained in water. Finally, some of the crushed and fractured rock never comes into contact with the ice. In this case, debris is evacuated in water flowing at the basement. However, crushing and fracturing leaves relatively large grade material so subsequent fluvial removal has to be powerful.

Bedrock abrasion is another method by which glacier ice erodes its basement. This process can be subdivided into two parts, abrasion of rock by pure ice and abrasion by impure ice containing sediment particles. For the former, it can be shown that with increased sliding velocity, overburden pressure and shear stress, the wear at the bed increases (Budd *et al*, 1979). For example, with sliding velocities between 50 and 300 metres per year, the abrasion of the granite by pure ice may be several millimetres (Budd *et al*, 1979). Softer and less resistant rock may experience greater levels of abrasive weathering by ice. The hardness of ice also changes with pressure and temperature. Localised increases in loading on the stoss side of bumps may reduce the pressure melting point of ice thus reducing ice temperatures (Robin, 1976). The ice then becomes harder, more resilient and gains an increased erosive potency. However, the abrasive power of a glacier is increased if angular rock fragments are present in the sole of the glacier. In this case the rate of bedrock wear will depend on the hardness of clast inclusion, concentration of debris in the ice, the force at which the clasts are applied to the rock and the velocity at which the glacier base is sliding.

Hallet (1979a) has suggested that the velocity of clast inclusions over bedrock is directly related to the sliding speed of the glacier irrespective of the shape of inclusion. However, Boulton (1974) proposed that although the velocity of bottom sediments in the ice is related to the glacier sliding speed, the geometry of clast is also crucial for the rate of abrasion. These two workers also disagree on the relationship between abrasion and effective force applied to clasts to erode the bed. Boulton (1974) suggested that the load on the clast in the ice pressing against the bedrock is related to the weight of clast, ice overburden pressure in a column above the clast and the pressure of water at the ice-rock interface. However, Hallet (1979a) envisages that the

effective pressure is independent of overlying ice pressure and more related to bed topography. Although both authors seem to differ in their views, they are able to practically apply their work Boulton (1974) applied his work to a variety of bedforms including corries and u-shaped valleys. Hallet (1979a) applied the results of his theory to explain how bedforms change with abrasion due to differing erosional rates depending on bed topography.

Finally, the mechanical action of water on bedrock can erode the basement substrata. This kind of erosion varies temporally since unlike the summer, water is unavailable at the base during winter. Water erodes the bed by two methods, rock cavitation at velocities greater than 12 m^{-1} and abrasion by particles entrained in the water (Drewry, 1987). The nature of the conduit is important for both mechanisms since Nye-channels will have greater wetted perimeters at the channel bed than R-channels. Cavitation occurs during fast, turbulent flows when low enough pressures within the water allow the creation of bubbles. If these bubbles grow, and move into regions of higher water pressure they burst. If this happens in close proximity to the bed then high impact forces near the rock can cause mechanical weathering of channel rock. Turbulence in the channel is also a significant factor when considering abrasion of the bed by bedload or suspended debris since increased turbulence produces increased particle velocity and erosion becomes more powerful. Clast size, hardness, concentration in the water and angle of attack of sediment at the bed also contribute to the rate of abrasion by water at the bed (Drewry, 1987).

Dissolution of rock is another way in which water can erode the bedrock. The solute load of glacier-fed streams, as indicated by electrical conductivity of meltwaters at the portal, reveals the source of water from the glacial environment (Collins, 1977).

Dissolution of bedrock and sediments in the ice is controlled by equilibria between available atmospherically derived hydrogen ions (from dissolved carbon dioxide) and oxidation of sulphides in the rock (Raiswell, 1984). Chemical activity varies during the year in response to changing water supply and delivery to glacier environments. During winter time, low flows have high conductivities since water supply is derived from stored meltwater within the glacier or groundwater flowing beneath. In both cases, the residence time of water is sufficient for chemical activity to weather the bedrock through cation exchange. During the summer however, flows are relatively dilute of solutes since surface meltwaters, comprising most of the summer flow budget, are quickly routed through englacial and subglacial conduits and do not have opportunity to exchange with sediments or bedrock sources. Subsequently, concentrations of dissolved bedrock cations in baseflows become diluted from mixing with the fast routed, solute-free water from the surface. On a diurnal scale over the summer, conductivity is inversely related to flow; at low flows solute concentrations are high and at high flows they are low. This reflects the changing water source during twenty-four hour periods. Discharge maxima are comprised of surface meltwaters which have a short residence time in the glacier. Thus, solute loads are relatively low. At night time, when discharge levels recede, the solute concentration increases because water is derived from stored aliquots near or at the bed.

This augmenting effect of solute concentrations at night time can be observed over longer periods in the summer if snowfall events cover the glacier surface and suppress ice melt (Collins, 1977). During the summer of 1975 at Gornergletscher, Switzerland, a snowfall event on the glacier reduced outwash flows for the next few days (Collins, 1977). Electrical conductivity increased suggesting that glacially derived

water was specifically being supplied from the subglacial region. It was not until several days later, when the snow layer had melted, that flows and conductivity resumed their diurnally cyclic characters.

All of these mechanisms of bedrock erosion are important to a greater or lesser degree. However, since each process is affected by different local conditions (for example, the type of underlying lithology, nature of the glacier sole - whether it is at the pressure-melting point or not, type of basal conduit or cavity system) it is difficult to quantify the relative importance of each. Consequently, when designing a model for subglacial erosion as inferred by water and sediment loads at the snout, it is appropriate to consider the different weathering types together, with the exception of chemical weathering, and not individually. Moreover, the distribution of sediment supply and entrainment of weathered basal sediments in meltwaters is critical when inferring subglacial erosion using the sediment record of a glacier-fed stream because sediment delivery depends not only on glacial erosion but also on meltwater routing configurations and their changing nature over the melt season.

2.3.2 Integration of Sediments with Meltwaters During the Ablation Season

During the melt season, weathered sediments at the glacier base are entrained into meltwaters providing discharges are powerful enough to overcome the inert weight of sediments at the bed and settling of particles once in motion (Collins, 1988). These subglacial sediments are perhaps, the most important debris source compared with sediments from englacial and subglacial regions. When the first meltwaters in spring

reach the bed, weathered sediments which have accumulated over winter and from the previous year's residue are easily entrained. After this initial flushing, sediment concentrations at the snout decline because accumulated sediment stores are flushed reducing the availability of debris for meltwater removal (Collins, 1988). Glacier erosion or removal of basal ice sediments subsequently becomes the main sediment source unless the drainage network changes location. During diurnally high flows, sediment accumulated since the previous event is evacuated. If the network is a linked-cavity configuration, only finer sediments will be removed since water fluxes may not be strong enough to entrain larger particles. Channelised flows however, are able to transport a larger range of sediments in suspension. If the rate of sediment production over the bed of a glacier is assumed to remain constant, the amount of sediment flushed at the snout will depend on the areal coverage of the bed by meltwaters.

The quantity of sediment stored at the bed reflects the rate of basal erosion by the glacier and the length of time since previous flows evacuated sediment from the bed. Hence, at the start of the melt season, large accumulations of sediment are readily entrained into flow (Hooke *et al*, 1985). Later in the melt season, when conduit flow is fully developed, suspended-sediment concentrations are lower because initial flushing of winter sediments in the spring depletes the supply (Østrem *et al*, 1967). However, sudden re-routing of englacial and subglacial conduits in the glacier can impinge on previously unworked sediment supplies (Collins, 1979a). This channel migration and tapping of new material produces raised sediment concentration levels in the outlet stream. Nevertheless, even though discharge increases through the ablation season, peaking when surface melting reaches its maximum and conduit networks are at their most efficient, exhaustion of sediment supply early on reduces subsequent sediment

discharge levels later in the season. Hence, the relationship between sediment delivery and discharge is not straightforward and warrants further discussion.

2.3.3 Discharge-Suspended-Sediment Relationships

Sediment is flushed from the glacier in two forms, bedload and suspended load. The former is conveyed along the bed of the channel by the force of water but is not suspended because particles are too large. Measurement of bedload in fluvioglacial rivers has been achieved by only a few researchers because typically fast flowing, turbulent streams reduce the durability of constructed bedload traps. Also, the sudden release of large volumes of ice- and debris-charged meltwater from large water stores within the glacier environment, may destroy such structures (Østrem, 1975). However, suspended-sediment concentrations are relatively easy to monitor and have received much attention in the past (Gurnell, 1987). Suspended-sediments can comprise between 40 and 50% of the total sediment flux from a glacier although Church and Gilbert (1975) calculated that they contributed over 80% to total sediment loads.

The relationship between suspended-sediment concentration and discharge has been one of the focuses of current research into fluvioglacial sediment transfer (Binda *et al*, 1985; Bogen, 1980; Borland, 1961; Collins, 1979a; Fenn *et al*, 1985; Mathews, 1964b; Østrem, 1975;). Østrem (1975) observed that in general, sediment transport in glacier fed streams increases with increased flows and declines with lower flows. Linear regression analysis has been applied to describe the relationship with varying levels of success to suspended-sediment and discharge data for different glacier-fed streams in

order to produce rating curves between the variables (Borland, 1961; Collins, 1979a; Østrem, 1975). This technique has been applied to discrete data sets for periods of flow varying from diurnal to annual time scales. When using regression analysis several assumptions have to be observed. Log transformations should reveal a linear rating relationship between variables and residuals should be random, have a zero average with normal distribution and constant variance and not be serially correlated (Gurnell, 1987). However, Fenn *et al* (1985) assessed the use of rating curves for data from monitoring periods of varying duration and observed that regression analysis often resulted in serial correlation of residuals which biased the rating curve. Also, due to estimations from log transformed data, predicted concentrations underestimated reality as warned by Walling (1977). Finally, observations showed that for different time periods at the same site, regression equations varied substantially from year to year and consequent predictions based on such analysis are inappropriate.

One of the reasons for the problems in developing accurate rating curves for suspended-sediment and discharge data is that the relationship exhibits hysteresis (Bogen, 1980; Collins, 1979a; Østrem, 1975). If discrete suspended-sediment and discharge observations are plotted in their time sequence, a looped relationship is often shown. This association occurs on all time scales ranging from diurnal events to annual cycles. The reason for these cyclic variations is two-fold. Firstly, the positions of sediment and discharge maxima on the hydrograph are separated by a lag. The reason for this characteristic is that on rising hydrograph limbs, comparatively more sediment is available for removal than similar flows on falling limbs; accumulated sediment from erosional processes after the previous event is immediately flushed. Thus, maximum concentrations of sediment coincide with maximum rates of increase in flow (Richards,

1984). Secondly, at the time of maximum discharge, suspended-sediment has already begun to decline with exhaustion of supply. This falling sediment limb is often more sudden than the rate of increasing concentrations. Hence, although supply of sediment to meltwaters is unlimited, transportation may become exhausted when flow exceeds present levels.

The relationship between suspended-sediment concentration and discharge is complicated by the recent history of the hydrograph and the nature of sediment supply and its exhaustion in addition to current flow levels. It has also been noted that clockwise hysteresis loops experience involutions in the record related to abrupt sediment flushing events from within the glacier (Collins, 1979a). Another problem in applying regression techniques is related to such sudden flush events from the glacier environment and their measurement. Proglacial streams are highly turbulent and are characterised by greatly varying sediment concentrations. Assuming a constant concentration through a section of the stream, temporally irregular pulse events from the glacier introduce noise into the discretely traced record. Re-entrainment of deposited proglacial channel sediments add to this noise component. This extraneous component can disguise the relationship between the variables making quantification of the relationship rather more complex than it possibly is.

Although limitations with regression analysis persist, it remains a popular tool for describing the relationship between flow and suspended-sediment in proglacial channels. Collins (1979a) established suspended-sediment concentration-discharge rating curves for rising and falling hydrograph limbs in waters draining Gornergletscher. Hammer and Smith (1983) calculated regression equations for these variables depending on whether data were collected earlier or later in the ablation season. However, for

adequate predictions of sediment transport into the future, it seems that regression analysis is an inadequate technique since it accounts for neither characteristic noise components nor the historical influences of hydrographs apparent in sediment delivery. Consequently, alternative empirical statistical techniques have been employed to address the problems which regression analysis cannot deal with.

2.4 Modelling Subglacial Erosion: Towards a Process-Orientated Approach

2.4.1 Non-regression Based Empirical Models

Regression analysis has proved to be inadequate in both long and short term modelling of the suspended-sediment-discharge relationship in proglacial channels. Even a multivariate approach adopted by Richards (1984) produced separate rating curves for different flow events in the same river during the summer. Consequently, a non-regression method was employed by Gurnell and Fenn (1984a; 1984b) to establish discharge-suspended-sediment rating curves.

Gurnell and Fenn (1984a) investigated the problem of strong serial autocorrelation in the relationship between suspended-sediment concentration and discharge by fitting a Box and Jenkins (1970) transfer function to data from the glacier de Tsidjiore Nouve. This related hourly change in suspended-sediment with the hourly change in discharge and incorporated a one hour lag (Gurnell, 1987). Data had to be prepared by filtering both data sets through a univariate time series model obtained from the independent variable (discharge), logarithmically transforming data and

calculating first differentials of both series. By examining the cross correlation function between both first differential series it was suggested that changing flows from one and two days before might influence the transfer function. A second method using cross- and autocorrelation time series analysis and a flow separation technique introduced by Collins (1979b) showed that closer association existed between subglacial flow and suspended-sediment concentration than between total or englacial flow and suspended-sediment concentration for the glacier de Tsidjiore Nouve (Gurnell and Fenn, 1984b). Therefore, it was suggested that a multivariate transfer function utilising englacial and subglacial flow components would improve prediction of sediment concentrations in this outwash channel.

Both time series modelling techniques implemented by Gurnell and Fenn (1984a; 1984b) are improvements on regression analysis methods although they both rely on long data sets for establishment of initial time series, a luxury which is not always available for the analysis of fluvioglacial characteristics. Furthermore, relationships become increasingly complex with transfer functions requiring lags, leads and rates of change of variables for data operations. Incorporating such intricate statistical relationships can cost predictive power outside of the data set especially since relationships are not always based on physical processes and so can only give approximate results. In addition, this kind of modelling technique is susceptible to sidetracking into certain limiting aspects of the methodology which do not improve overall predictions (Klemeš, 1982). Model fits may be improved without prior understanding of the related part of the processes at work. Hence, it appears reasonable that the modelling of subglacial erosion as indicated by suspended-sediment concentration and discharge is currently at the stage of needing a new framework in

which past empirically calculated relationships are developed into more process-orientated models. "True" simulation and prediction based on reality may then become possible.

2.4.2 Process-orientated Modelling

Modelling of subglacial erosion is fraught with conceptual difficulties about conditions of water routing and rates of denudation at the bed. Many different scenarios of subglacial conditions have been proposed for as many different glaciers. For example, source of sediment is a problem when designing a causal model of subglacial erosion; is the material flushed at the snout derived from subglacial erosion or does it originate from within the englacial environment as a result of subaerial erosional processes on valley sides? Also, suspended-sediment in meltwaters may not account for all transportation of weathered debris from the glacier sole since greater or lesser portions of the sediment load might be in the form of bedload traction and saltation. Furthermore, without adequate knowledge of the routing of water throughout the ablation season, the state of drainage development and characteristics of sediment removal may not be known. Since the englacial and subglacial environment are generally inaccessible for observation of such processes, inferences have to be made using empirical relationships between quality characteristics of fluvioglacial meltwaters. Thus, immediately, causal models in this field become based on inferences made from essentially untestable statistical relationships between the weathering of material in situ and its eventual removal from the glacier. However, empirical measures do not

necessarily reduce the validity of such a causal approach. If used properly, they may enhance assumptions made in the design of process-orientated models. Hence, it seems that fully- or semi-causal modelling approach is the way forward to simulation and forecasting of subglacial processes operating in an alpine glacier catchment.

Chapter 3

Study Region and Field Data Collection Sites

3.1 Regional Context

3.1.1 Introduction

The Karakoram mountain range lies north-west of the Greater Himalaya system and is bound by longitudes 72°-79° east and latitudes 34°-37° north in the Northern Areas of Pakistan (Figure 3.1). It forms a 650km arc trending from northwest to southeast on the northwestern flank of the Ladakh Himalayas. The western limits are marked by the Hindu Kush mountains while the Pamirs to the north provide a link between the Karakoram and Hindu Kush and the Kun Lun, Tian Shan and Trans Alai ranges (Tahirkheli and Jan, 1984).

The location of the Karakoram straddles four of Pakistan's political boundaries: those with India, China, the Soviet Union and Afghanistan. This is reflected in the ethno-cultural characteristics of the inhabitants. The border with India, however, is disputed and has continuously been contended since partitioning of India and Pakistan in 1947.

Although not as extensive as the Himalayas, the Karakoram contains elevation ranges as impressive. At 8611 metres above sea-level (a.s.l.), Mount Godwin Austin

FIGURE 3 1 THE KARAKORAM MOUNTAINS AND SURROUNDING RANGES
(adapted from Young, 1981)

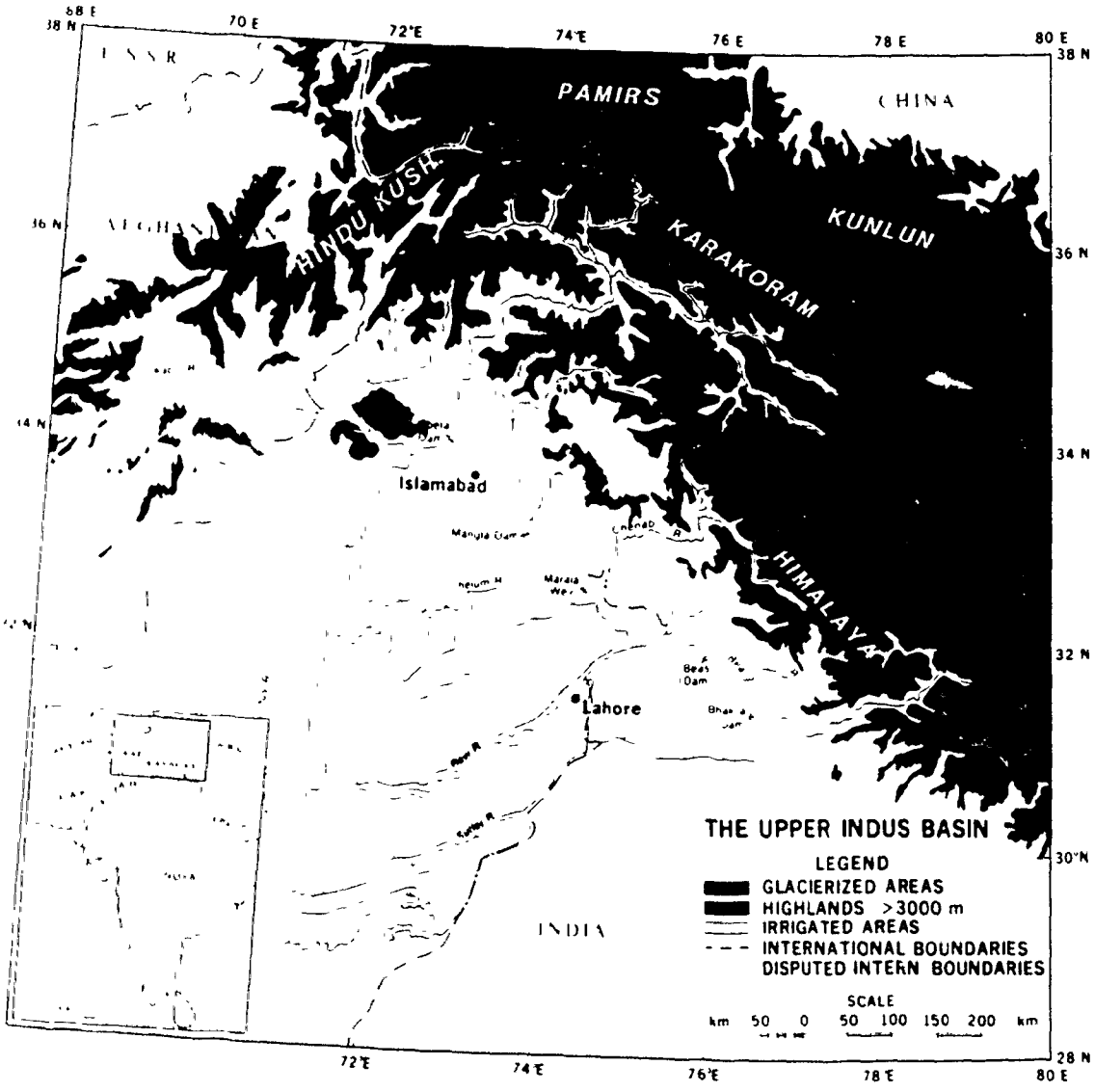

(K2) is located in the northeast of the Karakoram and is the second highest peak on earth. Not only are the mountains high, but slope gradients are among some of the greatest in the world (Goudie *et al*, 1984). Valleys are deeply incised by rivers producing altitudinal differences between valley floors and mountain summits typically in the order of 4000 to 6000m. Such elevation changes take place over relatively short horizontal distances. For example, Rakaposhi Peak rises 5940m over a distance of 11km from its Hunza Valley base at 1850m above sea level. Since these mountains rise into the mid troposphere and extend over a large area, they are effective in climatically isolating the region from southern and northern lowland air masses thus marking the transition between the Central and South Asian continental climate patterns (Wake, 1987; Goudie *et al*, 1984).

3.1.2 Climate and Weather

Between October and May, the Karakoram are heavily influenced by incident westerly air masses which at lower altitudes follow the sub-tropical westerly jet stream in the upper troposphere (Barry, 1981). In May, the jet stream over the Karakoram is weakened due to its diversion to the north. The strong westerly disturbances give way to easterly high pressure systems originating from the Tibetan Plateau (Flohn, 1968). These anticyclones persist until the jet stream regains momentum in October. However, this changing pattern in the upper atmosphere may be interrupted during the summer by destruction of Tibetan anticyclones by sub-tropical monsoons from the lowland

regions which reach the Karakoram and bring heavy rain- and snowfalls to the mountains (Finsterwalder, 1960).

The result of this general climatic trend is that from May to the end of September, warm weather persists in the mountains. Incident solar radiation facilitates melting from snow covered and glacierised areas and contributes to discharge to the rivers in the semi-arid southern lowlands. If the summer monsoons in the plains do not arrive until August or September, or are delayed over other countries in the Asian sub-continent, the Karakoram meltwater component reaching the lower Indus River becomes vitally important for agricultural, domestic and industrial purposes. In the winter time, the influx of westerly disturbances into the Karakoram often brings heavy snow and rain storms to the mountains. Thus, depleted glacial and snowpatch water stores from summer ablation become replenished during winter.

Topography not only influences broad climatic controls, but also affects local weather conditions. Orography increases precipitation with greater altitude and causes rainshadow effects on leeward sides of mountains (Barry, 1981). In addition, variable solar radiation intensities on slopes of different aspect and angle create spatially varying convective air patterns along with changing temperature lapse rates. Thus, different local climates exist within the Karakoram in response to varying topographical configurations; one valley's micro-climate may be somewhat different from adjacent valley's depending on topographical characteristics and orientation.

3.1.3 Glaciers

The Karakoram contains some of the longest glaciers in the world outside the polar regions (Goudie *et al*, 1984). One hundred are longer than 10km and fifteen are over 20km in length. Five of these exceed 50km from their accumulation head walls to snouts (Wake, 1987; Goudie *et al*, 1984). Furthermore, many of the glaciers have some of the steepest gradients in the world; accumulation areas, often above 7000m a.s.l. and with perennially sub-freezing temperatures, supply glaciers which descend to semi-arid valleys below 3000m a.s.l. (Field, 1975).

The areal extent of the Upper Indus Basin (UIB) is in the order of 250,000km^2. Total permanent glacier coverage of the Karakoram is approximately 15,000km^2. This amounts to 15% glacierisation for the main stem of the Indus above Attock. At the beginning of the summer ablation season, areal snowcoverage to the north of Tarbela Dam (located in the plains several kilometres north of Attock) is commonly greater than 70% (Hewitt, 1985). Hence, snow and ice meltwaters make an important contribution to annual flow in the Indus River.

3.1.4 Hydrology

Water supply to Pakistan is primarily delivered by the Indus River system which rises in northern India and Xijang (Tibet) and runs the length of Pakistan (3200km) before reaching the Arabian Sea. The five main tributaries of the Indus basin are the Kabul, Jhelum, Chenab, Ravi and Sutlej rivers. Approximately 70% of annual discharge

in the Indus is derived from snow and ice melt (Tarar, 1982). However, the Indus Water Treaty (1960) prevents Pakistan's use of snowmelt runoff from the heads of the Ravi and Sutlej since these supplies are allocated to India.

The Karakoram is almost entirely contained within the UIB. The heavily glacierised catchment area comprises 15% of the area of the UIB and contributes 25% of annual flows in the Indus (Goudie *et al*, 1984). The water source in this region is snow and ice melt from the glaciers and snow covered areas. Hence, in response to the climatic influences, strong seasonal flows characterise the annual river regime in the upper Indus with increased and decreased discharges during summer ablation and winter accumulation seasons respectively. Hydrograph records taken at selected Water and Power Development Authority (WAPDA) gauging sites in the lower UIB show that flows begin to rise between the end of March and beginning of April, as winter snow accumulations start to melt. During the summer, the increased glacier ice melt component produces peak flows in the Indus River. At stations in the upper portions of the UIB, snowmelt contributions do not increase trunk flows until May with peak flows from glacial melt not reaching arterial rivers until July and August. This is because temperature drops with increasing altitude. Thus, at higher elevations, temperatures do not increase sufficiently to generate snow and ice melt until well into the ablation season.

3.1.5 Glacier Erosion Systems

Erosion of the Karakoram landscape depends upon the continual tectonic uplift of the mountains and spatially varying lithology (Hewitt, 1989). It has been suggested that characteristic geomorphic processes and landforms can be classified according to topoclimatic conditions at different identifiable altitude bands (Hewitt, 1989). Ferguson (1984) has described the topographical link between erosional processes in regions of mountain systems. Steep slopes associated with high relief produce rapid mass movement events resulting in deposition in the lower slopes. High relief also increases precipitation at altitude due to orographic effects and leads to increased fluvial erosion on slopes. At altitudes above 4800m a.s.l. in the Karakoram, cold temperatures facilitate precipitation in the form of snowfall which feed glaciers. Thus, valley bottom and mountain-side erosional processes are linked by the presence of glaciers.

With such extensive glacierisation, the Karakoram is subject to intense glacier erosional forces. Weathering of underlying bedrock and sediments is achieved by extremely powerful abrasive, crushing and water erosion processes. With steep longitudinal slope gradients and large availability of subglacial and englacial meltwaters during summer, seasonal sliding of glaciers produces some very high erosion rates (Goudie *et al*, 1984). Glacial erosion is added to by massive ice overburden pressures; thicknesses can reach several hundreds of metres in the ablation area where sliding is active (Zhi-Bin *et al*, 1984).

The evidence for intense glacial erosion in the Karakoram is apparent around all glacier margins, along glacier-fed tributary channels and around the main arterial rivers which dissect the mountains. Lateral, medial and terminal moraines are composed

of enormous volumes of glacially-eroded sediments. In addition, sediments are deposited along the flood plains of proglacial rivers at times of high flow. Direct evidence of glacial erosion can be examined where recent deglaciated sections of bedrock exhibit polished surfaces, for example, Passu Glacier (Goudie *et al*, 1984). In all cases, locally deposited debris becomes the source for subsequent re-working by sudden inundations as a result of the release of large volumes of stored water from within glacier systems (Hewitt, 1982).

Perhaps the most obvious proof of active glacier erosion processes in the Karakoram is the highly concentrated suspended-sediment loads in glacier-fed streams during the summer. Although bedload and dissolved solid transportation is apparent, suspended-sediment probably contributes the majority of sediment load in the main trunk rivers (Ferguson, 1984).

Measurement of suspended-sediment in rivers may be the best way to investigate erosional rates over large, topographically non-uniform areas. For this reason, WAPDA initiated a sediment monitoring programme to examine fluvial transport rates of eroded debris from the Karakoram. The level of importance of this programme was raised when it was discovered that high sediment yields from the Indus River are responsible for filling the 84km long lake behind the Tarbella Dam. The Indus River annually discharges 500 million tonnes of sediment (both solid and dissolved) into the Arabian Sea (Meybeck, 1976). Most of this load has its source in the Karakoram and Hindu Kush (Ferguson *et al*, 1984). In 1980, the International Karakoram Project (IKP) supplemented WAPDA investigations by undertaking detailed suspended-sediment concentration measurements in the Hunza basin (Miller, 1984). WAPDA (1976) established that the annual sediment yield of the Hunza River between 1966 and 1975

was 4800 tonnes per square kilometre (equivalent to a lowering of the surface by 1.8mm, Ferguson, 1984). Periodicity in sediment delivery from glacial sources was e.. nined by IKP members in detail to investigate sediment source and short-term fluctuations in its record (Ferguson, 1984; Ferguson *et al*, 1984).

Since the flow regimes of rivers in the Karakoram are dominated by glaciers, sediment loads are highly seasonal in their temporal variability, typically with over 90% of annual sediment fluxes occurring during the four months from June to September (Ferguson, 1984). The seasonality of sediment concentrations in glacier-fed rivers is also shown by hysteresis in the relationship between suspended-sediment and discharge as indicated, for example, by Hunza River data in 1973 (Ferguson, 1984). However, varying proportions of suspended-sediment are not derived directly from subglacial erosion processes during the summer. Slope processes on surrounding valley sides contribute sediment to sub-, en- and supraglacial drainage networks in addition to supplying outwash streams in proglacial environments. This sediment input to the glacier hydrologic system is probably more important in the Karakoram than in other glacierised alpine regions of the world since slope gradients are steep and rock avalanching is commonplace during the summer. Nevertheless, suspended-sediments in glacier-fed streams during the summer ablation season will also be produced from subglacial weathering which increases at this time as glacier sliding is enhanced. Hence, during the 1987 and 1988 ablation seasons, fluvioglacial meltwater sediment and solute characteristics were measured in outwash rivers draining two glaciers in the Karakoram.

Figure 3.2 The Hunza Valley, N. Pakistan. (Adapted from Collins, Unpubl.)

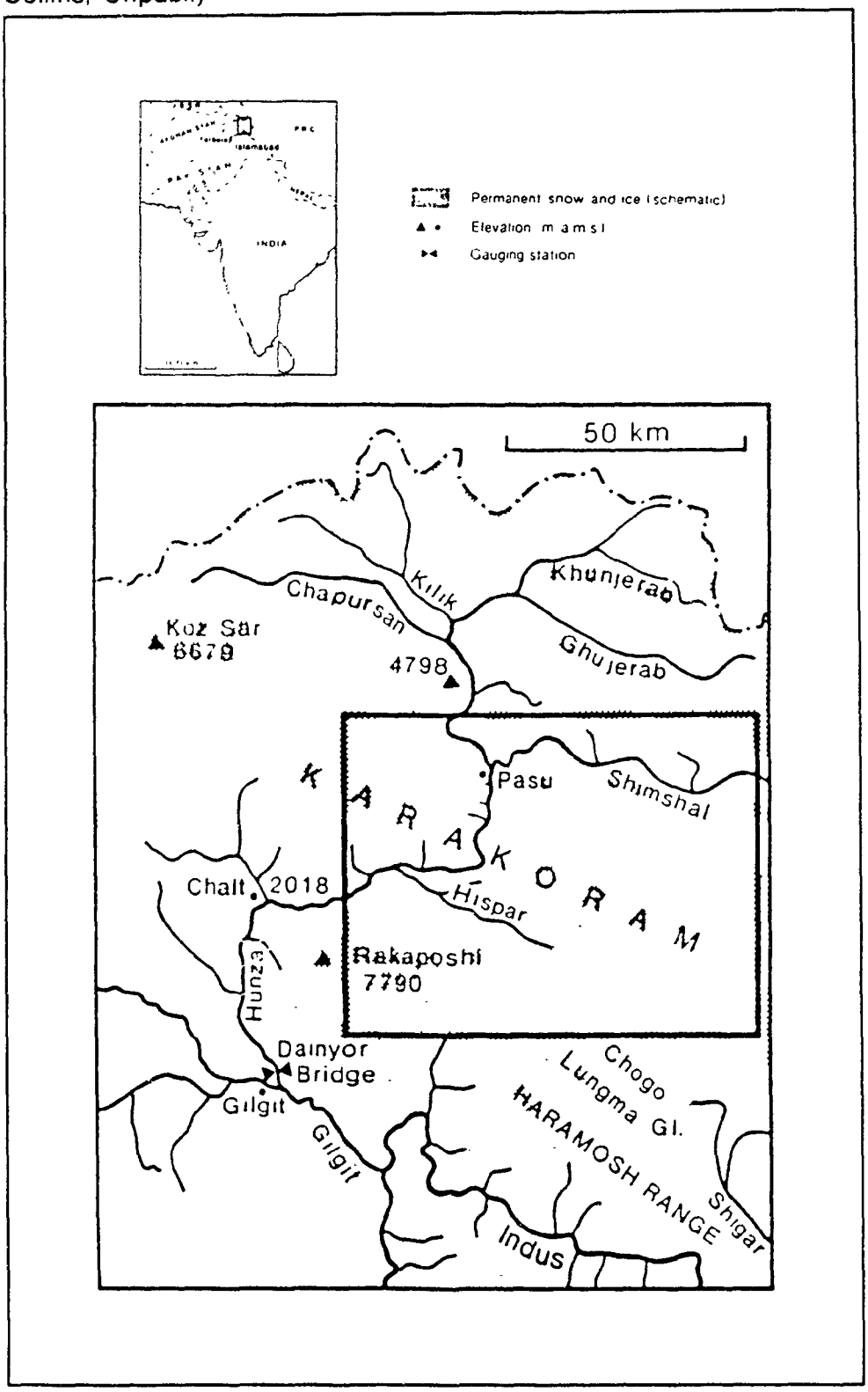

Figure 3.3 The central Hunza Valley. (Adapted from Collins, Unpubl.)

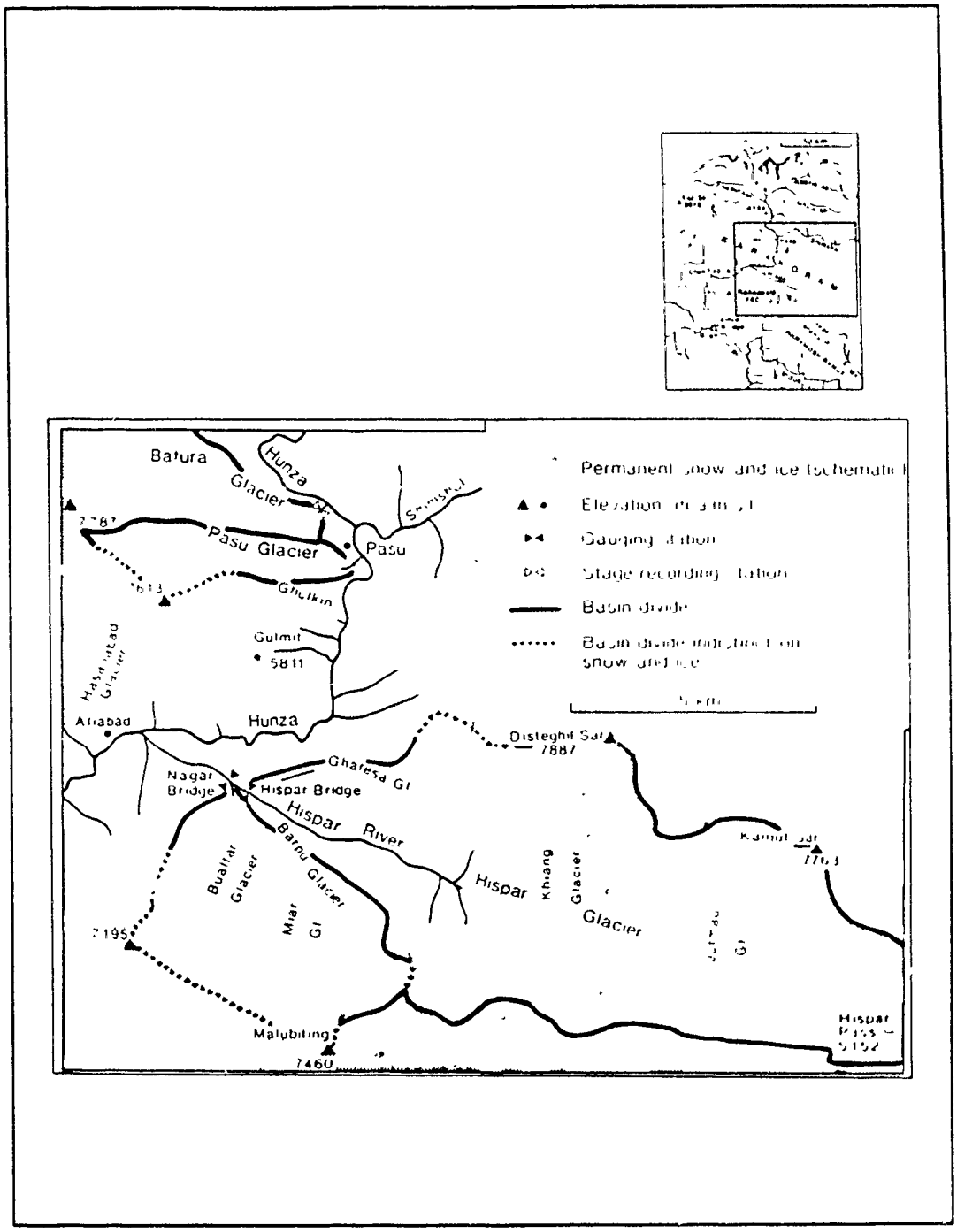

3.2 Specific Location of Sites

The Hunza Valley in the upper Indus catchment lies northeast of Gilgit in the western Karakoram (Figure 3.2). A relatively large proportion of its 13,000km^2 area is covered with glaciers. The largest glaciers in the Hunza Valley are located in the middle stretches of its course (Figure 3.3). The Batura and Hispar Glaciers at 59 and 62km are the longest in this region (48% and 55% glacierisation respectively for each basin).

Flow measurements in the UIB by WAPDA at Dainyor Bridge (upstream of the confluence of the Hunza River with the Gilgit River) and Partab Bridge (below the confluence of the Gilgit River and Indus River) show that the Hunza contributes 22% of the annual flow to the upper Indus at Partab Bridge (Ferguson, 1984). This contribution is spectacular considering the Hunza basin only occupies 9% of the total Karakoram area. Furthermore, 39% of total sediment loads at Partab Bridge originate in the Hunza Valley. Hence, the Hunza Valley makes an important contribution to annual flows in the Indus River.

3.2.1 Bualtar Glacier

The Bualtar (or Hopar) Glacier (74°45' east, 36°08' north) is a temperate alpine glacier and forms the final contribution to the Barpu-Miar-Sumaiyar Bar system (Figure 3.4). The glacier is situated in a tributary sub-basin of the Hispar River catchment which joins the left bank of the Hunza River at longitude 74°38' east, latitude 36°18'

Figure 3.4 The Bualtar Glacier and Barpu Glacier System. (Adapted from Collins, Unpubl.)

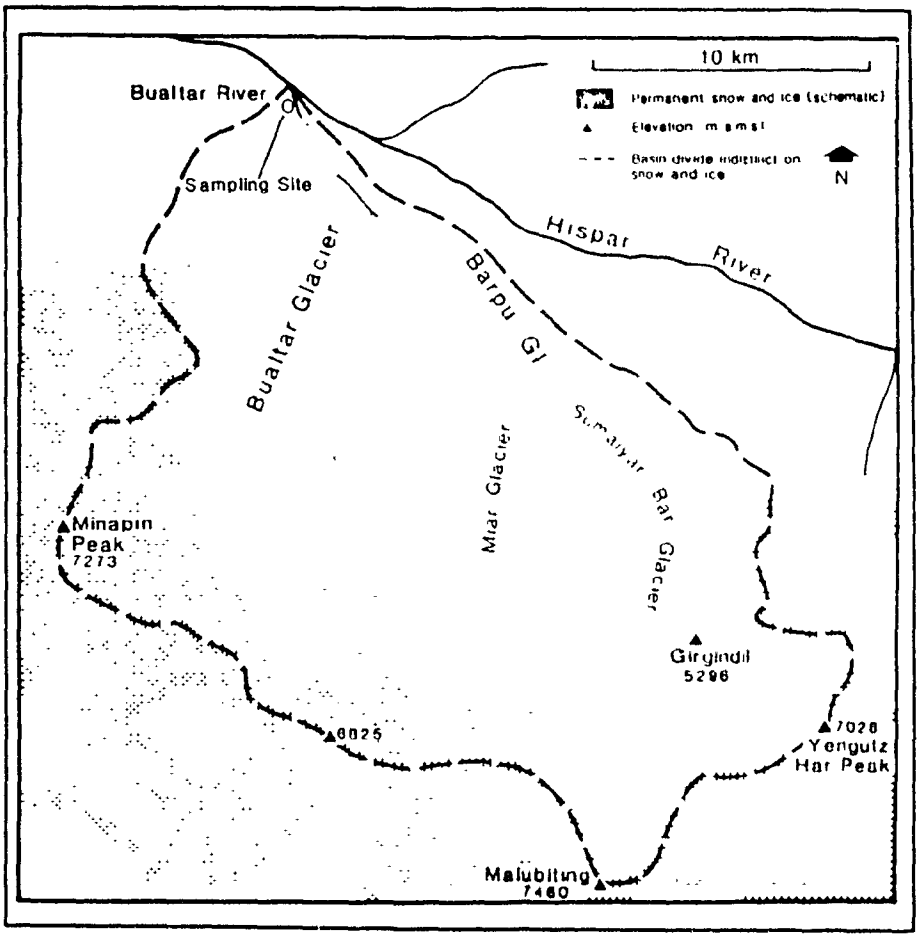

north. It descends 20km north northeast from the Rakaposhi Range and has an areal coverage of approximately 80km^2 which translates to a basin glacierisation of about 20%. The average width of glacier is about 1km and the maximum glacier elevation is at 7275m a.s.l. with the terminus at about 2438m a.s.l.. The Bualtar ablation area comprises 28% of the total glacial area with the equilibrium line at 4268m a.s.l. (statistics are taken from the Pakistan Glacier Inventory).

The geology of the bedrock beneath most of the Bualtar Glacier is the Chalt formation which is comprised of green sandstone, arenaceous quartzite, green schists and beds of crystalline limestone. The lower ablation zone is underlain by the Dumordo formation comprising marble, gneiss and micaschist.

Steepest slopes over the Bualtar Glacier occur above the equilibrium line where the glacier ascends into the Bagrot and Phuparash groups of the Rakaposhi massif. The accumulation zone experiences frequent snow avalanching throughout the year similar to many other Karakoram glaciers. It is probable that temperatures do not rise above freezing for most of the year in the upper accumulation zone. Between approximately 4000 and 5000m a.s.l., low winter temperatures are replaced by warmer, humid weather in the summer (Hewitt, 1989). However, since the aspect is predominantly northeast facing, the summer season is shorter than for glaciers with south facing orientations. Hence, persistence of snow cover in this catchment is prolonged compared with south facing glaciers.

In the ablation zone, below 4268m a.s.l., slopes are gentler with gradients less than the average (15%) for the entire glacier. The surrounding steep, unstable valley sides exhibit active slope processes. Rock avalanches and large landslides have deposited a thick debris layer on the Bualtar surface. At least one such event has

initiated localised glacier surging (Hewitt, 1988). The intense buckling of ice in the mid-ablation zone section is probably a result of such "pseudo-surging" behaviour. The Bualtar ablation zone moves, on average, at 0.6 to 0.8m day^{-1} during late winter/spring seasons although locally increased movements resulting from massive deposition of landslide material on the surface are of the order of 7m day^{-1} (Hewitt, 1988).

Air temperatures in this section of the glacier are warm during summer although its north northeast aspect potentially reduces the length of melt season. In winter, temperatures drop and moderate snowfall covers the ground for between 3 and 8 months of the year.

The Barpu Glacier system converges on the Bualtar Glacier two thirds of the way down its ablation zone. At the intersection of these glaciers there is a small seasonal outwash channel from the Barpu system which presumably joins summer subglacial meltwater flows beneath the Bualtar. The Bualtar snout is a further 5km downstream from the confluence with the Barpu Glacier.

The Bualtar River drains into the Hispar River at approximately 1km below the Bualtar Glacier terminus (about 25km downstream from the Hispar Glacier snout). Although the proglacial river issues from one portal during each ablation season, it may switch positions from the right to the left side of the terminus from year to year. In addition, examination of summer meltwater flows from the Bualtar Glacier is complicated by inputs to the glacier derived from snow and ice ablation from the Barpu Glacier system. Groundwater flows from around and beneath the glacier are envisaged to be negligible during the summer ablation season compared with snowmelt and glacier ice melt.

Suspended-sediment in the Bualtar River is derived not only from the subglacial environments beneath the Bualtar Glacier and Barpu system glaciers but also from active slope processes operating in this valley. Unstable valley sides are frequently subject to rock avalanching which deposit sediments on glacier surfaces (Hewitt, 1988) and below the Glacier terminus where it becomes re-entrained by river water. Hence, suspended-sediment concentration in the Bualtar River partially will be composed of non-glacially eroded sources.

3.2.2 Batura Glacier

The Batura Glacier is located at longitude 74°35' east, latitude 36°34' north on the right bank of the Hunza River (Figure 3.5). The basin has an area of 687km^2 of which 332km^2 is covered by glacier ice (48% catchment glacierisation). The highest point in the basin is at 7795m a.s.l. in the Batura Muztagh, and the lowest point is at about 2740m a.s.l. at the snout. The Batura Glacier itself occupies 285km^2 or 41% of the catchment. The remaining 7% glacierised area is from smaller tributary glaciers. The Batura Glacier is 59.2km long and has an average width of 1.8km. 51% of the glacier occupies the accumulation zone while the remaining 49% comprises the ablation zone (Batura Glacier Investigation Group, 1979).

The glacier trends in an east-southeasterly direction. Hence, because of its aspect, duration of ablation seasons is longer for the Batura glacier than north facing glaciers. The transient snowline fluctuates between 4700 and 5300m a.s.l. (Batura Glacier Investigation Group, 1979). Gravimetric techniques reveal that the Batura has

FIGURE 3.5 THE BATURA GLACIER

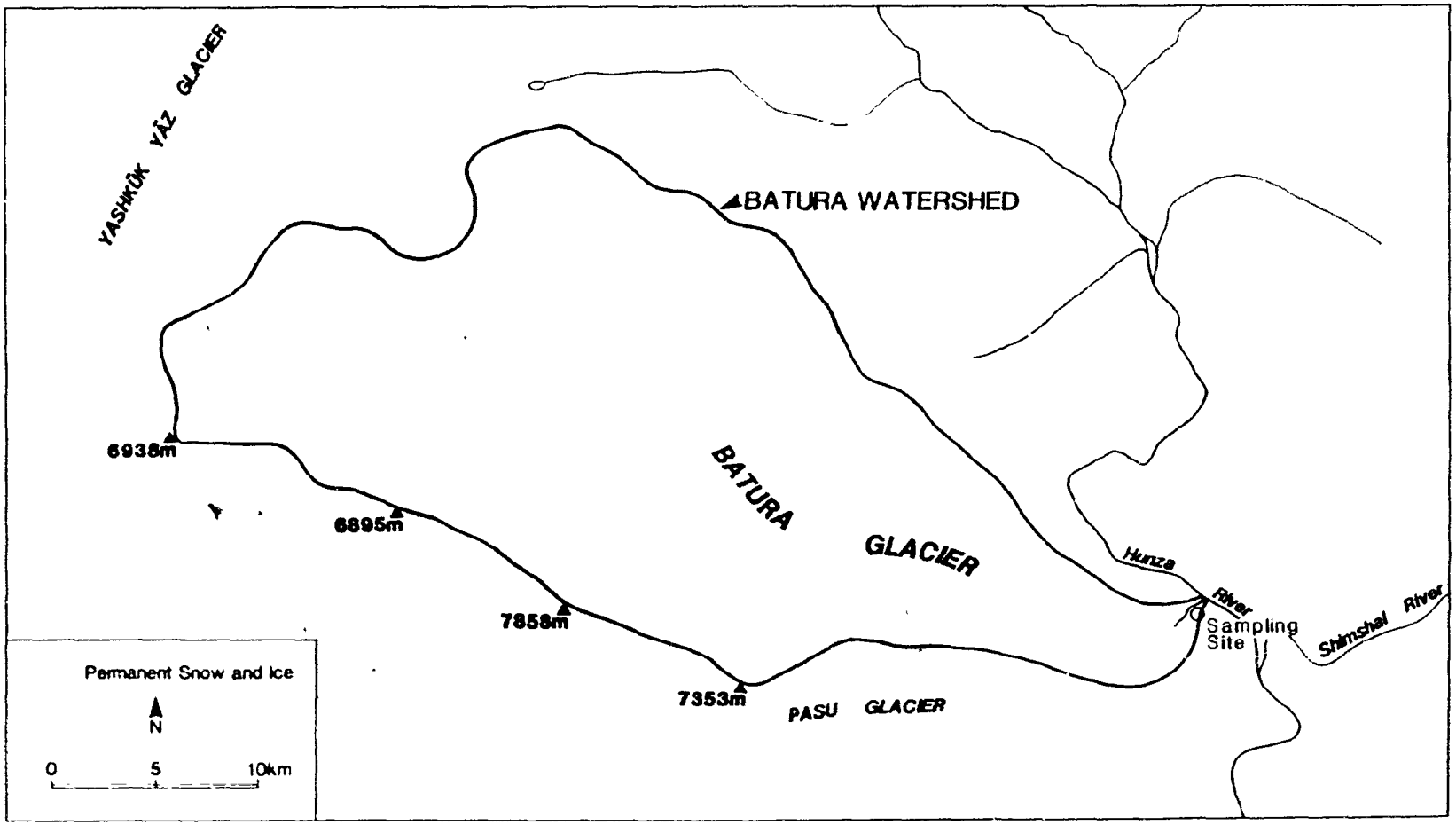

an average depth of 82m with a deepest measured thickness of 432m at 20km above the terminus. From 1974 to 1975, average ice velocity was about $35ma^{-1}$ in the snout region with maximum summer ice flows of the order of $520ma^{-1}$ 20km above the snout (Batura Glacier Investigation Group, 1979).

The geology of the Batura Glacier is varied. In the lower regions it is underlain by Skarmi limestone and Ghujhal dolomite. This gives way to Pasu slates in the lower middle portion. The geology of the upper regions consist of a granodiorite basement.

Generally, the surface of the Batura Glacier is debris free. It is only in the lower 3km that debris concentrations on the surface increase. Two thirds of the snout area itself is covered in moraine and small surface lakes are common. It is probable that these sediments in the lower regions probably influence sediment characteristics of the glacial outwash channel which meets the Hunza River 2.5km below the Batura terminus.

Since the glacier is so large it is difficult to investigate the nature of groundwater flows which join the system. It seems reasonable to expect such flows exist since flow in the Batura River does not cease during winter (Batura Glacier Investigation Group, 1979). However, the relative contributions to total annual flow of extraneous groundwater flows (for example, valley springs on lower valley slopes) and the winter release of stored summer waters is unknown. During summer it is assumed that snow and ice meltwater flows overshadow groundwater runoff components.

Chapter Four

Field Data Collection Techniques

4.1 Bualtar Glacier, 1987

4.1.1 Discharge Measur ment

The Bualtar glacier-fed river is extremely turbulent and fast flowing during the summer ablation season. Furthermore, it is highly charged with both suspended-sediment and bedload material at this time making precise, discrete measurement of discharge very difficult. Even continuous, direct measurement of changing water level (stage) using fixed depth transducers is problematical since there are few places along the river bank from which to firmly anchor a submerged probe. The reason for this is that the outwash plain is strewn with sediments ranging from fines to large boulders several metres in diameter. Consequently, discharge in the outflow stream from the Bualtar Glacier had to be measured indirectly using a subtraction technique of flow data from a monitoring station upstream and downstream of the confluence of the Bualtar river with the Hispar river.

Hispar Bridge and Nagar Bridge stream-gauging sites are respectively located on the Hispar River upstream and downstream of the confluence of the Bualtar River with the Hispar River (Figure 3.3). At both sites, on each hour of the day from

08:00hrs to 16:00hrs, WAPDA employees record the changing river water level against previously installed stage boards. This continues all year except for public and religious holidays. In addition to stage observations, WAPDA has undertaken a stream discharge gauging programme during the summer on selected rivers in the Karakoram mountains.

At both Hispar and Nagar Bridges, flow is measured during the summer season at different times of the day when the Hispar river is at different levels of flow. River stage is also recorded at the time of gauging. Thus, it is possible to associate different river discharges with different stage levels. Flow velocity varies across the river so in order to calculate discharge at each site it is necessary to measure stream velocities at different positions in the profile and calculate the associated cross-sectional area. This is undertaken by lowering a flowmeter into the water from each bridge at regular intervals across the river (Lewin, 1981; Shaw, 1984). At each interval, where possible, water velocity is measured at 0.2x, 0.6x and 0.8x the river depth. The area of each segment is known since water depth at each interval and horizontal spacing between intervals are recorded during gauging. Hence, for each segment, discharge is the product of segmental area and average velocity at that position. Total river discharge for each site is obtained by summing all discharges of segments across the river. Although the time taken to gauge the Hispar river at both sites is approximately half an hour, it is assumed that the calculated discharge represents the instantaneous flow on the hour when measurement began.

Since flow in glacier-fed streams is known to vary over twenty-four hour periods in the summer, it is important that such discharge measurements are conducted at different times during periods of varying flow levels. It is then possible to calibrate gauged flows at a variety of times during different days with continuously monitored

WAPDA stage readings taken at the same time. However, a major problem with this method of water flow measurement undertaken by WAPDA is that no measurements are taken during the evening and at night when the majority of meltwater from the Hispar and Bualtar Glaciers flows into the Hunza River. Hence, a supplementary measurement programme was initiated to monitor flow over consecutive 24hour cycles during the 1987 ablation season from 30 July to 27 August.

Druck pressure transducers were installed in the Hispar river beneath Hispar and Nagar Bridges at sites on the river of least turbulence. Both probes were firmly attached to temporary solid Dexian angle-iron structures at positions in the river's vertical profiles where it was probable that the transducers would neither emerge from the water as diurnal flows subsided nor would become buried beneath deposited sediment from the river. The probes were connected to Technolog Tinyloggers which are solid state, battery powered digital loggers. The transducers measured the changing overlying pressure head of water and converted this reading to an electrical signal which was recorded by the loggers. The loggers are calibrated to transform this signal into centimetres above an arbitrary preset value.

Digital recorders were programmed to log varying river stage every fifteen minutes beginning on the hour. Each fifteen minute reading is an averaged stage data value calculated from the measured pressure head during the ten seconds prior to the programmed on-minute reading. This accounts for short-term fluctuations in water level. The reason for such frequent recording is that both Bualtar and Hispar glacier-fed streams are highly turbulent producing a rapidly fluctuating noise component. By taking the mean of observations around each hour, a more representative hourly stage record is obtained. Care was taken that hourly WAPDA stage readings coincided with the

automatically monitored stage from the transducers and loggers. Also, if the probes had to be re-sited as a result of siltation or emergence, the time of repositioning and corresponding logged stage was recorded together with the position of the water level on the stage board. Time-checking of instruments was undertaken each day in order to ensure that the equipment functioned properly and that probes did not become buried or emerge from the water. The water level on the stage board was also recorded to provide a check on WAPDA observations.

At the end of the field season, data loggers were returned to the laboratory where recorded stage data were downloaded onto computer. Hourly stage data for both sites was calculated from the mean of the five, fifteen minute observations around each hour: those two at thirty and fifteen minutes before the hour, the observation on the hour, and the two readings after at quarter and half past the hour. Although this produces a weighted mean, it is assumed that the result is representative of stage for the hour.

Calculation of discharge on the Hispar River at Hispar and Nagar Bridges was accomplished using all three types of data described above. Rating equations were devised by implementing the sums of least squares linear regression technique to relate WAPDA stage records to associated gauged discharge data. The relative errors involved using this calibration method for different segments of paired stage and discharge data were examined using the root mean square error technique. Consequently, it was then possible to choose optimum fitting calibration curves. Since this data only described flow conditions in the Hispar river during daytime, rating equations were calculated to relate discrete hourly pressure transducer data with WAPDA stage records. The continuously logged stage record had to be prepared in order to assign default values

to missing data and remove sudden 'jumps' in the record caused by repositioning of probes in the river. This latter problem was overcome by comparing paired stage values, consisting of WAPDA stage data, with automatically logged data. Once this had been done it was possible to calibrate digitally recorded data with WAPDA stage records and then convert the outcome to discharge data using the calibration equations calculated for the WAPDA stage and gauging data.

The record of discrete, instantaneous discharge data for the Bualtar River during the monitoring period in 1987 was calculated by subtraction of hourly simultaneous discharge data at Hispar Bridge from that of Nagar Bridge on the Hispar River. The data were smoothed through a running average filter to remove biases introduced to the time series by occasional non-synchronous paired values in the Nagar and Hispar Bridge records.

4.1.2 Suspended-Sediment Concentration Measurement

Turbulence in the Bualtar River during the summer ablation season produces well mixed suspended-sediment concentrations. For this reason it was possible to directly measure concentrations in the river (Østrem *et al*, 1971). A site was chosen 0.5km downstream from the glacier portal on the left bank of the Bualtar River where it was safe to install a North Hants Engineering Company automatic water sampler. Water samples were unable to be taker nearer the glacier snout since the river bank was not well defined and any installations would have been washed away by diurnal flood events. One problem with the site was that in-channel sediments were not always

comprised of glacially eroded material. Some sediments were derived from re-worked fluvioglacial sediment deposits adjacent to the outwash river course. However, compared with sub- and englacially derived material, this source of debris was assumed to have a limited influence on suspended-sediment concentrations since late summer flows were receding and flow energy available for re-working of peripheral outwash sediments was declining.

Monitoring of suspended-sediment concentration took place from 30 July to 27 August. The automatic liquid sampler was programmed to collect hourly samples of water, each sample being taken on the hour. Samples were collected in separate flasks which were connected to the river by individual polythene hoses, the nozzles of which were submerged in river water At the start of a twenty-four hour period flasks were evacuated of air using a stirrup pump and temporarily sealed by a trigger-release mechanism. A mechanically sprung clock arm released each trigger on the hour during twenty-four hour cycles thus releasing bottle vacuums (500 mmHg) and sucking water from the river. Each sample took between 100 to 300 ml over approximately five seconds. Sample volumes less than 100 ml were discarded. At the end of each day's cycle, sample volumes were measured and the collected aliquots were filtered under pressure through pre-weighed Whatman Number One filter papers (initial pore penetration size 2 μm). Flasks were rinsed and re-attached to their hoses ready for the next 24 hour cycle. Each hose was also rinsed to remove residual particles from the tubing. After filtration, sediment-laden filter papers were sealed in plastic bags and returned to the laboratory for analysis.

Problems arose during the course of sampling as a result of defects with the automatic sampler. Unfortunately the trigger arm was faulty on several occasions

resulting in loss of samples. Also, the Bualtar River has an exceptionally high concentration of suspended-sediment during the summer. Occasionally sediment became lodged in the tubing during the intake of water from the river thus blocking the hose and preventing water and sediment from entering flasks. Samples were eitner totally lost or the collected water parcel had an un-representatively low concentration because sediment in the sampled water was unable to pass the obstruction even though water reached the bottle. To reduce these errors and biases during the season, the diurnal cycle was rotated so that each bottle with associated trigger and hose did not sample on the same hour over consecutive days.

In the laboratory, sediment-laden filter papers were dried for four days and weighed on an infra-red heating balance. Suspended-sediment concentration for each sample was calculated by subtracting the weight of each pre-weighed filter paper from the weight of its dried, sediment-laden state and dividing by the volume of sample collected:

$$S_c = \frac{[(WS-FPW)x1000]}{V} \text{ mg } l^{-1} \qquad (4.1)$$

where S_c is the suspended-sediment concentration, WS is the weight of the sediment-laden filter paper in grammes, FPW is the weight of the pre-weighed filter paper in grammes and V is the volume of sample in litres.

Calculated concentration data were transferred to a computer format for further analysis with discharge. Unusually high or low outliers were removed from the sediment concentration time series when it was clear that they were not surrounded by discrete rising and falling sub-series. However, this was done with knowledge of the

accompanying discharge and electrical conductivity records which indicate timings of sudden pulse events.

4.1.3 Electrical Conductivity Measurement

Electrical conductivity, a surrogate indicator of total dissolved solids in river water, was measured at the same site as suspended-sediment concentration from 30 July to 27 August. A robust shielded cell was anchored to an installed angle-iron frame so that the probe remained immersed in water at a turbulent, well aerated section of the stream. The cell was connected to a Walden Precision Apparatus CM-25 meter and the signal traced onto a connected analogue Rustrak chart recorder every two seconds. The cell constant for the conductivity cell was known to be unity from previous tests. Since it was not an objective to compare electrical conductivity between different sites, standardisation to 25°C of the traced reading was unnecessary. Also, standardisation techniques have been shown to be inappropriate for glacial meltwaters (Collins, 1977). The reason for this is that conversion of data to 25°C from temperatures near freezing introduces high percentage errors which overshadow measurement errors.

The chart recorder and meter were timechecked each day and the battery level was inspected to ensure that power was not fading. The cell was also examined each day to safeguard against blockage between the conductor plates by lodged suspended debris. At the end of the season, the charts were returned to the laboratory where their traces were transferred to computer with the aid of a digitising package.

4.2 Batura Glacier, 1988

4.2.1 Stage Measurement

In 1988, WAPDA did not undertake a streamflow gauging programme on the outwash river from the Batura Glacier. Furthermore, continual daytime observations of water level were not taken. However, changing stage was continuously monitored from 4 August to 14 August in 1988 using a Druck pressure transducer and Technolog Tinylog.

Stage was measured 1.5km downstream from the glacier portal on the right bank of the river along a section which had been reinforced with steel mesh and boulders (Figure 3.5). This proved to be an ideal site since although the river was turbulent, relative safety for instruments was provided by steps in the reinforcement structure. Furthermore, the surrounding outwash plain, like that below the Bualtar terminus, is covered with moraines and fluvioglacial debris making emplacement of equipment along most of the river bank unsafe. Following installation of the Druck probe, similar methods were used to monitor stage and the same precautionary steps were taken as those for the Bualtar river (section 4.1.1). Timechecking was frequently undertaken and included water level recording against the stage board to check that the logger and transducer remained precise throughout the duration of monitoring. At the end of the season, the logger was returned to the laboratory where stored data were downloaded to computer. Fifteen minute readings were averaged to hourly values, missing data were assigned defaults and 'jumps' in data were removed by comparing paired observations of automatically logged data with stage board records. It was not

necessary to filter the final hourly time series since data were of a high quality without bias.

4.2.2 Suspended-Sediment Concentration Measurement

The method and type of equipment employed to calculate hourly suspended-sediment concentration was the same as that at Bualtar in 1987 (section 4.1.2). At the Batura River in 1988, it was not possible to sample river water at the same site as stage measurements were taken. This was because hosing was not long enough to reach the river from the automatic sampler placed on the step. Hence, a location was chosen 25m downstream from the stage monitoring site where the sampler would safely reach the water without too much threat of being washed away. Unfortunately, the sample record was incomplete because major problems were encountered with the clock and trigger mechanism. Thus, although sampling was undertaken from 16 July to 14 August, the record is intermittent and only records from 4 August to 14 August are used since this segment coincides with stage data.

Filtration of samples was undertaken in the field and processing of filter papers was done in the laboratory. Data were transferred to computer and outliers removed with a knowledge of stage and electrical conductivity.

4.2.3 Electrical Conductivity Measurement

Electrical conductivity was measured at the same location as stage using similar equipment which was employed at the Bualtar River in 1987 (section 4.1.3). The cell was attached to the river bank reinforcement structure and care was taken to ensure that the conductor plates became neither clogged with sediment nor emerged from the water at low flows. The Rustrak charts containing the recorded conductivity data were returned to the laboratory where they were digitised onto computer.

The record of conductivity begins on 20 July and ends on 14 August. However, for hydrological interpretation with stage and suspended-sediment concentration data, only data contained within the segment from 4 August to the 14 August are useful.

Chapter Five

Interpretation of Results

5.1 Bualtar 1987

5.1.1 Discharge

Discharge in the Bualtar River from 30 July to 27 August, 1987 is shown in Figure 5.1. The record is broken on two occasions, from 1 August to 2 August and briefly on 9 August, when the data logger at Hispar Bridge was inoperative. Data reveal a changing cyclic pattern which is compri- of two parts, a diurnally fluctuating component superimposed on a base flow.

The base flow component is marked by fal.ng discharge from 30 July to 4 August when a minimum flow of 73.8 m^3s^{-1} was recorded at 08:00hrs. This is in response to cooler weather conditions experienced during the period. Discharges sharply increase over the next seven days as cloud cover is reduced and temperatures increase. Rates of increase of discharge are relatively reduced for the following thirteen days because sunny days, yielding high rates of incoming solar radiation, are interspersed with cloudy days with reduced solar energy. On 17 August discharge begins to decline until 19 August when rapidly increasing flows continue over the following day to produce a peak discharge for the measurement period of 164.4 m^3s^{-1} at 17:00hrs on 20

Figure 5.1 Instantaneous discharge in the Bualtar River, 1987.

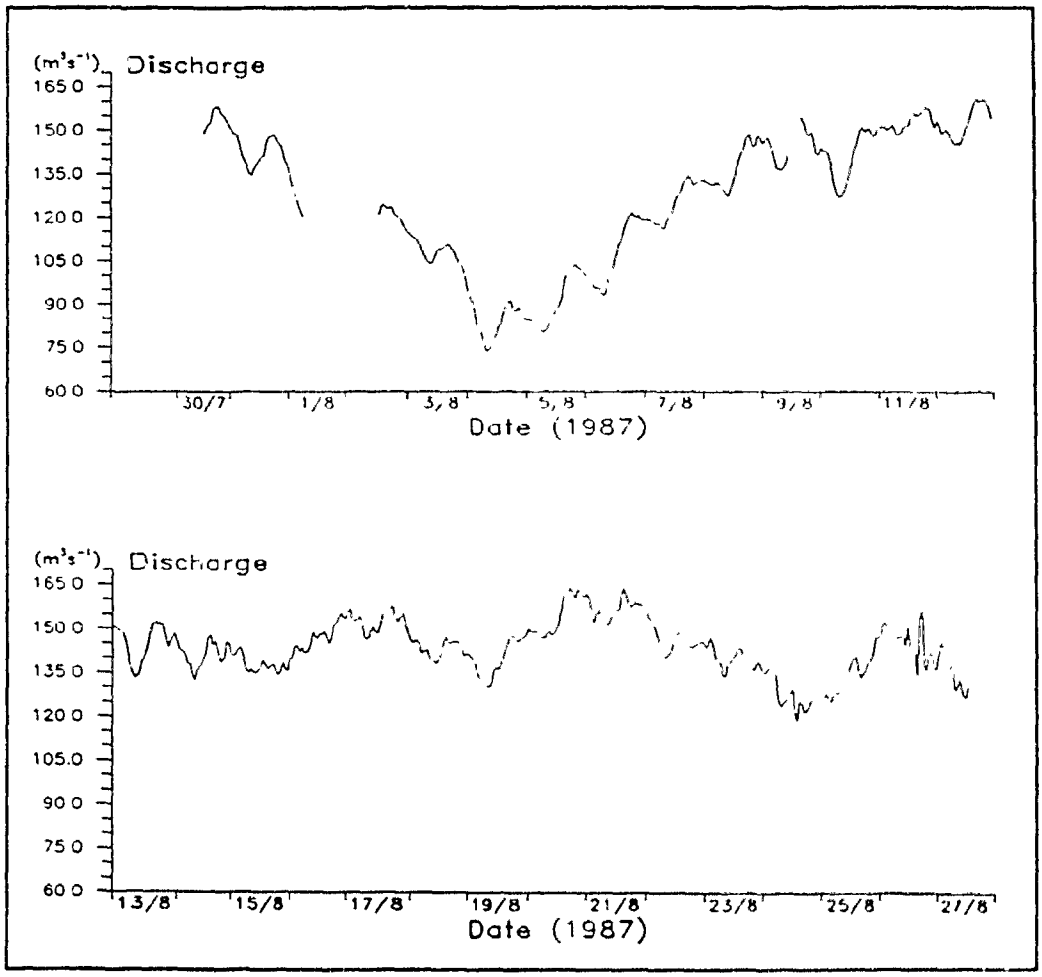

August. During this period, radiation inputs were probably at their maximum since there were no clouds present. Subsequent flows over the next four days recede to a minimum of 119.0 m^3s^{-1} at 14:00hrs on 24 August before increasing to 157.2 m^3s^{-1} at 16:00hrs on 25 August. The final two days of the monitoring period are characterised by decreasing discharge.

Figure 5.2 shows the daily minimum, maximum and mean discharge values occurring during the measurement period. Base flow characteristics are well defined with a period length of approximately three to four weeks. Unfortunately, since the record does not extend over the whole summer, inferences about the exact duration of these longer cycles are speculative; although the cycle here begins on 6 August, its termination might be on the 24 August but it could also be soon after the end of the monitoring period. It is possible that this long-term variation coincides with the influx of an easterly high pressure system from the Tibetan Plateau which produces sustained melting periods of two to four weeks' duration. The range in discharge between diurnal maxima and minima remains constant throughout the whole period with mean flows approximately mid-way between maxima and minima for most days. Mean discharge for the whole period is 136.1 m^3s^{-1} with a standard deviation of 19.4 m^3s^{-1}. This indicates that daily discharge data tends to be normally distributed.

Superimposed on the base flow characteristics are diurnal fluctuations caused by varying diurnal temperature regime over the glacier surface. Discharge maxima generally occur between 18:00 and 23:00hrs each day with minima between 05:00 and 08:00hrs. Rising limbs of diurnal flood hydrographs[1] are generally steeper than falling

[1]Flood hydrograph here is defined as the record of diurnally increasing and decreasing discharge in the outwash channel.

Figure 5.2 Daily average, minimum and maximum discharge in the Bualtar River, 1987.

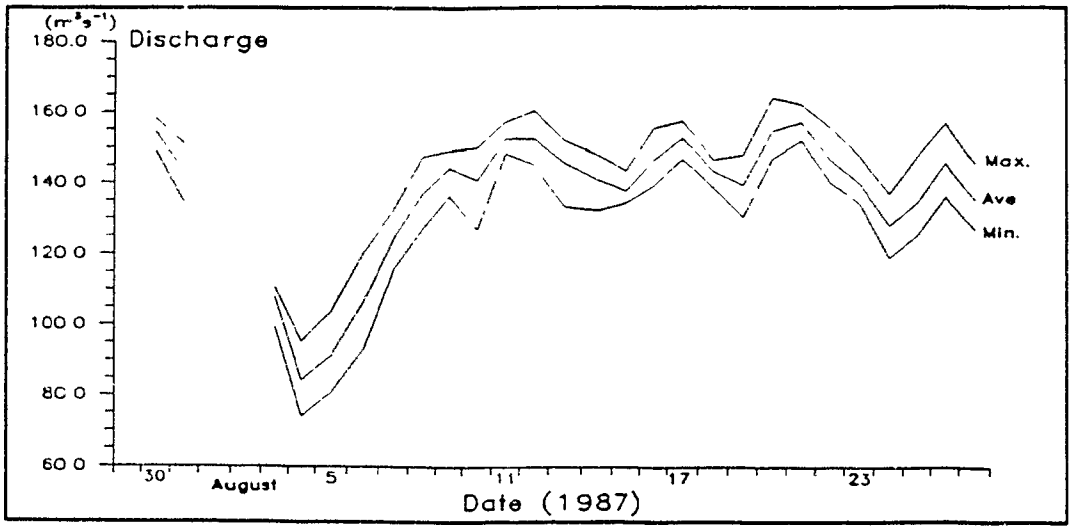

limbs indicating that the rate of increase in flow for each cycle is greater than the rate of recession. However, apart from the hydrographs from 30 July to 6 August, most cycles are not characterised by simple rising and falling discharges. Many hydrographs are composed of multiple peaks or have recession limbs with sudden, short-term increases and decreases superimposed on the series. It is probable that both types of variation in hydrograph characteristics are caused by waters from the Barpu-Miar-Sumaiyar-Bar Glaciers not reaching the outlet until after peak Bualtar flows have subsided. Hence, discharge remains high as the Barpu-Miar-Sumaiyar-Bar meltwaters reach the Bualtar portal.

Two other mechanisms cause deviations in flow characteristics from the usual regular diurnal periodicity. Firstly, on 15 and 16 August, diurnal cycles are damped as flows rise. This was possibly caused by increased cloud cover which augmented flows by contributing water to the conduit network as a result of precipitation events. Later, in the evening, release of subglacially stored water in the Bualtar-Barpu systems continued to increase flows until the diurnal pattern was restored on 17 August. Secondly, 25 to 26 August, discharge again deviates from its normal diurnal pattern. On 25 August, flow peaks early at 13:00hrs before falling for the following two hours. During the rest of the day it increases to a maximum of 152.8 m^3s^{-1} at 00:01hrs on 26 August before declining to a minimum of 134.9 m^3s^{-1} at 15:00hrs later that day. A sudden increase in discharge is shown by a spike with a peak of 157.2 m^3s^{-1} at 17:00hrs and flows immediately return to previous levels. Flow then assumes a more normal character in the evening of 26 August with discharge increasing to a maximum of 146.0 m^3s^{-1} at 01:00hrs on 27 August and then declining at the end of the record. Characteristics of flow during these penultimate two days may be explained by a

possible blockage in arterial conduits in the early afternoon of 25 August. Discharge declines as the impediment prevents the passage of meltwater through the glacier. However, the blockage is cleared shortly afterwards allowing discharge to increase rapidly. On the following day, as flows decline in early afternoon, another blockage of the drainage system causes a sudden fall in flow. Meltwater becomes temporarily stored under pressure and with the removal of the obstruction, the sudden release of stored water produces the sudden, sharp discharge increase shown in mid-afternoon. After the stored water has been expelled, discharge rapidly returns to its normal flow levels in the early evening. Further interpretation of discharge data is possible only after analysis of electrical conductivity and suspended-sediment concentration.

5.1.2 Electrical Conductivity

The record of electrical conductivity data in the Bualtar River (Figure 5.3) illustrates that solute concentration is inversely proportional to discharge. Thus, when flows are minimal, electrical conductivity is maximal. Furthermore, rates of change in total dissolved solids content is inversely in phase with the rate of change in flow. Hence, gradients of rising limbs of diurnal solute concentration cycles are steeper than on falling limbs.

Mean electrical conductivity is 112.2 μScm^{-1} with a standard deviation of 22.0 μScm^{-1}. Maximum observed solute concentration (conductivity of 181.3 μScm^{-1}) was measured at 09:00hrs on 4 August. This value coincides with minimum discharge when water is derived predominantly from subglacial water sources which have undergone

Figure 5.3 Electrical conductivity and discharge in the Bualtar River, 1987.

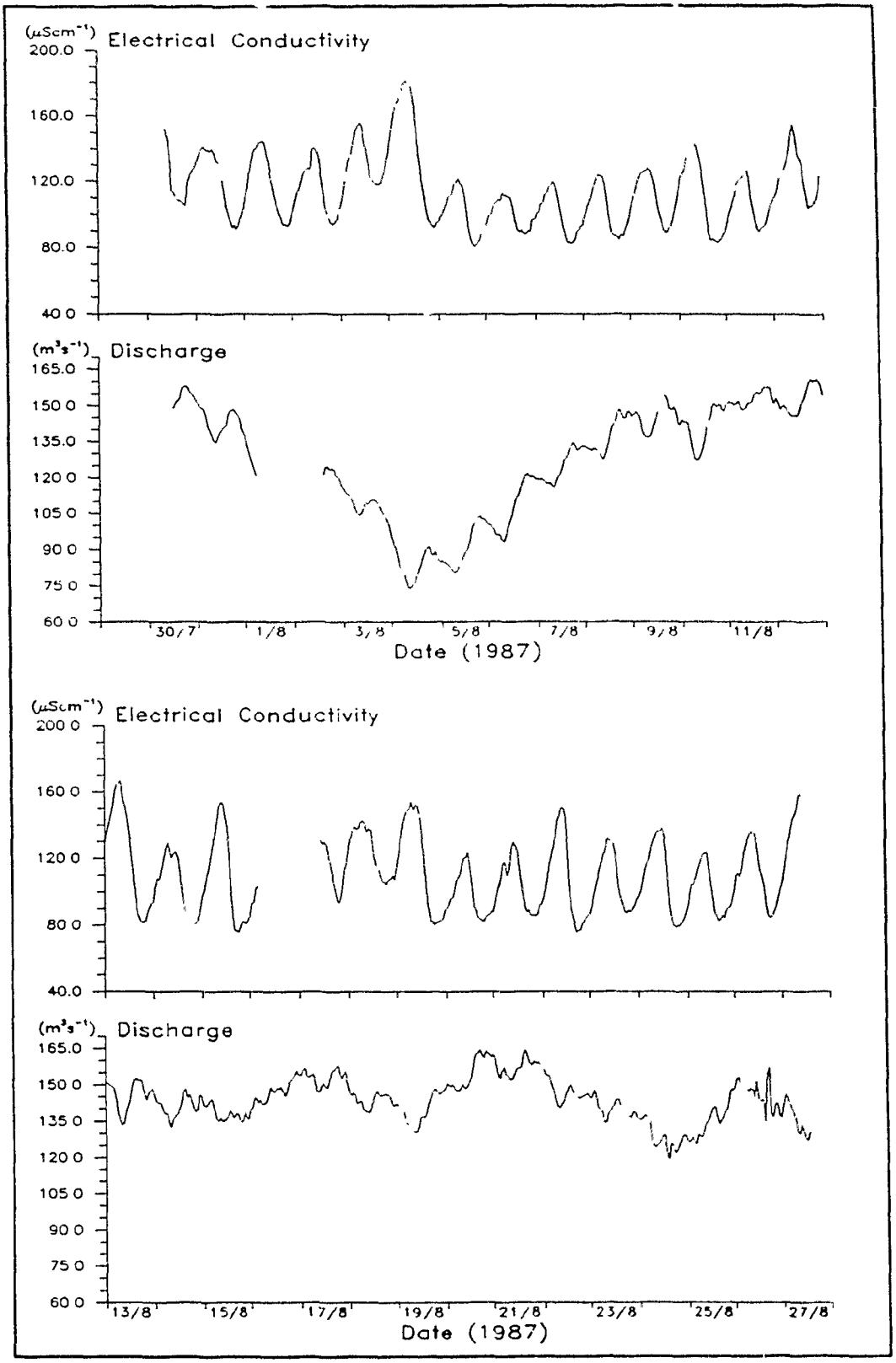

chemical enrichment through contact with bedrock and sediments at the base. Minimum conductivity was measured at 18:00hrs on 14 August when a value of 75.0 μScm^{-1} was recorded. This should coincide with peak flows when water is most dilute although in this case it does not. One possible explanation is that on 14 August, a greater proportion of meltwater was derived from glaciers which comprise the Barpu system. Unusually dilute meltwaters issuing from the Bualtar Glacier surface were further diluted by solute-free waters draining the Barpu system glaciers. Further evidence for this influence is provided by the fact that this particular hydrograph is characterised by a double peak, the first maximum being at 14:00hrs and the second, derived from the Barpu system, at 22:00hrs. Although the magnitude of the second peak flow at 22:00hrs is 4.7 m^3s^{-1} less than the first, it is protracted in duration and includes a second, smaller sub-peak. This suggests that an important contribution is made to daily flow on this occasion by the Barpu system meltwaters, more so than to the hydrograph event at maximum flow on 20 August. At maximum discharge on 20 August, the level of solute concentration does not fall to the recorded minimum of the whole period because meltwater solute concentrations remain high and the relative contribution of flow from the Barpu system is less than on 14 August.

Diurnal fluctuations in conductivity are well matched with discharge variations as relative contributions of water sources change from solute-rich, subglacially-derived waters in early morning to solute-free, surface ice melt in early evening (Raiswell, 1984). Furthermore, short-term fluctuations in solute concentrations aid in the interpretation of perturbations in the discharge record. For example, on the flow recession limb on the morning of 18 August, a sudden pulse in discharge produces a small sudden increase in the discharge trace of 1.0 m^3s^{-1} at 02:00hrs. At the start of the

pulse, conductivity increases but immediately after the slightly increased flow, it drops before rising again as discharge declines to its previous recession level. It is possible that this sudden spike on the recession limb, which is accompanied by a reduction in conductivity, is caused by the inclusion of englacially trapped, solute-free water which suddenly becomes incorporated into arterial flows. Flow in the outwash channel increases as the parcel of water initiates a kinematic wave effect producing an increase in discharge downstream two hours before the aliquot of water arrives and alters the chemical signature of the water (Glover and Johnson, 1974). A similar situation was recorded early in the morning of 21 August.

Another example where the record of solute concentration aids in the interpretation of discharge time series is for the period between 25 and 27 August. On 25 August, when flow rises to its first peak at 13:00hrs, conductivity reaches a minimum shortly afterwards at 15:00hrs. However, the subsequent increase in discharge is accompanied by an increase in solute concentration which continues after flows begin to fall from 00:00hrs on 26 August. Concentration peaks to a conductivity of 135.5 μScm^{-1} at 09:00hrs on 26 August and constantly declines to a minimum of 85.7 μScm^{-1} at 17:00hrs later that day. Both spikes on the recession flow of 26 August (a smaller one at 12:00hrs and the main one at 17:00hrs) are not associated with any perturbations in solute concentration. Hence, the sudden fluctuations in discharge might have been caused by a blockage in the conduit system rather than a sudden inclusion of subglacially stored water within the glacier.

Although diurnal variations in solute concentration are closely related to changing discharges, the base flow component of conductivity does not exhibit such a close association. The reason for this phenomenon is that sources of solute-rich water,

often from subglacial cavities, become progressively flushed over consecutive diurnal hydrographs (Collins, 1977, 1979b). This implies that solute sources become exhausted unless new stores are constantly tapped. The Bualtar record exhibits prominent flushing events on several occasions which disrupt base flow solute levels which might otherwise be expected from the discharge record.

From 30 July to 4 August, conductivities increase and flow declines. As subsequent flows begin to increase, conductivities drop and remain within a relatively constant range between 80.0 and 160.0 μScm^{-1} from 5 to 12 August. During this period, amplitudes of diurnal fluctuations gradually increase probably as increased basal flows, under increased water pressure, gain access to wider solute stores at the bed. The culmination of this period is a maximum solute concentration at 08:00hrs on 13 August indicated by a peak conductivity of 166.7 μScm^{-1}. On the following day, the solute concentration maximum is relatively less (129.3 μScm^{-1}) for a similar discharge. This indicates short-term exhaustion of dissolved solid supply on the previous day. Flushing of solute supply is also shown on 18 and 19 August, and 22 August with respective flows on following days producing relatively lower solute concentration peaks in response to exhausted supply. This flushing and exhaustion of supply from within the glacier is shown more clearly in the record of solute load.

An index of solute load is the product of electrical conductivity and discharge. Since it is an index and not an absolute value it cannot be used for accurate calculations of total dissolved solid load. However, it is useful for examination of varying relative rates of solute removal from a glacier. Figure 5.4 shows the index of solute load record for the measurement period. Maximum solute transportation rates on 13, 19 and 22 August are clearly followed by reductions in diurnal solute load peaks

Figure 5.4 Index of solute load and discharge in the Bualtar River, 1987.

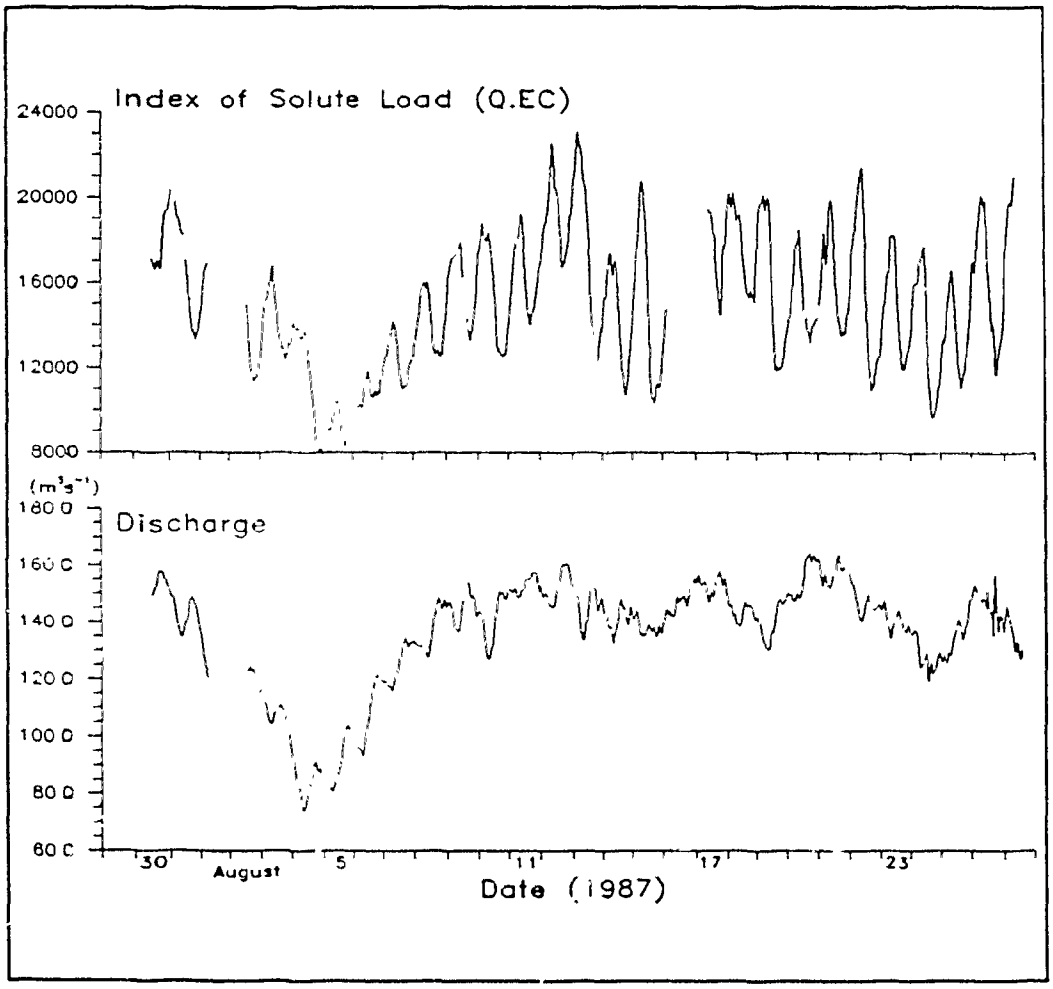

on subsequent days. Hence, flushing-exhaustion mechanisms are operative in outwash flows from the Bualtar Glacier during this period.

The index of solute load trace is characterised by a more prominent base flow than electrical conductivity data. Although diurnal fluctuations are inversely in phase with discharge, varying base flow solute loads reflect changing discharges. Increased solute removal from the glacier system occurs at times of elevated flow levels and minimum solute loads coincide with reduced discharges. However, these observations have to be treated with care since not only is the relationship between discharge and solute load spurious by definition, but electrical conductivity in the Bualtar River is complicated by inputs in solute load from the Barpu system. Hydrometeorological controls vary throughout the whole basin in time and space; conditions in the Bualtar basin on any occasion may be rather different than those over the rest of the system at the same time. Hence, contributions to flow from the Barpu system may temper or accentuate hydrochemical characteristics of meltwaters draining the Bualtar Glacier.

5.1.3 Suspended-Sediment

Suspended-sediment concentrations in the Bualtar River from 30 July to 27 August are shown in figure 5.5. Unfortunately the first ten days of the record contain many missing values as a result of problems with field data collection. Although it is possible to relate base flow variations in sediment concentrations, detailed analysis and interpretation of diurnal variations over this period are not possible. However, the

Figure 5.5 Instantaneous suspended-sediment concentration and discharge in the Bualtar River, 1987.

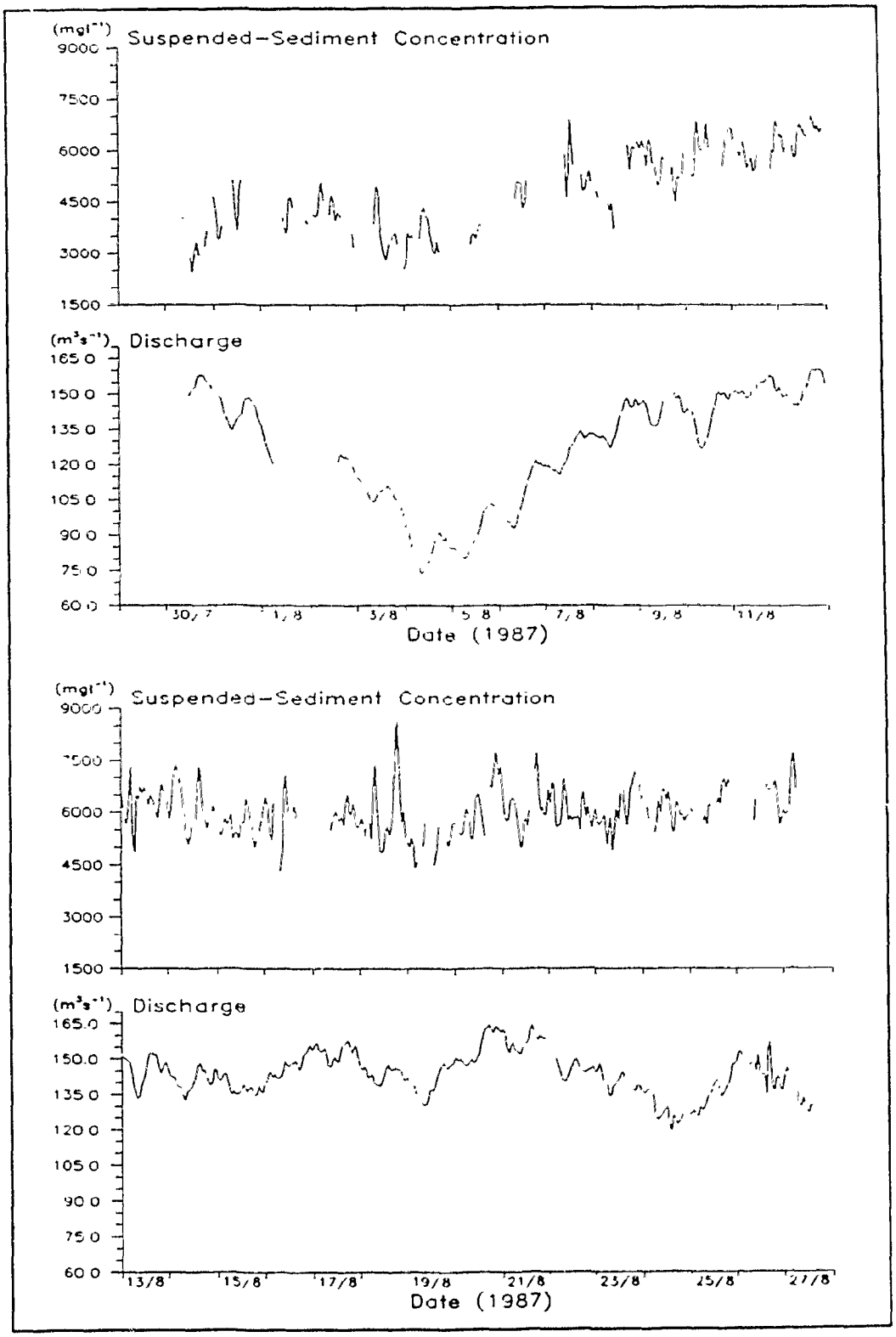

remaining section of the record exhibits a relatively high quality time series with few missing data.

Sediment concentration data are characterised by a daily flow component, cyclic variations on a diurnal scale and short-term fluctuations over four to five hours. The shorter term variations are superimposed on the longer term cycles. The average concentration is 5591 mgl^{-1} with a standard deviation of 1057 mgl^{-1}. All data remain within a range between 2430 and 8670 mgl^{-1} with a maximum concentration of 8670 mgl^{-1} at 19:00hrs on 18 August and a minimum value of 2430 mgl^{-1} at 12:00hrs on 30 August. Figure 5.6 shows this range in suspended-sediment concentration with daily minimum, maximum and mean data plotted. Data appear to be relatively normally distributed on a daily basis with daily means generally mid-way between maxima and minima.

Examination of data shows that with the exception of two periods between 30 July and 1 August, and between 22 and 25 August, the daily trend in sediment concentration is generally directly in phase with discharge data. The reason for this is that assuming an adequate sediment supply, river competency increases with increased flows (Hjulström, 1935). Concentrations decline with receding discharge from 2 to 4 August and subsequently increase with rising flows from 5 to 13 August. Between 13 and 16 August, the range of suspended-sediment concentration remains between 4550 and 7500 mgl^{-1}. However, from mid-afternoon on 16 to mid-morning on 17 August, a break in sediment data prevents comparison with discharge. On 17 August, suspended-sediment concentrations decline with discharge to a minimum of 4416 mgl^{-1} at 04:00hrs on 19 August. This coincides with the falling daily hydrograph over this period. In the afternoon of 19 August, rising daily flows are accompanied by increasing sediment

Figure 5.6 Daily average, minimum and maximum suspended-sediment concentration in the Bualtar River, 1987.

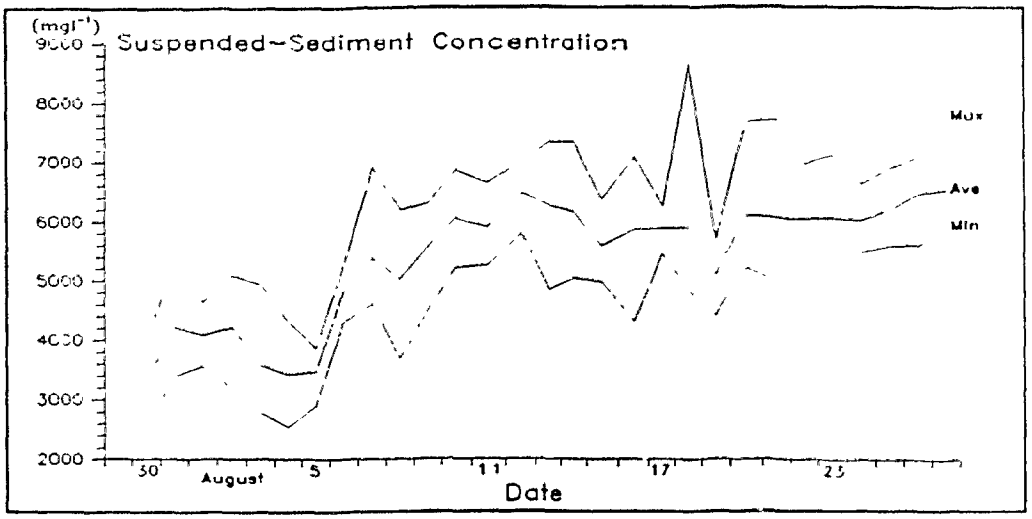

concentrations both of which reach maxima in the evening of 20 August. Suspended-sediment concentrations remain high for the remainder of the monitoring period even though discharge recedes to 24 August and then rises until 26 August before falling over the final three days.

Inspection of diurnally changing sediment concentration reveals that the time series at this scale is not as well defined as daily variations in sediment concentration. Studies elsewhere have shown that suspended-sediment concentration diurnally increases with rising flows often reaching maxima at times of greatest rate of increase in discharge before starting to decline at peak discharge and continuing to decrease as flows subside (Østrem, 1975; Richards, 1984). Others have reported that sediment concentration peaks may occur both before and after discharge maxima or indeed have no pattern at all (Binda *et al*, 1985; Collins, 1979a). The reason for such weakly defined cycles in the Bualtar River is because short-term concentration fluctuations, of the order of several hours duration, disguise what might otherwise be a simple, cyclicly varying series. These short-term variations are related to two influences on suspended-sediment transport in the outwash channel. Firstly, since outwash flows from the Bualtar Glacier incorporate meltwaters from the Barpu Glacier system, it is reasonable to assume that sediments from beneath and within the Barpu Glacier system are also injected into meltwaters issuing from the Bualtar Glacier. Sudden flush events from the contributing Barpu system add short-term pulses to the sediment trace in the outwash channel. Secondly, the Bualtar Glacier is heavily laden with sediment derived from surrounding slopes. Slumping of such sediments into supraglacial or marginal channels can produce sudden spikes in the sediment concentration record. However, although

those short duration fluctuations disguise diurnal variations in suspended-sediment concentration, it is possible to observe 24 hour cycles in the time series.

Unfortunately, diurnally changing patterns of sediment concentration are less discernable for most of the first ten days than the rest of the measurement period. However, through comparison with inferred base flow concentrations, it is possible to approximate peak concentrations during this segment of time series. On 3 August, a maximum sediment concentration occurs at around 09:00hrs. This precedes an early diurnal peak discharge by five hours. A similar pattern occurs on the following day when a maximum concentration in suspended-sediment concentration precedes peak flows in the evening by several hours. On 7 August, a diurnal concentration peak is synchronous with the flow peak at 16:00hrs.

From 10 August onwards, hourly detail in the suspended-sediment concentration time series is better defined than the first few days. Diurnal peaks in sediment concentration occur between 16:00 and 23:00hrs each day although their timings do not always coincide with associated discharge maxima. On the evenings of 10 and 11 August, concentration maxima in suspended-sediment lag behind peak flows by several hours. On 12 August, peak concentrations coincide with maximum flow at 06:00hrs. Over the next three days, although concentration maxima accompany discharges before, after and during peak flows, the record contains several well defined pulses in sediment concentration. The second pulse in the sediment record observed at 21:00hrs on the falling hydrograph limb of 13 August is possibly in response to a sudden release of stored water from within the glacier system. Since it coincides with the maximum rate of increase of flow for this event and a small drop in rising solute concentration (Figure 5.3), the aliquot of water containing the sediment may have been derived from

an en- or supraglacial store. On release from its store, water may have been able to re-work sediments deposited during the falling diurnal flow. A similar event occurred on the second smaller flow maximum superimposed on the declining flow level of 14 August. During 15 and 16 August when daily flow increases and diurnal discharge cycles are suppressed, suspended-sediment concentration increases at times of short-term (several hours) flow peaks or maximum increase in rates of flow.

The segment in the time series from 17 to 19 August contains the peak concentration in suspended-sediment for the whole monitoring period. On 17 August, peak flow at 18:00hrs produces an unremarkable concentration maximum of 6561 mgl^{-1}. This flow maximum is the culmination of three days' continual increase in discharge. Hence, it should be expected that this flow would result in high concentrations in suspended sediment as observed, for example, on 20 August. However, deposition of sediment in a subglacial store or clogging of subglacial peripheral conduits by entrained sediment may not have caused outwash concentrations to markedly increase at this time. On the recessional flow limb during the morning of 18 August, the second of two sudden increases in discharge at 06:00hrs is accompanied by an increase in suspended-sediment concentration of 2197 mgl^{-1}. The sediment concentration of this parcel of water coincides with a slight reduction in peak conductivity for the duration of pulse. This peak concentration represents partial flushing of accumulated sediment from storage. Remaining sediment from the period is totally removed by raised flow levels on 18 August. However, this interpretation is complicated by the position of concentration maximum on the hydrograph. Since it coincides with the second, smaller peak of two discharge maxima, it is possible that meltwaters contain sediments not only from beneath the Bualtar Glacier but also from

the Barpu Glacier system. Nevertheless, subsequent short-term exhaustion of supply beneath the Bualtar is shown by low concentration values on 19 August indicating the sediment availability is reduced.

Another sediment flush event is exhibited during 20 and 21 August. Increase in suspended-sediment concentration accompanies the flow level increase from 19 to 20 August. Peak discharge for the whole measuring period at 17:00hrs on 20 August, produces a maximum sediment concentration of 7724 mgl^{-1} at 21:00hrs. Debris supply is reduced on 21 August as concentrations rapidly decline. However, discharge levels do not decline greatly and a flow maximum in the afternoon is only marginally less than the previous day's peak flow. Sediment concentrations at this time rapidly increase to a peak concentration of 7740 mgl^{-1} suggesting the incorporation of a new supply.

For the remaining segment of data and despite falling flows between 22 and 24 August, suspended-sediment concentrations remain high with relatively well defined diurnal fluctuations. During daily receding flows, concentrations remain high possibly because the subglacial conduit network pattern changed after the flushing event of 20 August. With reorganisation of some secondary passageways, new sediment stores become available for removal from beneath the glacier. Sediment pulses over this last section are synchronous either with sudden releases of water from within the glacier system or when diurnal flows experience maximum rates of increase.

The varying magnitude in suspended-sediment removal from the Bualtar Glacier during the measurement period is shown by the suspended-sediment load time series plot in Figure 5.7. Sediment load is the product of discharge and suspended-sediment concentration and is a useful measure of instantaneous sediment flux. Maximum load is observed on 18 August at 19:00hrs when a peak sediment load of 1265 Kgs^{-1}

Figure 5.7 Instantaneous suspended-sediment load and discharge in the Bualtar River, 1987

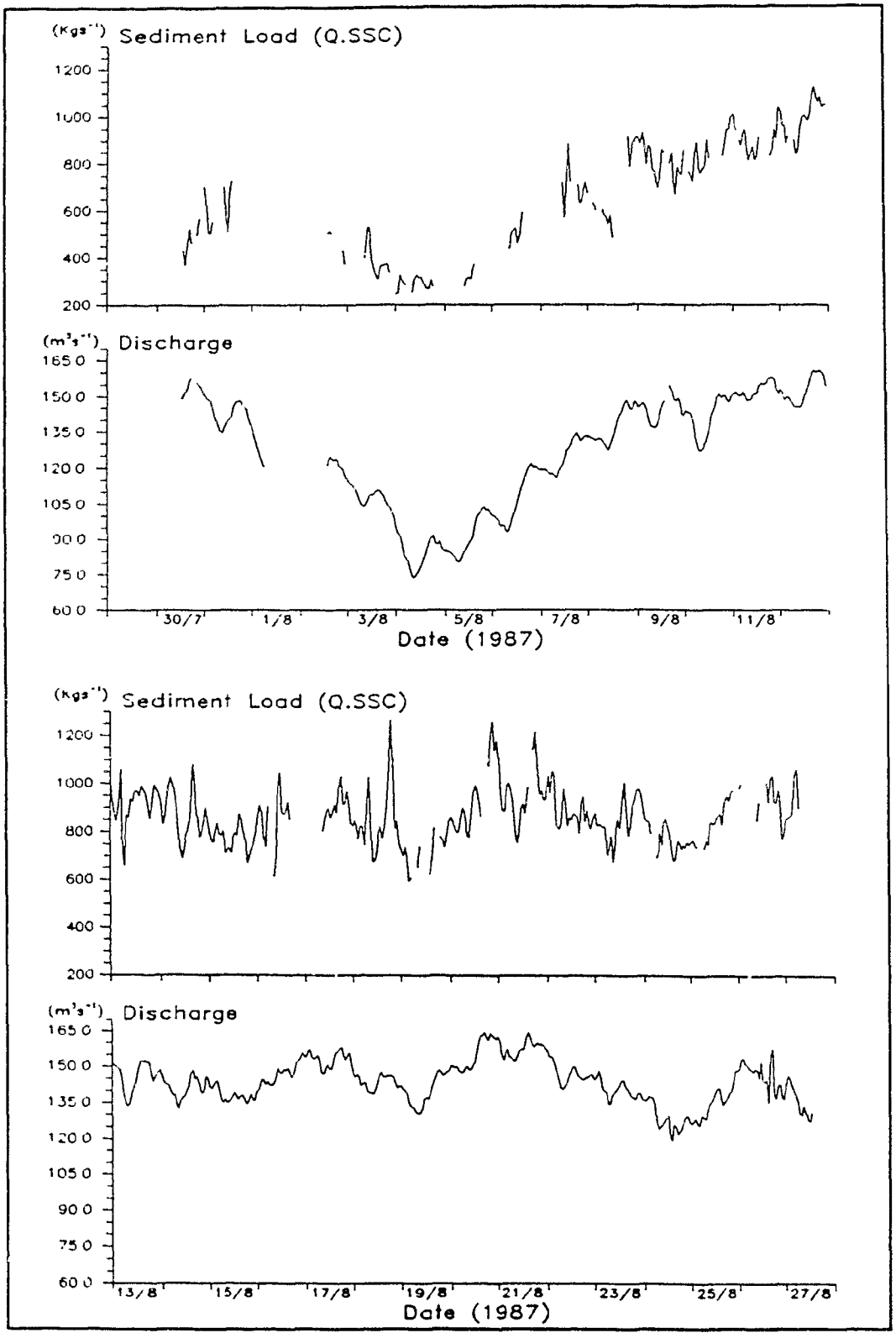

coincides with maximum sediment concentration. The minimum sediment load for the period was recorded at 00:00hrs on 4 August, several hours before the minimum flow for the measurement period. Data are in phase with variations in both discharge and sediment concentrations on all time scales although this is to be expected since load is a function of discharge.

Short-term suspended-sediment concentration pulses are evident in the sediment load series indicating that the sudden flushes are not simple concentrating effects produced by falling flow levels. Diurnal periodicity in suspended-sediment removal from the glacier system is well portrayed by the data. This is to be expected since load is derived from discharge which exhibits a stronger diurnal periodicity than sediment concentration. Diurnal maxima in sediment removal tend to coincide with simple diurnal peak flows in the outwash channel. However, on some occasions when diurnal flows are characterised by compound discharge maxima, sediment concentrations coincide with secondary flow maxima which are probably comprised of meltwaters draining the Barpu system.

Long-term variations in daily sediment flux are in phase with fluctuations in discharge. Since load is a direct function of discharge, this is to be expected. However, when examining total sediment removal from glacier systems by glacier-fed streams, and hence inferring subglacial erosional processes, it is more meaningful to use suspended-sediment fluxes rather than concentrations since concentrations alone do not indicate sediment loading of meltwaters. Nevertheless, suspended-sediment fluxes are a function of associated concentrations. Hence, the relationship between outwash flow levels and suspended-sediment concentrations is integral to the design of a process-

orientated model which simulates and predicts subglacial erosion as inferred by sediment loading of fluvioglacial waters.

5.1.4 Discharge-Suspended-Sediment Concentration Relationships: An Empirical Approach I

A good association between daily suspended-sediment concentration and discharge is expected since with increased discharges, greater volumes of water per unit time pass through the fluvioglacial system than at low flows. Hence, increased flow rates produce increased available energy in water to remove eroded sediments. However, on a diurnal scale the relationship is complicated by short, frequently occurring sediment pulse events. Furthermore, different diurnal peak concentrations lead, lag and coincide with different flow maxima producing a complex relationship between variables at this time scale.

Linear regression analysis of the relationship between suspended-sediment concentration and discharge in glacier-fed streams has been applied to paired data over diurnal and longer time scales by several authors (Bogen, 1980; Collins, 1979a; Østrem, 1975). Regression analysis demands that the relationship between discharge and concentration be linear with residuals in the dependant variable (suspended-sediment concentration) randomly and normally distributed with constant variance, zero mean and not serially autocorrelated (Gurnell and Fenn, 1984a). A scatter plot of paired Bualtar discharge and sediment concentration for the entire data set reveals that the two variables are unremarkably related; a strong linear trend does not emerge (Appendix

I, Figure A.1). This is also shown by a low Pearson's Product Moment correlation coefficient for data of 0.59. Log transformation of both data sets does not significantly improve linearity in the relationship (Appendix I, Figure A.2) with the correlation coefficient only rising to 0.62. If linear regression analysis is applied to transformed paired data at different time scales, a variety of different rating equations of the form $S = aQ^b$ are obtained with varying associated coefficients of determinations (Appendix I, Table A.1).

The rating equation for paired discharge and concentration values for the whole measurement period produces a total explanation in suspended-sediment concentration (S) from discharge (Q) of 38% (calculated R^2 value). Investigation of the Student's T-test for the whole of the discharge data set shows that samples were collected without statistical bias. Examination of predicted suspended-sediment data indicates that although residuals are normally distributed, both standard deviation and standard error around the mean are unacceptably high. Hence, it appears that a rating equation defining the statistical relationship between variables for the entire data set is inadequate for not only descriptive purposes, but also for possible predictive applications. In an attempt to improve regression model fit, the time series was broken into segments of shorter duration.

All paired data were subdivided into rising and falling flow hydrograph subsections to investigate whether individual rating equations could be generated to successfully describe the relationship between flow and sediment concentration during characteristically distinctive periods. The results are shown in Appendix I, Table A.1. T-test analysis confirmed that discharge data for each period were randomly selected from larger populations thus minimising sample bias. However, the best fitting rating

equation only had 65.6% of the variation in concentration explained by variation in discharge. This was on the falling flow limb of 3 August. All other calculated rating equations had R^2 values (a measure of the goodness of rating curve fit) less than 60% with the majority being less than 40%.

The relationship between sediment load and discharge could be examined using linear regression analysis. However, improved fits of rating curves would result from such an approach since both series are directly related. Hence, the relationship is statistically spurious invalidating such a technique for these data.

A major factor influencing the fit of generated linear regression curves is hysteresis between suspended-sediment concentration and discharge data. Concentration peaks on rising and falling diurnal flow limbs produce clockwise and anticlockwise hysteresis loops during diurnal flow cycles. Clockwise loops indicate greater concentration peaks prior to flow maxima at times of maximum increasing discharge than at similar flow levels on recessional limbs. Anticlockwise curves however, describe diurnal sediment concentration peaks at times of declining flow. Selected examples of diurnal hysteresis are shown in Figure 5.8. The graphs chosen show the simplest of loops since during other periods, traces are disguised by exceptionally convoluted patterns. Each graph in Figure 5.8 consists of paired sediment concentration and discharge data sequentially plotted from minimum flow on one day to minimum flow on the next. Although two figures (Figures 5.8A and 5.8C) each have a couple of missing values in their time plots, it is assumed that the plotted graphs are representative of meltwater characteristics at these times.

Figure 5.8A shows clockwise hysteresis between 19:00hrs on 10 August to 07:00hrs on 11 August. The looped plot relates to the second of two flow maxima

Figure 5.8 Sequentially plotted paired discharge and suspended-sediment concentration data during four different sub-periods in the 1987 Bualtar record. (A) is from 19:00hrs on 10/8 to 07:00hrs on 11/8, (B) is from 08:00hrs on 13/8 to 08:00hrs on 14/8. (C) is from 08:00hrs on 18/8 to 09:00hrs on 19/8. (D) is from 08:00hrs on 22/8 to 07:00hrs on 23/8.

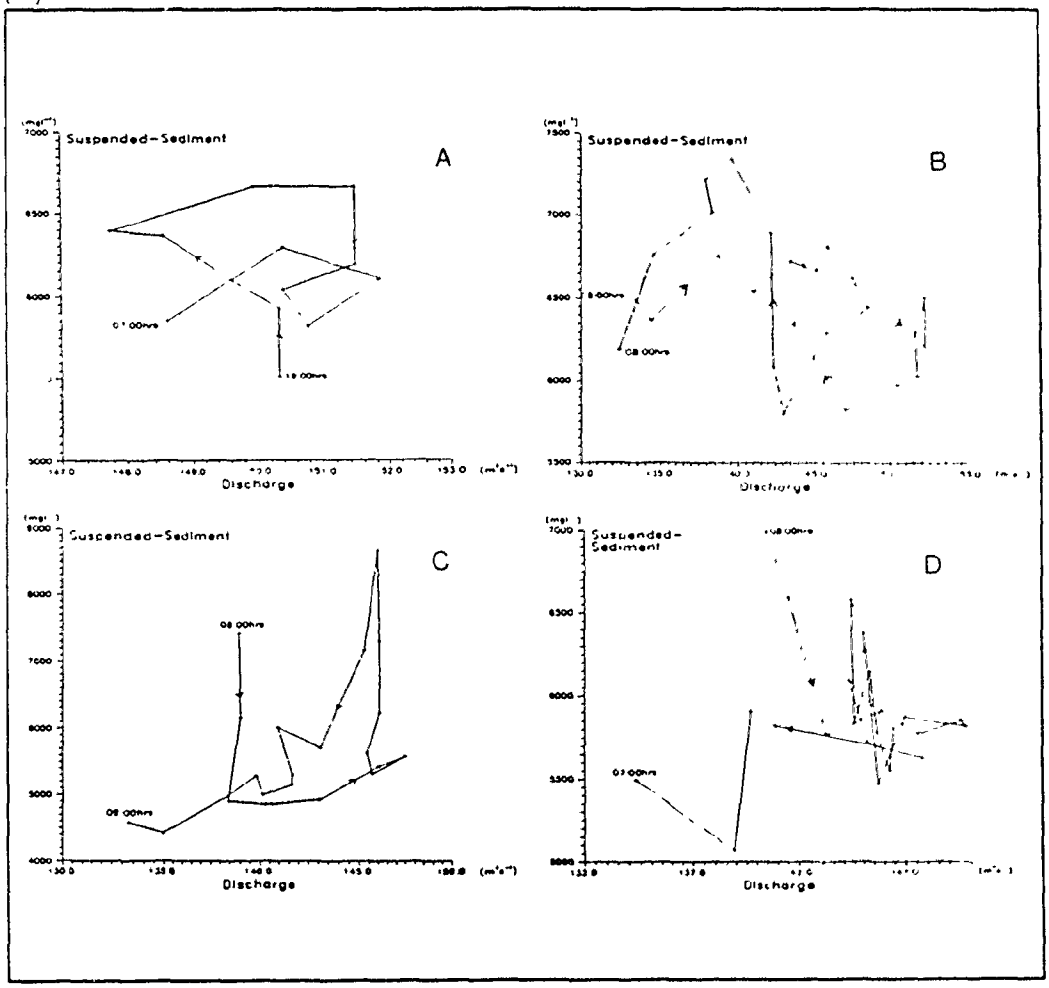

recorded at this time. As flows decline in the evening after the first discharge peak of 10 August, suspended-sediment concentrations increase to 22:00hrs when low flows begin to rise again. Both discharge and concentrations increase for the next hour and sediment concentration peaks between 23:00hrs and 00.00hrs. Flows remain high while sediment concentration decreases for the following 3 hours. The involution in the cycle (a smaller loop on the main cycle) relates to a sediment pulse event at 05:00hrs on 11 August. Figure 5.8B shows connected paired flow and concentration data for the 24 hour period beginning at 08:00hrs on 13 August. Two sediment pulses during this period occur on the rising and falling limbs of a secondary flow peak after the diurnal flow maximum on 13 August. This produces both clockwise and anticlockwise hysteresis loops in the trace. Figure 5.8C shows the sediment and discharge plot from 08:00hrs to 09:00hrs on 18 to 19 August respectively. Diurnal peak flow precedes the sediment concentration maximum by six hours producing a well defined anticlockwise loop. Plotted paired data for a 23 hour period from 08:00hrs on 22 August (Figure 5.8D) shows that the relationship between concentration and flow is complex with many involutions in the data. Again, these intricate cycles are caused by the sudden pulse events in concentration record which may not be attributable to changing rates of flow.

Hysteresis in the relationship between suspended-sediment concentration and discharge data constantly changes over the monitoring period as shown in the variety of different looped patterns in Figure 5.8. The reason for this constantly changing nature is that exhaustion of sediment supply occurs when previous flows are greater than current discharges. Hence, unless account can be taken of the historical element in sediment concentration and discharge data, empirical methods, especially linear

regression analysis, will be unable to successfully describe relationships between these variables.

5.1.5 Summary of Bualtar Results

Discharge data exhibit variations in flow at three time scales. The longer period of day to day flow has a duration of between three to four weeks and probably coincides with the influx of warm air from an easterly high pressure system. Diurnal cycles are well defined over most of the period although peak flows on some days are comprised of two maxima, the second peak presumably being a result of the delayed input to the Bualtar drainage system of meltwaters from the Barpu Glacier. Shorter term spikes in the data record are the result of sudden releases of stored water from sub-, en- or supraglacial pockets into the main drainage network. Suspended-sediment concentrations are also characterised at three time scales. Long-term variations in sediment concentration match the changing daily discharge record for most of the measurement period. At a diurnal scale, fluctuations in concentration are not as well defined as flow variations since the trend is complicated by short-term pulses in concentration of several hours duration. However, variations in the total instantaneous sediment transport record are more closely matched with fluctuations in the discharge record. Variations over all three time scales are better defined than concentration fluctuations.

The empirical relationship between discharge and suspended-sediment concentration in the Bualtar River is poor. Regression analysis used to predict sediment

concentrations from flow data succeeds in neither fully describing nor explaining variations in concentration at long-term and diurnal time scales. One reason for poor statistical explanation of sediment concentrations by discharge is that s ally autocorrelated residuals in regression analysis are produced by hysteresis in tne relationship between flow and concentration data. Hysteresis relationships constantly change over the whole time series indicating that recent hydrograph history might be an important factor in explaining sediment concentration levels.

5.2 Batura 1988

5.2.1 Stage

Flow level (stage) of water in the Batura River between 4 and 14 August, 1988, is shown in Figure 5.9. Apart from a short break in the record on 13 August, the time series is continuous. Maximum stage for the entire period was 1.56 m and was measured at 23:00hrs on 13 August. Minimum flow of 0.97 m was recorded at the start of the monitoring period on 4 August. The time series is characterised by steadily rising daily flow levels on most days except for 11 and 12 August when stage slightly dropped. Warm weather for the duration of the period provided favourable melting conditions which caused the gradual increase in stage. The first two days experienced minor cloud coverage while maximum incoming solar radiation was incident at the lower reaches of the glacier over the following four days since cloud cover here was

Figure 5.9 Water stage in the Batura River, 1988.

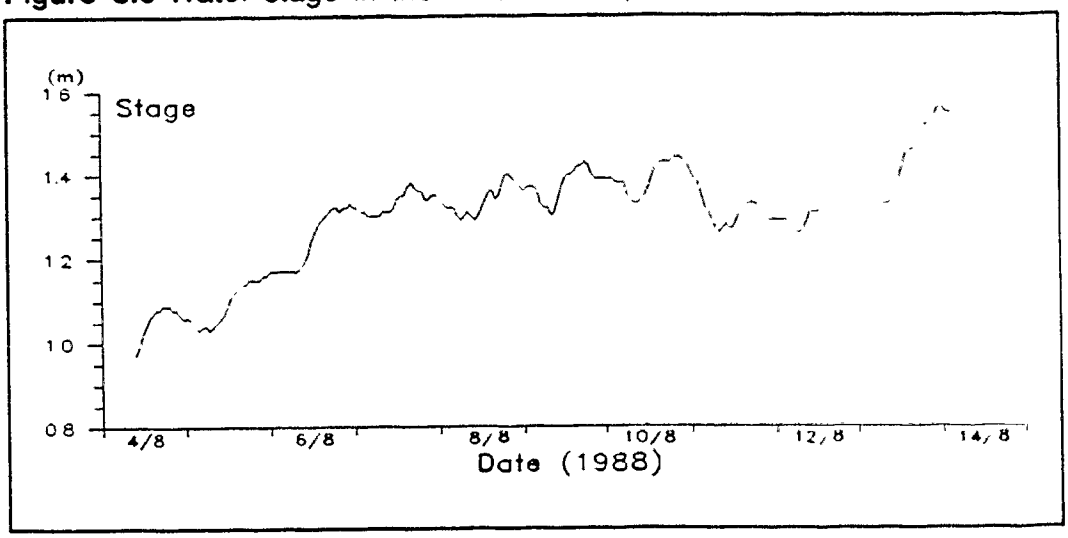

Figure 5.10 Daily average, minimum and maximum stage values in the Batura River, 1988.

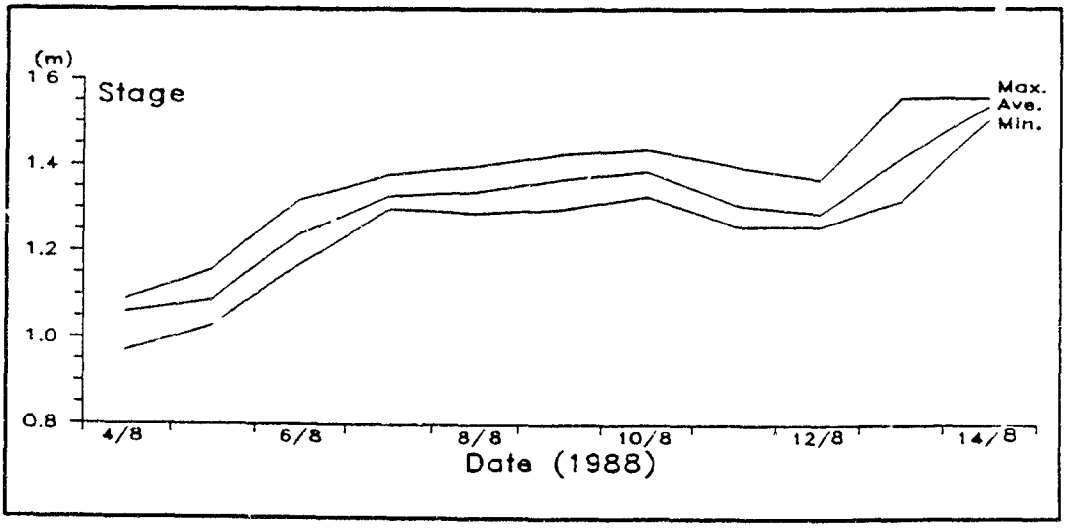

minimal. Increased cloud cover on 11 August produced the drop in stage which did not recover previous flow levels until 12 and 13 August.

Diurnal fluctuations in stage are pronounced with peak flow levels at the staging site generally between 17:00hrs and 23:00hrs each day. Minimum diurnal stage readings occur between 05:00hrs and 09:00hrs. Rising hydrograph limbs are steeper than their recessional counterparts suggesting that routing of surface meltwater takes place through an efficient englacial and subglacial drainage system. This is expected since stage measurements were taken well into the ablation season when glacier drainage networks are at their most developed for the year.

Figure 5.10 is a plot of daily minimum, maximum and mean stage values for the monitoring period. The rising flow regime is well defined by high quality data which have a mean of 1.03m and standard deviation of 0.13 m for the whole period. Daily mean flow levels are mid-way between daily maximum and minimum flows indicating normal distribution of data.

5.2.2 Electrical Conductivity

Variations in total dissolved solids in the Batura River during the monitoring period, are indicated by the electrical conductivity time series in Figure 5.11. Solute concentrations are contained within a conductivity range of 309.0 to 570.7 μScm^{-1}. The average electrical conductivity of all data is 405.0 μScm^{-1} with a standard deviation of 63.3 μScm^{-1}. The conductivity trace is inversely proportional to stage at two time scales, daily and diurnal. The entire time series is characterised by falling daily solute

Figure 5.11 Electrical Conductivity and stage in the Batura River, 1988.

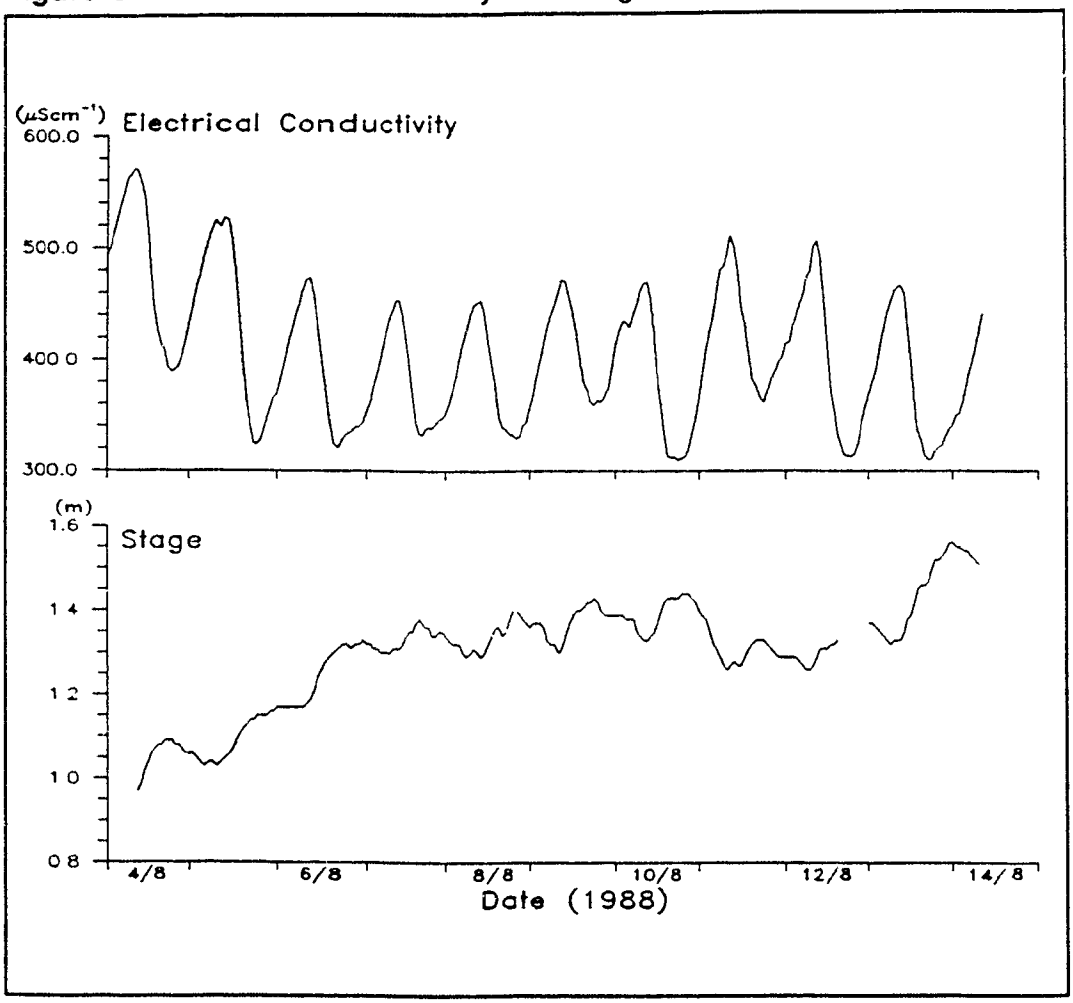

concentrations with exceptions on 11 and 12 August when the daily conductivity level increases as flows drop. However, on 13 and 14 August, solute concentrations continue to decline as discharge levels increase.

Maximum solute concentrations during each day coincide with minimum flows when solute-rich meltwaters originate from the glacier bed. Minimum concentrations are associated with peak flows comprised of fast routed, relatively solute-free surface meltwaters. Diurnal fluctuations in the conductivity record have asymmetrical forms with relatively gently rising and sharply falling limbs. The reason for this phenomenon is that following discharge maxima, flows gradually decline producing a slow build-up of solute concentration in out-flowing meltwaters as the subglacial flow component increases. Conductivity peaks when meltwaters are predominantly derived from relatively slow moving subglacial flows which have ample opportunity to dissolve bedrock and sediments at the ice-rock interface. At maximum solar radiation intensity (at about 13:30hrs), melting of surface ice produces solute-free meltwaters which are quickly drained through the Batura to the outwash stream. Hence, the solute-rich subglacial flow component, which is closest to equilibrium with mineral particles, becomes mixed with less concentrated supraglacially derived waters and quickly lowers conductivity in the outwash channel (Collins, 1977).

On the falling diurnal discharge limb of 9 to 10 August, flow levels become constant for several hours before resuming their decline to a minimum of 1.33m at 08:00hrs on 10 August. This change in rate of discharge decline is accompanied by a sudden short drop in conductivity before solute concentrations continue to rise to a peak of 469.3 μScm^{-1} at 09:00hrs. It is probable that the sudden levelling of flow trace and associated depression in conductivity are related to release of a solute-free water

store from within the glacier. This is a reasonable explanation considering that the lower section of the Batura Glacier surface is pitted with pools of water. Sudden drainage of a pool would temporarily reduce flow decline and solute concentration increases in the outlet stream. It is possible to explain the other few short duration conductivity suppressions in the same way.

Compared with conductivity data collected from the Bualtar Glacier in 1987, characteristics of solute concentration in the outwash stream of the Batura Glacier in 1988 are uneventful. Unfortunately, the length of record for the Batura Glacier in 1988 is not long enough to examine longer flow trends in solute transport. However, the level of solute concentration in the Batura River during the measurement period is greater than concentrations measured in the Bualtar Glacier in the previous year. Hence, data collected do provide a useful indication of the magnitude and nature of changing solute concentration characteristics in meltwaters draining one of the largest Karakoram glaciers during this period in the ablation season.

5.2.3 Suspended-Sediment

Suspended-sediment concentration data collected from the Batura River are shown together with stage in Figure 5.12. Many observations are missing as a result of technical problems with field equipment. Consequently, it is not possible to interpret conclusively detailed sediment concentration characteristics for all data although it is possible to relate general trends in data.

Figure 5.12 Suspended-sediment concentration and stage in the Batura River, 1988.

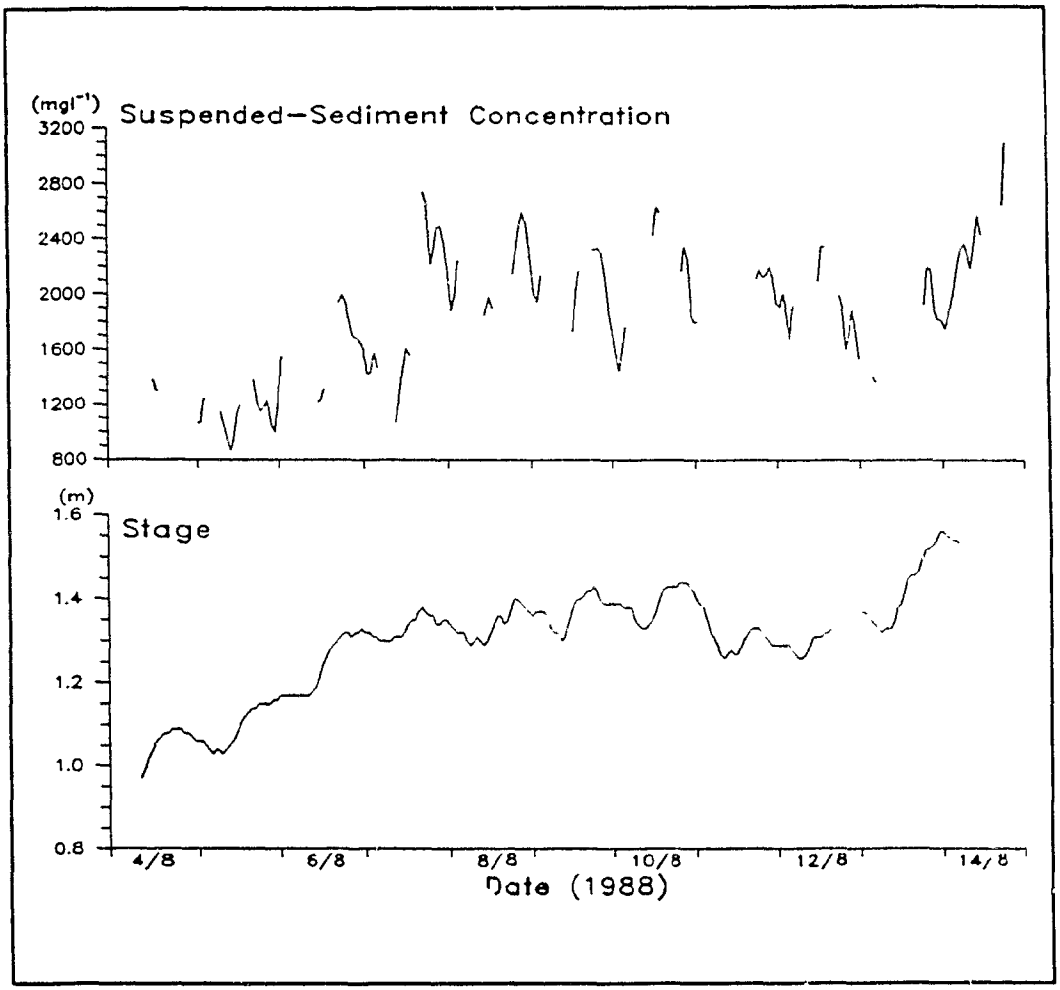

Figure 5.13 Daily average, minimum and maximum suspended-sediment concentration in the Batura River, 1988.

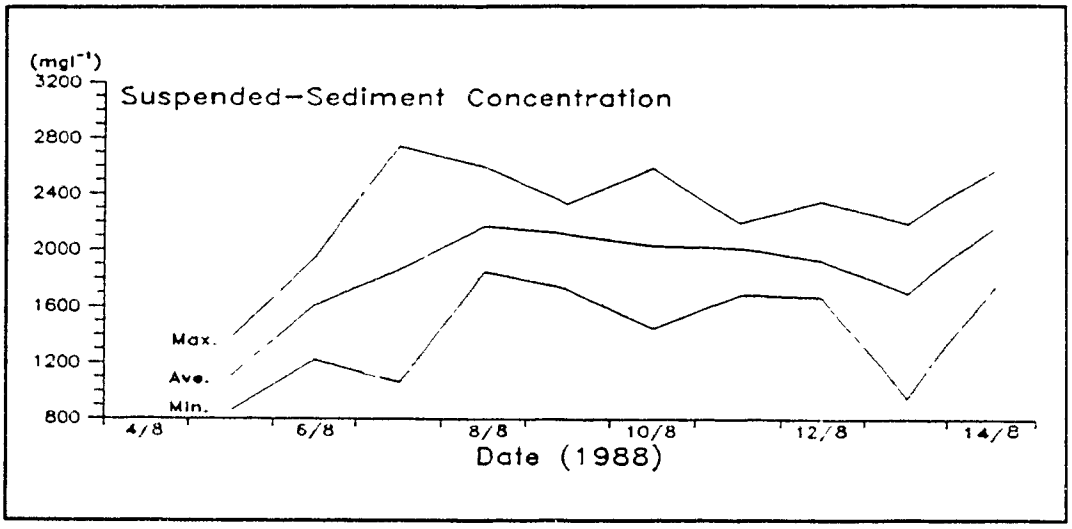

Sediment concentrations are contained within a range between 860 and 3200 mgl^{-1} (Figure 5.13). However, although the maximum sampled concentration for the whole period was 3110 mgl^{-1} at 19:00hrs on 14 August, lack of surrounding data values in the time series prevents confidence in this observation. Furthermore, simultaneous flow data were not collected preventing possible verification of this observation. Instead, a maximum concentration of 2745 mgl^{-1} is assumed to occur at 17:00hrs on 7 August when sharply rising and falling concentrations before and after the measured peak suggest a maximum of at least this magnitude. A minimum suspended-sediment concentration of 865 mgl^{-1} was sampled at 10:00hrs on 5 August. The mean concentration for the time series is 1858 mgl^{-1} with a standard deviation of 473 mgl^{-1}. Although paucity of suspended-sediment concentration data introduces bias to interpretation of the plot of maximum, mean and minimum concentration, calculations using all available daily data show that mean sediment concentrations lie mid-way between maximum and minimum daily values suggesting near normal distribution of data.

Daily concentrations of suspended-sediment in the Batura River are well related with changes in flow levels. Rate of increasing concentration is high from the start of the measurement period until maximum flushing on 7 August. Daily concentrations decline for the following two days and subsequently remain at a constant level until 13 August. The final segment of data on 14 August is characterised by rapidly increasing suspended-sediment concentration.

Plotted available data indicate that sediment concentration sections within the time series exhibit sharply increasing and decreasing trends over short time periods. This suggests that data are characteristic of highly fluctuating suspended-sediment

Figure 5.14 Index of suspended-sediment load and stage in the Batura River, 1988.

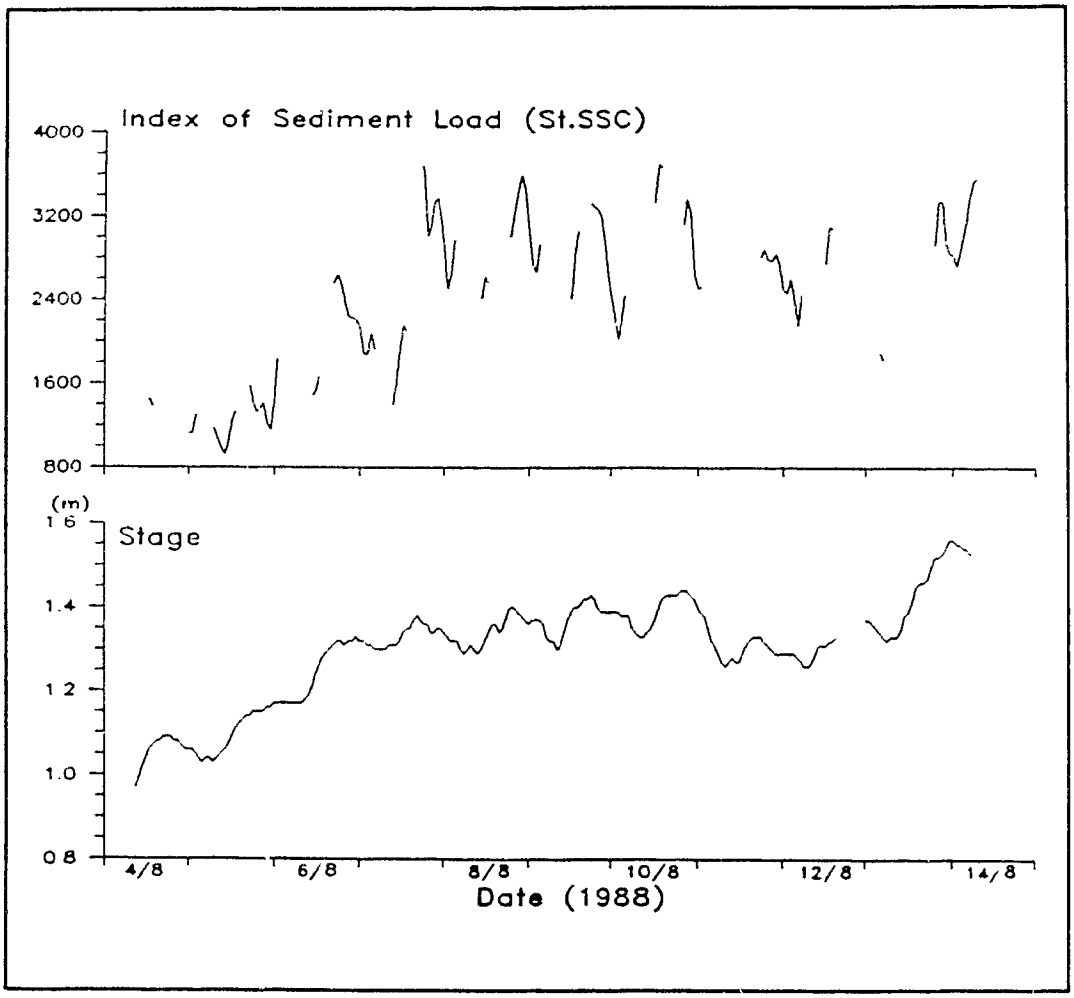

concentrations in glacier-fed streams. Peak diurnal suspended-sediment concentrations coincide with or lag behind by two or three hours maximum flow observations on 6, 7, 8, 9 and 11 August. It is not apparent when diurnal concentration minima occur although it is probable that they coincide with times of minimum flow.

Short-term fluctuations in concentration during the monitoring period can only be related to changing flow characteristics on two occasions. A sudden concentration pulse in the Batura River at 22:00hrs on 7 August is accompanied by in spike in the flow record suggesting sudden release of stored water from within the glacier. A similar event is exhibited at 02:00hrs on 12 August. However, on this occasion flow levels are not inverted but become constant for three hours before continuing to decline.

Figure 5.14 shows the index of suspended-sediment load for the period calculated from stage and suspended-sediment concentration data. Since streamflow gauging on the Batura River was not undertaken in 1988, discharge could not be calculated from rating curves, hence the sediment flux record is an index which can only be used for inferences of relative variations in sediment transport rates. Both daily and diurnal sediment load variations directly coincide with changes in flow at these time scales. Furthermore, sediment pulses in the flux record are synchronous with spikes in the flow series.

5.2.4 Stage-Suspended-sediment Concentration Relationships: An Empirical Approach II

Relationships between stage and suspended-sediment concentration data were investigated using statistical techniques. Rating equations from linear regression analysis were derived for the entire data set and for smaller segments which contained sufficient numbers of paired observations to allow regression analysis.

A scatter plot of all flow and concentration data showed that the relationship between variables is not particularly strong. In order to improve linearity for the purpose of statistical analysis, stage and suspended-sediment concentration data are log transformed. The Pearson's Product Moment correlation coefficient of all paired data is 0.71.

Results of a Student's T-test indicate that data measurements were taken without statistical bias. Table A.2 in Appendix II shows linear regression statistics for rating curves fitted to paired observations for the whole data set and smaller subsections. Regression equations are of the form $SSC=aSt^b$ where SSC is suspended-sediment concentration, St is stage and a and b are constants.

A rating curve derived for the whole data set has a poor coefficient of determination of 51% even though the correlation is high. Further analysis indicates that residuals in the dependent variable have a mean value of -50.0 with a high standard deviation and standard error around the mean. Serial autocorrelation of residuals also emerges after analysis.

Since the longest segments of data subsections are comprised of relatively few observations, it is inappropriate to break the record into shorter period individual rising

and falling flows for regression analysis. Rating equations are obtained for longer sections containing both rising and falling flows for three periods: 6 to 7 August, 8 to 9 August and 13 to 14 August. Correlation coefficients are low for the first two segments. The third, however, has a high negative coefficient of -0.84. The rating curve produces 70% of explanation in suspended-sediment concentration from stage data. Hence, with a zero mean of residuals and low standard deviation, this subsection shows close association of stage with concentration. The other rating equations, however, have poor goodness of fits and high standard deviations suggesting that paired data are not closely associated for these periods.

One of the reasons for poorly fitting rating equations in two of the subsections is the influence of hysteresis in the relationship between stage and suspended-sediment concentration. Figure 5.15 shows sequentially plotted paired observations of hourly concentration and stage during the three subsections for which regression equations were derived. Figure 5.15A exhibits a strong clockwise hysteresis loop from 17:00hrs on 6 August to 04:00hrs on 7 August with hourly sediment concentrations peaking on the rising diurnal flow limb. However, an anticlockwise loop characterises the plot from 19:00hrs to 03:00hrs on 8 and 9 August respectively (Figure 5.15B). Here, suspended-sediment concentration reaches a diurnal maximum three hours after peak flow for the day. Finally, peak stage on 13 August is preceded and followed by sediment concentration peaks. This is exhibited in Figure 5.15C which shows plotted paired data from 19:00hrs on 13 August to 07:00hrs the next day. Initially rising concentrations reach the first maxima at 20:00hrs. As flows increase, sediment concentrations fall to a minimum value of 1750 mgl^{-1} at 01:00hrs. However, subsequent declining discharges are accompanied by increasing concentrations to the end of the plot. Thus, since

Figure 5.15 Sequentially plotted paired stage and suspended-sediment concentration data during three different sub-periods in the 1988 Batura record. (A) is from 17:00hrs on 6/8 to 04:00hrs on 7/8. (B) is from 19:00hrs on 8/8 to 03:00hrs on 9/8. (C) is from 19:00hrs on 13/8 to 07:00hrs on 14/8.

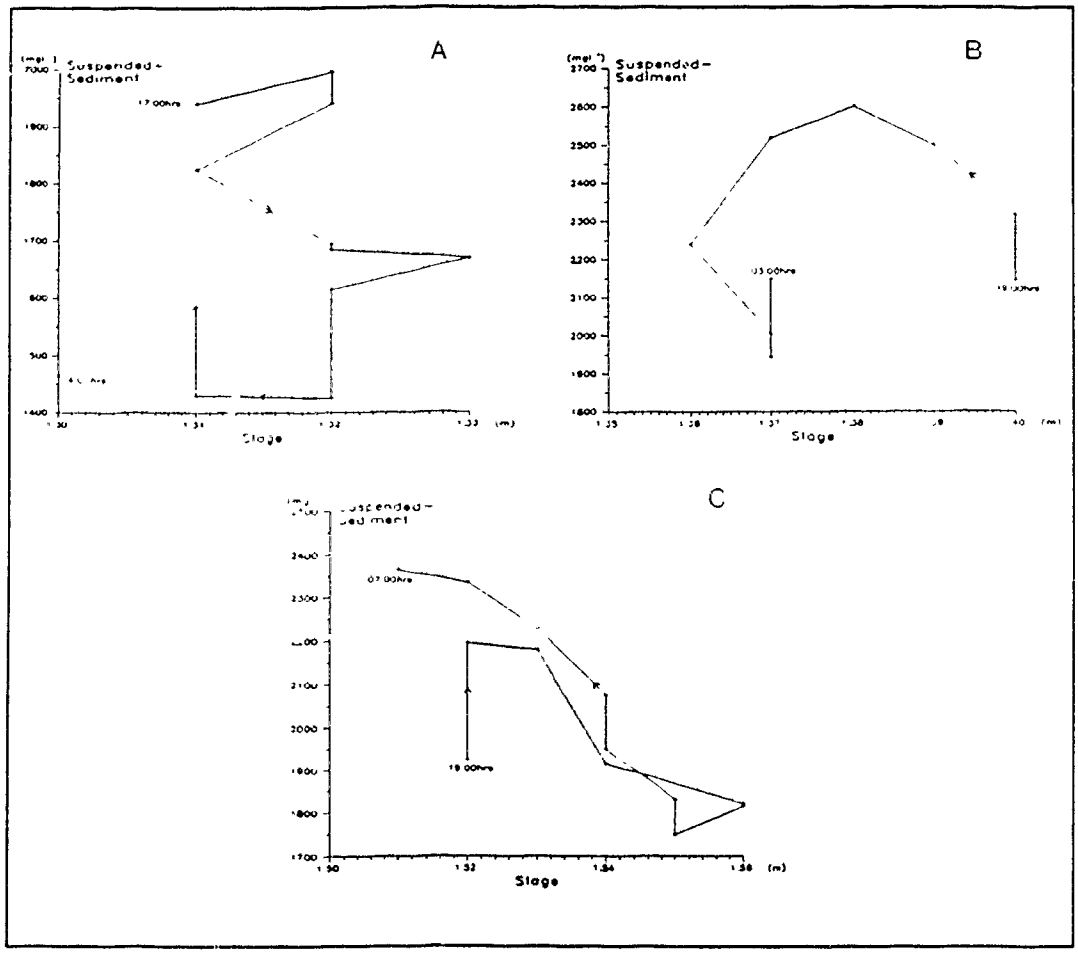

minimum and maximum concentrations and flows coincide, the relationship is more linear than the other two subsections. Hence, a good fit of predicted concentration values derived from the rating curve is a consequence of weaker hysteresis between variables during this subsection of data than for other periods.

5.2.5 Summary of Batura Results

Stage data consist of diurnally fluctuating flow cycles superimposed on a rising daily discharge trend which is a result of sustained favourable melting conditions. Repeating 24 hour flow peaks are in response to variations in incoming solar radiation. Although a lack of hourly suspended-sediment concentration data prevents detailed analysis of sediment transport from the Batura Glacier, during the period of measurement, daily increasing trends of sediment concentration are in phase with rising flow levels. Detailed analysis of selected concentration data segments at an hourly level indicates that sediment concentration maxima occur within a two hour period either preceding or following peak flows.

Analysis of the empirical relationship between flow and suspended-sediment concentration suggests a high correlation between variables during periods comprised of data for the whole series and the subsection from 13 to 14 August. However, linear regression analysis produces rating equations for these periods which neither adequately describe nor explain the relationship between stage and concentration. Serially autocorrelated residuals, as a result of hysteresis in the association between variables, reduce the degree of fit for calculated statistical relationships. Furthermore, hysteresis

loops change suggesting that it is not unreasonable to expect changing stage-concentration relationships on other occasions.

5.3 Data Errors

It is possible that errors in the data have produced biases in the plots of all three variables (discharge/stage, suspended-sediment concentration and electrical conductivity). However, attempts were made to minimise the errors throughout collection of data and subsequent analysis.

In the field during both years, conductivity cells, pressure transducers and sediment sampling nozzles were firmly anchored at sites of measurement so that they did not move from their locations in the rivers. Errors in electrical conductivity records are minimal since all data observations comprise a very gradually changing trace with little or no extraneous noise. For data processing purposes, hourly values were calculated from ten minute observations extracted from the charts. The five values surrounding each hour were averaged to produce on-hour data. Stage data were processed in the same way since downloaded digital data of fifteen minute intervals were averaged using five observations surrounding each hour to produce the on-hour reading. In addition, discharge rating equations for both Nagar and Hispar Bridge were applied to respective data sets. In the absence of the original copies, it is assumed that derivation of these rating equations was founded upon accurate and representative data. However, even if the gauging data were not accurately taken, relative variations in flow would still be useful since automatically measured stage at both bridges was achieved

with precision, *i.e.* relative changes are accurate for the whole period. However, suspended-sediment concentration data provide the most scope for error.

Since sediment samples were taken at an hourly frequency and not over shorter intervals, sampling biases could produce errors in the final data. In the field precautions were taken to reduce such sampling errors (see section 4.1.2). However, due to the turbulent nature of flow in glacier-fed streams, unless huge sediment traps are constructed, it is impossible to completely remove all biases from point sampling of suspended-sediment concentration. Data in both sets are assumed to be fairly representative with trace lines of connected observations composed only of consecutive hourly values; missing values are not inferred from observations on either side in series. Furthermore, outliers have been removed to prevent further bias in empirical analysis. The greatest problems come from comparison of sediment concentration data with discharge. It is assumed that hourly point samples are representative of concentrations during the following hour. Since samples were not taken more often (the clock mechanism on the sampler only had a 24 hour cycle), it is not possible to calculate averaged hourly data from a more detailed data set. This bias might be one cause for the weak statistical relationship between concentrations and flow data. However, lagging the sediment data by one hour does not improve relationships since sediment concentration maxima only rarely coincide with flow peaks during the whole time series. Most days are characterised by pulse events and diurnal concentration maxima which precede or lag discharge maxima by at least two hours. Hence, it is assumed that sampled suspended-sediment concentrations in both time series are representative of hydrological conditions in the Bualtar and Batura Rivers for their respective measurement periods.

5.4 Discussion of Results: A Justification for Choosing a Non-Empirical Approach to Model Flow-Suspended-sediment Concentration Relationships

It is clear that linear regression analysis fails to describe adequately or explain variations in suspended-sediment concentrations as predicted by discharge and stage for both the Bualtar and Batura Rivers in 1987 and 1988 respectively. This failure occurs on all time scales since the relationship is inadequately modelled over whole periods and shorter subsections of the time series. There are various reasons for the lack of explanation afforded by linear regression analysis to explain the relationship.

At a diurnal scale, hysteresis between concentration and discharge data produces serial autocorrelation of residuals from regression analysis. Hence, one of the criteria for linear regression analysis is not met. Since there is an unlimited supply of sediment within both glaciers, the cause of hysteresis between sediment concentration and flow data is related to supply of sediments to the drainage network rather than the absolute volume of stored sediment within the glacier.

Subglacial rivers transport most supplied sediment from the glacier bed and at flow maxima, all proximate sediments will become flushed as stream competency is increased. During periods of warm weather, conduits at the bed laterally expand incorporating newly exposed tills or sediments from the channel margins. Hence, daily transportation during warm weather periods increases in the Bualtar and Batura Rivers as indicated by rising daily flux data. However, supply of sediment to the drainage network from sites of sediment production over the glacier bed is through smaller basal or englacial tributary conduits. Sediment flows in these channels are not constant since conduit configurations are unstable and susceptible to sudden reorganisation in response

to changing flow dynamics of overlying ice. Hence, conduits which have access to high concentrations of sediment in ice or at the base, may become sealed and new channels open which have access to a more limited local supply of material. Sudden random sediment pulse events in the outwash stream may be the result of unworked sediment store inclusions into flow as channels migrate across their bed and within the ice. This appears to be a common occurrence in the Bualtar record which is characterised by frequent spikes in the sediment concentration time series. However, another factor influencing the timing of sediment discharge maxima is related to the recent history of the hydrograph.

At times of rising discharge, flowing water may re-entrain channel sediment which has been deposited on previous recessional flow limbs. If such local sediment stores are unlimited, maximum sediment transport rates will coincide with peak flows. Subsequent rates of decline in concentration will be greater than rates of increase for each diurnal cycle since sediment supply becomes exhausted as flows increase thus reducing availability of sediment for removal on falling hydrograph limbs. However, depending on the magnitude of increasing flow, limited sediment supplies may become exhausted at times of increasing diurnal flows. Concentrations of fluvially transported sediments in suspension may peak before discharge reaches its daily maximum. Discharge levels at which sediments were laid down are critical for re-entrainment on later occasions since unless previous flows are exceeded, stream energy will not be capable of re-initiating debris removal. Hence, flushing events are characterised by simultaneously increasing concentrations and flow levels to the point either at which limited local sediment supply is exhausted or when flow levels reach their point of maximum energy. The former is characterised by peak sediment transport rates prior

to flow maxima as available sediment is flushed followed by sharply falling concentrations as a result of sediment exhaustion. The latter is described in sediment and discharge time series by simultaneously peaking variables, again with high rates of sediment concentration decline on falling hydrograph limbs. Both phenomena are shown in the Bualtar and Batura time series on several occasions during the measurement periods. For hours or days afterwards, sediment concentrations may remain low since waters do not have access to readily available sediment supplies. If exhaustion occurs on a rising trend of daily discharge, concentrations may decline as increased flows and reduced sediment supplies cause dilution of outwash waters, for example on 18 August, 1987 in the Bualtar River. If an unremarkable maximum flushing event of stored sediments coincides with peak flows for a period, subsequent suspended-sediment concentrations may remain high as a result of a concentrating effect produced by lowered water volumes and non-exhaustion of sediment supply. This could explain flow in the Bualtar River after the discharge maximum for the entire period on 20 August. However, the main flushing event for the whole series occurred two days prior to this peak flow suggesting that all available sediment was removed. Hence, maintenance of high sediment concentrations in meltwaters might have been related to three processes. Firstly, sudden reorganisation of secondary conduits within the glacier may have created increased availability of fresh, unworked sediments for removal. Secondly, increased sediment concentrations from the Barpu Glacier might have maintained high concentrations. Finally, new stores of sediment may have become impinged upon by glacial meltwaters as a result of supply exposure caused by changing glacier ice dynamics.

Maximum rates of sediment transport from both glaciers are also exhibited on falling flow limbs indicating that another mechanism must be involved in removing sediment from within the glacier environment. At times of maximum discharge increase, water flow in main arterial Röthlisberger or Nye channels may occupy the entire channel cross-section. Mechanical friction with ice enlarges the cross-sectional area at a rate exceeding the ice overburden pressure (Röthlisberger, 1972). However, channel enlargement takes place over several days and does not produce significant changes from one hour to the next (Shreve, 1972). Hence, excess water probably becomes forced out beneath the glacier at the ice-rock interface and joins secondary tributary conduits. Assuming adequate supply, raised water levels in the peripheral channels facilitate increased removal of glacially eroded sediment. Subsequent increased concentrations in the outwash channel after peak flows may result from a delayed contribution by these smaller channels to arterial flow. Excess water, which becomes forced out of the main channels at high flow, may also become stored at the bed and might not be released until impinged upon by smaller subglacial channels. Depending on the size of water pool, sudden inclusion into the fluvioglacial network may cause pulses in sediment transport in the outwash channel.

The complexity of interplay between sediment transfer processes is undoubtedly the main reason why statistically derived relationships between suspended-sediment transport and flow rates in glacier-fed streams have limited success in describing time series. The inability of empirical models to account for acting geomorphological processes within the glacier produces poor predictions of changing streamflow characteristics. Furthermore, temporally varying hydrological characteristics in outwash meltwaters do not only reflect current conduit configurations, availability and magnitude

of sediment sources, general glacier motion and rates of bedrock weathering by ice within the glacier system, but also depend on the recent historical variations in hydrological characteristics in the glacial system. Although some recent papers have sought to address this historical aspect using time series analysis (e.g. Gurnell and Fenn, 1984a), fundamental processes are ignored allowing results of simulations, often with high degrees of fit, to be based on pure statistics. Therefore, it is the intention here to diverge from traditional empirical techniques and employ a process-orientated approach which eventually might result in a more realistic explanation of the relationship between subglacial weathering of bedrock and hydrological characteristic in two glacier-fed streams.

Chapter Six

Development of a Model of Sub-glacial Erosion

6.1 Introduction

Investigations of empirical relationships between discharge and suspended-sediment concentration in glacier-fed streams have been described by several authors for various periods of measurement in different rivers (e.g. Bogen, 1980; Collins, 1979a; Gurnell and Fenn, 1984a; Liestøl, 1967; Østrem, 1975). Although useful for understanding certain aspects of sediment supply and delivery through fluvioglacial systems, results are founded upon techniques which are purely statistical by nature. Hence, it is dangerous to apply empirically derived rating relationships to data outside time series upon which such models are based (Klemeš, 1982). Furthermore, within control data sets, series of short duration trends observed over several hours indicate that fluctuations of both discharge and sediment transport will complicate statistical sediment-discharge relationships. Thus, it is hoped that predictive capabilities of these relationships will be improved by implementing and improving a process-orientated, finite differencing model as devised by Keeley (1986).

The model has been adapted from its original form which predicts changing suspended-sediment concentration in fluvioglacial streams. Processes of subglacial weathering and subsequent fluvioglacial removal of weathered sediments by meltwaters

are the main factors affecting sediment characteristics in outwash streams. Hence, prediction of suspended-sediment concentration has been modified to prediction of suspended load since both rates of weathering and fluvioglacial debris transfer characteristics are reflected by sediment load to a greater extent than by concentration.

6.2 Model Design

6.2.1 Description of the Model and Assumptions

The model is driven primarily by subglacial water flow in the central R-channel. An assumption is made that water flow in the outwash channel is composed entirely of subglacial meltwater from the arterial conduit. It is likely that waters beneath the Bualtar and Batura Glaciers are channelled into an arborescent network system which becomes increasingly divergent from the main channels further up-glacier. However, since it is impossible to inspect directly either subglacial and englacial sediment sources or the routing of water within both glaciers, the model envisages each glacier as a one dimensional cross-section at a flat ice-rock interface comprised of different cells each of which has a sediment capacity.

The profile width is delineated by the number of cells within the glacier; larger glaciers will have a greater width with more cells and total sediment loading while smaller glaciers will have fewer cells. When simulating sediment transport from glaciers of different sizes, initial choice of width for each glacier is arbitrary since an expression of relative glacier size is needed rather than absolute size. A central,

primary cell contains the main drainage channel comprised of water and suspended-sediment. The channel never closes during winter and persists over melt seasons. Peripheral, secondary cells on either side of the main channel have capacities which are less than that of the main channel. At the start of the period, all cells are initialised with a sediment content. If modelling begins at the start of the season (spring melt), all secondary cells receive the same content which represents eroded and deposited sediment from the winter plus deposited fluvioglacial material from previous meltwater activity at the bed i.e. from the preceding summer. If modelling begins at any other time during the summer, the initial sediment store in the main channel is small since water constantly flushes sediments from the river during the season. In the peripheral cells after the spring melt, sediment in each cell decreases from the profile extremities towards the central channel. The reason for this is related to the way in which meltwater flushes each cell at each timestep (time interval) as explained below.

At each timestep, water is supplied to the main channel cell in response to release of stored water from surface melt and englacial pools. Initial channel capacity is defined by a previously dominant discharge using a mechanism related to the channel geometry equilibrium theories proposed by Röthlisberger (1972) and Shreve (1972). Channel expansion is driven through frictional melting by conduit water on the sides while channel closure is the product of ice overburden pressure. Hence, in the model design, if discharge exceeds channel capacity, conduit cross-sectional area becomes enlarged for the next time interval. The increased water pressure at this time forces water to spread out over the cross-profile into secondary cells (a process modelled by the WASH function). If discharge in the main channel is less than the previous channel capacity, pressures are too low to cause lateral spreading of water over extensive bed

areas and flows are confined to the arterial conduit. Furthermore, the sediment capacity of central cell decreases for the next timestep since the influence of ice overburden pressure on conduit size becomes greater than frictional melting of the sides.

With the exception of the central cell, sediment is supplied to each secondary cell in the cross-profile at a constant rate (a process known as recharge). This is in response to direct, in situ, subglacial erosion of bedrock. All methods of weathering (see section 2.3.1, Chapter 2) are included in the model and the rate of supply of material to the bed does not change over the period of simulation. Peripheral cells have a pre-determined finite capacity which, once reached, does not permit further deposition of eroded sediment into "full" cells. Sediment is supplied to the main channel from in-channel scour and abrasion by fluvial action since erosion of bedrock by ice here is minimal. The magnitude of sediment erosion by the river (RECHX) varies depending on channel capacity determined in the WASH function. At greater excess water flows, RECHX increases since flowing meltwater has more available energy for erosion.

It is assumed that sediment removal from glacier systems increases proportionally with raised arterial water flow levels. When flow in the main channel exceeds channel capacity and water is washed out into the peripheral regions, sediment is removed from the secondary cells as a result of entrainment. Debris-laden water subsequently re-joins the main channel and is expelled from the glacier at the terminus. The magnitude of sediment transport in the outwash stream depends on the number of cells activated during lateral spreading of water from the main cell; the greater the excess water, the more secondary cell sediment loadings are incorporated into the final outwash. However, when excess water reaches a cell, not all debris is flushed since the amount of sediment removed from each cell at each timestep is proportional to

proximity of the cell to the main channel. Available energy in water for debris entrainment decreases for a given flood with increased distance from the channel. Thus, during rising flow limbs, cells located close to the main channel have most of their deposits removed. Cell flushing decreases with distance from the conduit so that remote cells in the profile have less sediment removed. This is the reason why initial sediment loading in each secondary cell is not constant for all cells when modelling is initiated during periods after the spring event. Initialisation depends on the balance between previous flows, channel geometry and sediment loading in secondary cells as a result of sediment production at the bed. At the next timestep, eroded sediment from the glacier bed (RECH) is added to remaining sediment in each cell from the previous timestep. It is hoped that this refinement to initialisation and removal of sediment from each cell will improve sediment transport prediction.

Excess water calculated by the WASH function depends on comparison between instantaneous flow magnitude and a previous average flow magnitude derived from a preceding period in the time series. Rate of increase in discharge controls the number of cells affected by excess flushing of water on an increasing flow limb. During rising flow limbs, simulated sediment concentrations are greater than for similar flow levels on falling hydrograph limbs when excess water is less and fewer cells are incorporated into the outwash. This relates well with characteristic sediment-discharge hysteresis relationships in glacier-fed streams which produce diurnal sediment concentration and transport maxima on rising hydrograph limbs when rates of increasing flows are greatest (Richards, 1984). At times of minimum flow, only a relatively few cells close to the main channel have subglacially eroded material removed since excess wash is

minimal. In this case, suspended-sediment loads in the outwash stream are lower than at times of increasing flows.

In conclusion, the model attempts to account for historical aspects of sediment transport in glacier-fed streams. This is achieved primarily on two scales. Firstly, over long periods of several days, the size of central channel changes depending on varying flow levels prior to the time of modelling. Hence, the relative magnitude of flow at each modeled timestep compared with the pre-defined channel capacity influences the amount of debris flushed from the system as sediment flows are activated from outlying cells. Secondly, on a diurnal time scale, at times of increasing flow, more sediment is removed from the system than for similar flows over recessional flow periods. This short-term process is superimposed on the changing day to day flow levels and is accomplished through the WASH function.

6.2.2 Model Parameters

The five parameters employed by the model are conceptualisations of processes operating at the glacier bed during each year. The reason for using so few is to keep the model as simple as possible and to minimise the chance of obtaining results based on spurious relationships in the model. If many more parameters are used, the risk of spuriousness between relationships increases since the number of possible combinations of parameter values increases. The five parameters used are (Keeley, 1986):

RECH. This parameter defines the rate of sediment supply to each secondary cell at the glacier bed. Sediment is constantly delivered at each timestep to cells through subglacial erosion including bedrock failure, bedrock abrasion by ice and sediments in the ice, and the mechanical action of water on the bed at the ice-rock interface. Sediment is also delivered to each cell by melting of debris-laden ice from above;

RECHX. This parameter dictates the rate of sediment recharge made to the primary cell containing the subglacial channel. Subglacial erosion has a minimal effect in the central channel so sediment is produced through in-channel weathering by water on bedrock. Hence, the variable size of RECHX is directly related to channel capacity since wider channels have more opportunity to weather their basements than smaller ones. During the ablation season, the primary cell is always larger than secondary cells so RECHX is always greater than RECH;

FULL. Secondary cells have a finite capacity which once reached, prevents further accumulation of sediment. Once a cell is full, the sediment armours the bed from subglacial weathering. In this state, sediments become deformed. Furthermore, the sediment in the cell insulates the overlying glacier sole from geothermal heat fluxes from below which contribute to melting of basal ice. Hence, sediment meltout from within glacier ice is retarded. FULL is held constant and represents the point at which no more sediment is added to each secondary cell;

INIT. Sediment loadings in each secondary cell at the start of the modelling period are initialised by the parameter INIT. If simulation begins at the very start of the melt season, the first loading value is added equally to each cell representing the winter accumulation of subglacially eroded sediments and material deposited during most recent flows. However, if modelling begins later in the season, it is assumed that all cells do not contain equal amounts of sediment as a result of varying subglacial activity through the season (weathering, deposition and flushing). Hence, increasing fractions of INIT are added from the central cell outwards towards the margins where it is likely that minimal fluvial action has taken place;

INITX. This defines initial sediment loading in the primary cell at the onset of modelling. The parameter relates to accumulated sediments in the main conduit as a result of deposition or weathering during a previous period. At the beginning of the ablation season, INITX represents sediment build-up as a result of deposition from previous year's flows and winter erosional activity at the bed by ice. In this case INITX is always larger than INIT since the main cell is larger than the peripheral cells. However, if monitoring begins later in the season, INITX is small since sediment is constantly flushed from the conduit during previous flow events.

All parameters are expressed as weights of subglacially-eroded sediment with units in mg. Sediment particle size distribution is assumed to be homogeneous in each cell and across the whole profile.

6.2.3 Data Set Requirements

Ideally, modelling requires two sets of flow data for simulation of suspended-sediment load. The first set is used to calibrate the model in preparation for simulation of the second set.

Calibration entails model parameter optimisation. Optimum values are chosen which produce the best fit of predicted sediment load when compared with the actual measured sediment load for the chosen calibration period. However, selected parameter values must remain physically realistic not only in terms of the processes which they represent, but also with respect to the other parameters used.

Once calibration has been achieved, the second data set is used to establish how well the model performs. By comparing simulated with actual data, the validity of the model can be established. If optimum parameter values generate data that do not predict actual observations, the algorithm has to be re-assessed. Hence, model performance is dependent on the representativeness of calibration data subsets compared with the rest of the data. If subsets are unrepresentative, simulation predictive power is reduced. This factor has great importance for modelling fluvioglacial sediment transport since water quality characteristics are temporally variable.

6.2.4 Programme Description

The programme used to simulate processes within the subglacial environment is shown in Appendix III. Originally, the algorithm was developed in Fortran 77.

However, conversion of the model to Turbo Pascal 5.0 was undertaken in order to increase versatility for this user. Seven main components contribute to the model design. The relationship between each part is schematically represented in Figure 6.1.

Part 1 of the model prompts for the five parameters described above and reads the discharge or stage data set into an array Q[K]. The number of cells along the cross-profile at the bed of the glacier is defined by the constant WIDTH and the period used as a reference from which to calculate previous channel capacity is defined by KKMAX. Contained within this first section is the procedure FLUSH.

The second part of the model initialises all cells with a store of sediment, the magnitude of which is defined by INIT and INITX. Since discharge, sediment concentrations and loads in the Bualtar and Batura Rivers were measured in late summer, both INIT and INITX are small because sediment supplies at the bed will have become depleted. The original model has been adapted to account for the decreasing energy of water for entrainment as it becomes forced under pressure away from the central cell. Unless modelling begins at the onset of the spring melt event, subglacial removal of sediment by river activity is assumed to have taken place during the summer leaving only small quantities of debris in accessible areas of the bed close to the main channel and large stores untapped towards the margins.

Part 3 calculates the size of central channel for the WASH function in Part 4. At each timestep, channel capacity is proportional to average flow for the previous 24 hours (AVQ). At the start of the modelling period, when there are not enough previous observations to generate a 24 hour average, a subsidiary parameter INITQ is used to define the channel capacity. For convenience when modelling 1987 and 1988 data,

Figure 6.1 Schematic flow diagram of a model of subglaciai erosion.

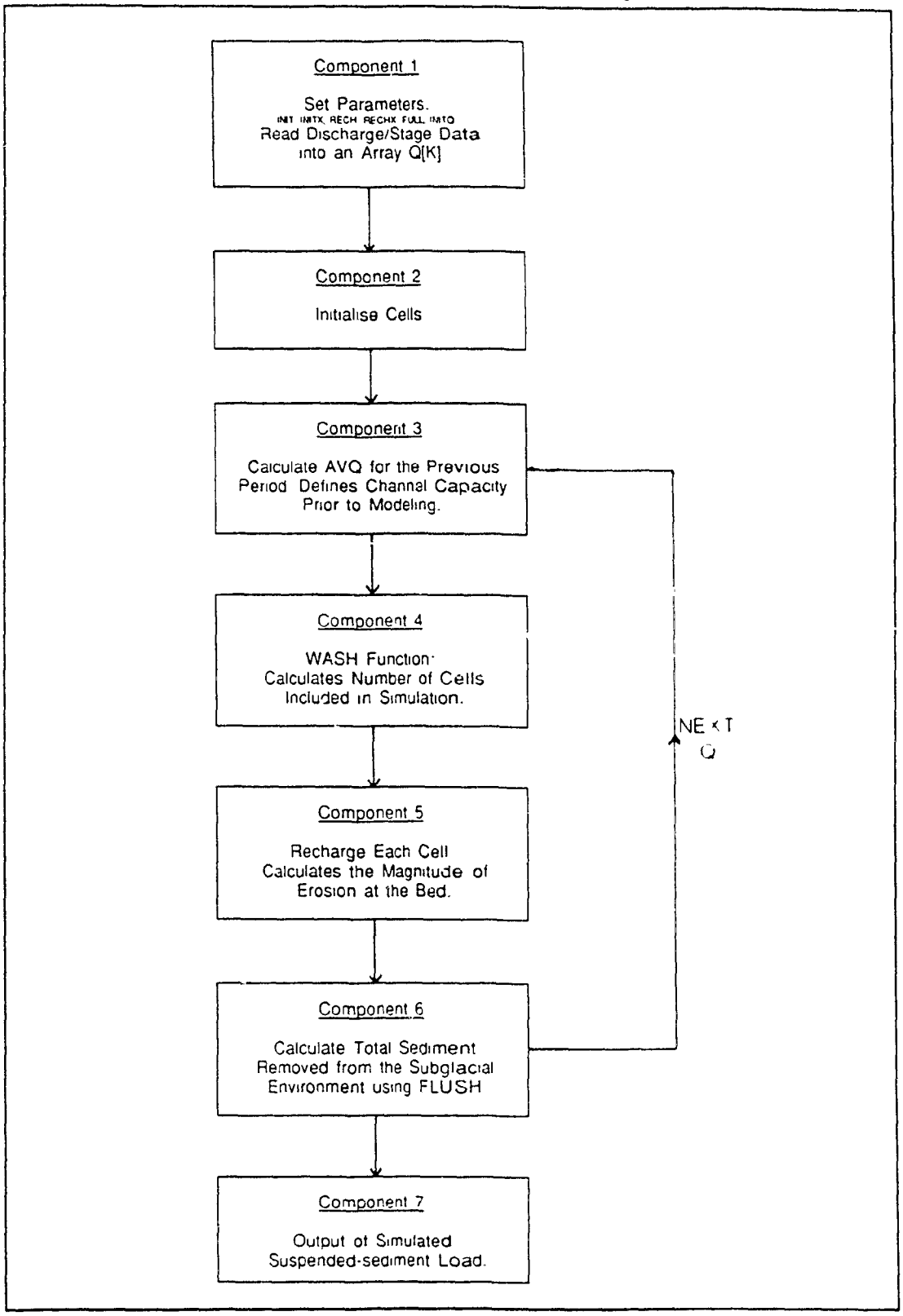

INITQ was set equal to the first discharge observation since previous discharges were not known.

The WASH function is the fourth component in the model. This converts flow in the main channel to a lateral flood if discharges are greater than previous 24 hour flows (AVQ). WASH is calculated from the equation:

$$WASH = \frac{[Q(K).A - AVQ.A]}{X} \qquad (6.1)$$

where Q[K] is the flow at each timestep, A is a conversion factor depending on whether discharge or stage is used, AVQ is the channel capacity and X is a constant which is related to the position of water flow observations in the time series. The role of A is to convert channel discharge or stage magnitude in ɔ an integer value which determines the number of cells affected by the flood. If stage is used, A is set at 100 and if discharge data is used, A becomes a factor converting real observations to integer values. If Q[K] is on a rising diurnal limb, X is less than 1 producing a large WASH; if Q[K] is on a receding flow limb, X is greater than 1 resulting in a smaller WASH. Thus, an attempt has been made to adapt the original model to include a "clockwise" hysteresis relationship between sediment transport and discharge. In the WASH function, rising flows produce greater lateral spreading of water than similar discharges on falling hydrograph limbs. Hence, potentially more sediment is flushed on these occasions than on receding limbs.

Part 5 is the section which relates sediment erosion at the glacier bed to the model. At each timestep, weathered debris is added to each cell at the bed at a

constant rate. It is envisaged that at times of increased glacier sliding, erosion at the bed increases providing cells with a greater sediment loading. Since ice velocities of both glaciers were not measured, it is assumed that the rate of recharge to each secondary cell is constant throughout modelling periods. Recharge of sediment to the main cell is a function of WASH since at times of greater discharge, fluvial erosion at the bed increases.

Part 6 initiates the FLUSH function which calculates the magnitude of sediment removed from cells encompassed in the WASH function at each timestep. For a given WASH, incorporated cells distant from the central cell have less sediment entrained than cells close to the main conduit. This is also a modification to the original model since subglacial sediment stores which are remote from the main conduit accumulate sediments that do not become flushed until high magnitude flows. Total sediment removed from the glacier at each timestep is the total amount of material mobilised in each cell by flood water. At this point, the modeled sediment is expressed by a concentration. The total load is calculated from the product of predicted sediment concentration and the original discharge or stage. If stage is used to drive the model, predicted sediment load is an index.

Part 7 sends predicted suspended-sediment load data to the output file in preparation for analysis of results.

6.3 Results of Modelling

Results of modelling are presented in two sections. Firstly, simulation of 1987 Bualtar suspended-sediment load data is reported and secondly, modelling of the Batura sediment flux in 1988 is described. It is intended to relate only the best-fit predictions for both sites and not all simulations since emphasis is placed on demonstration of comparative effectiveness of the process orientated approach with an empirical strategy. However, calibration of the model can be achieved using various combinations of different parameter values. Thus, references are made to different simulations in order to clarify rationales behind the final choices.

Predictions of sediment load based on optimised parameters used by Keeley (1986) are not appropriate here for four reasons. Firstly, since modelling sought to simulate suspended-sediment concentrations in 1986, re-calibration is required if sediment flux is to be predicted. Secondly, changes to the design of component parts within the algorithm, necessitate changes to input parameters. Thirdly, in 1986, collected stage data was used to drive the model which has now been adapted to incorporate either discharge or stage data. Finally, temporally varying glaciological, hydrometeorological and fluvial conditions in subglacial environments of different glaciers will produce a wide variety of inter-relationships between subglacial processes represented by the model. Hence, in 1986 conditions were different from those in 1987 and 1988.

6.3.1 Bualtar River

The best-fit prediction of suspended-sediment load in the Bualtar River during the measurement period in 1987 is shown in the time series plot in Figure 6.2. Calibration of the model was achieved using hourly discharge data for the first ten days of monitoring from 30 July to 8 August. This period was chosen because although the sediment record contains missing data, variability in daily flow levels is relatively high. Calibration parameters are also shown in Figure 6.2.

The number of cells chosen for the cross-profile is 1000 (WIDTH) and AVQ is the mean discharge from the 24 hour record prior to each time interval (KKMAX=24). Modelling was undertaken for data in the late ablation season. Hence, INIT and INITQ are assigned low values (20 and 30 mg respectively) compared with those used by Keeley in 1986 since it is assumed that accessible sediment available for removal earlier in the season had been flushed before data were collected. Also, the conduit network at this time will be at its maximum efficiency (Collins, 1989). Hence, RECHX is given a value which is considerably greater than RECH because in-channel scour of the conduit bed produces more significant amounts of weathered material in the channel than are produced in each peripheral cell. The capacity (FULL) of each secondary cell is large because it is envisaged that with progressively increased erosive and fluvial action at the bed through the summer, subglacial storage capacity of sediment increases. INITQ is set to the first discharge value in the time series.

Day to day fluctuations in simulated sediment load are in phase with actual values for the whole data set. For the first ten days, magnitudes of predicted observations are fitted well with measured data. This is to be expected since calibration

Figure 6.2 Predicted (dashed line) and measured (solid line) suspended-sediment load in the Bualtar River, 1987: the inset shows calibration parameter values.

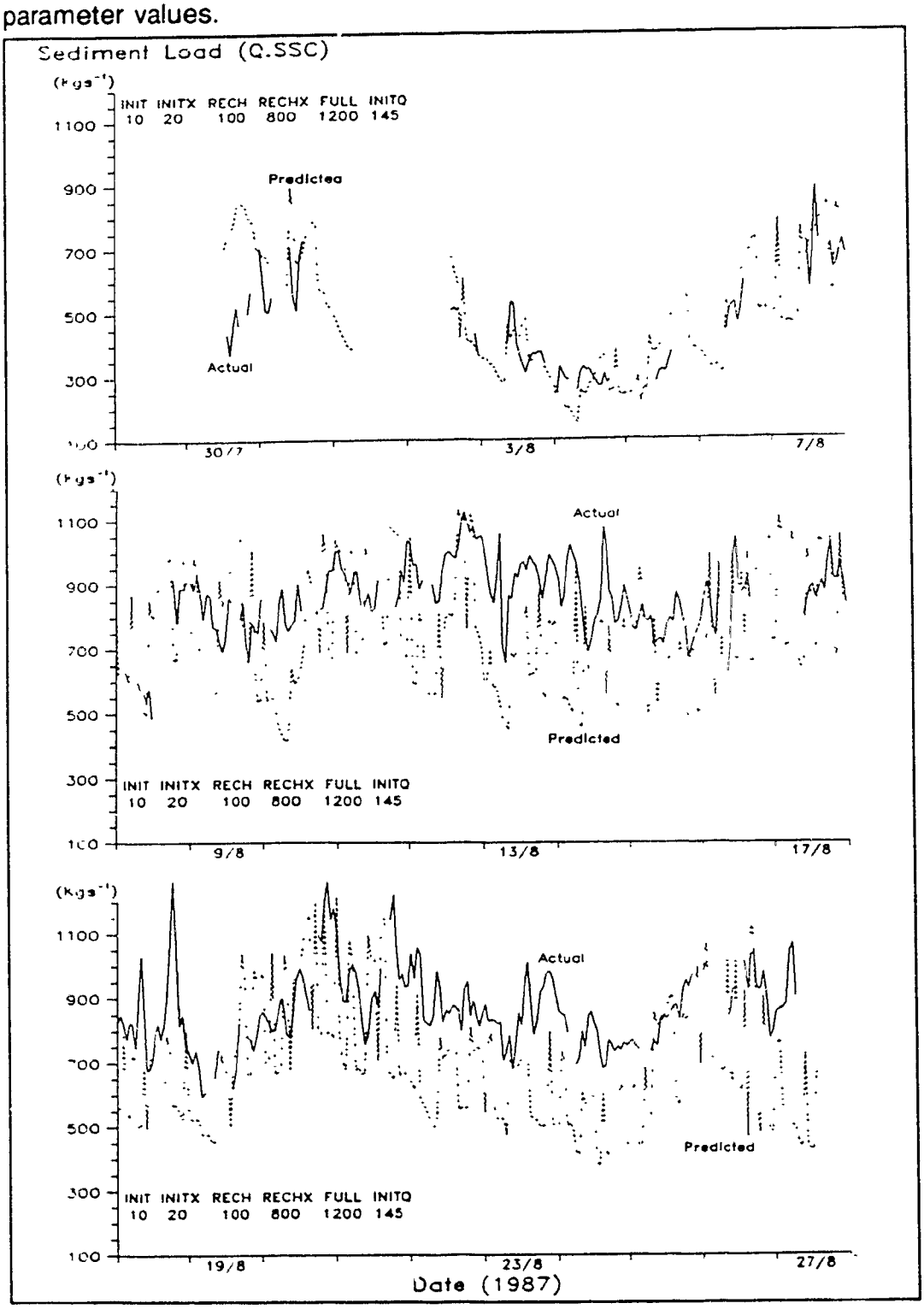

of the model was undertaken using this data sub-section. From 11 August onwards, simulated data generally show levels of sediment flux lower than those of actual sediment load. However, the magnitude of fluctuation at this time scale is the same order of magnitude as that in the actual flux series.

The short-term trend in the simulated data series is characterised by frequent, high magnitude fluctuations of 200-300 Kgs^{-1} over 1-4 hours. On several days, predicted sediment maxima almost coincide with measured values in both timing and magnitude, for example, at 19:00hrs on 12 August and at 10:00hrs on 16 August. Furthermore, short duration variations in predicted load maxima temporally coincide with measured load although relative magnitudes of these variations have a poor fit. Maximum measured load on 18 August is not predicted well by the model since sediment fluxes only slightly increase from the declining daily flux trend.

Figure 6.3 is a scatter plot of paired predicted load and measured flux. There appears to be a direct relationship between variables shown by a linearly increasing trend in the plot. However, this trend is not strong since data are spatially dispersed in the plot between 600 and 1000 Kgs^{-1}. The correlation coefficient between predicted and actual sediment load is 0.54. The standard deviation of predicted load is 218 Kgs^{-1} (for measured data, the standard deviation is 198 Kgs^{-1}) with a mean value of 658 Kgs^{-1} for all observations (for measured data, the mean is 795 Kgs^{-1}). Plotted histograms of measured and predicted load reveal near normal distributions for both sets of data although simulated data are slightly negatively skewed and measured data are slightly positively skewed. It should be noted that the incomplete observed load data set introduces bias to comparisons between standard deviation tests for measured and predicted data.

Figure 6.3 Scatter-plot of predicted and observed suspended-sediment load in the Bualtar River, 1987: the inset shows calibration parameter values.

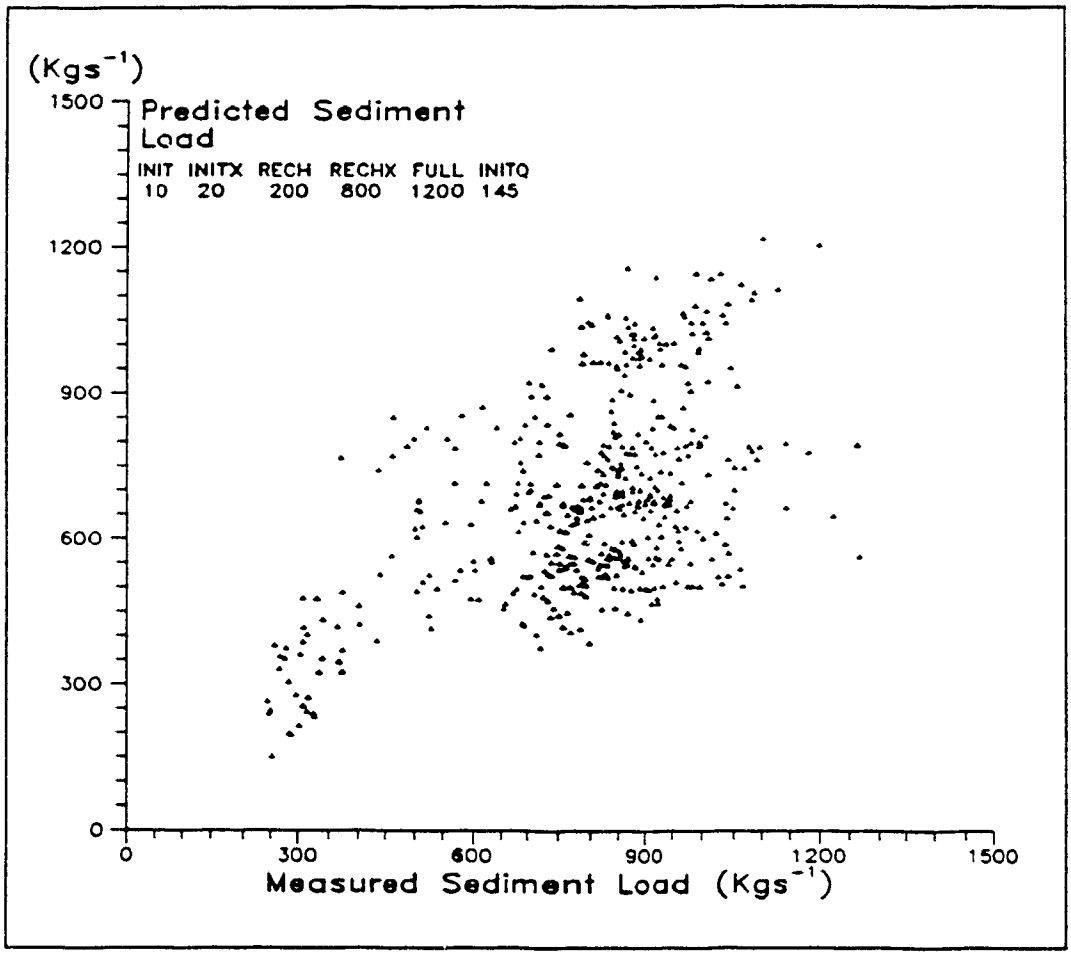

Calibration using different parameter values produced different output results. INIT and INITX and INITQ remained unchanged during parameter optimisation while the other three were varied. By reducing FULL and keeping RECH and RECHX constant, the magnitude of fluctuation decreased since more cells became full with sediment and subsequent erosion at the bed effectively stopped. Consequently, modelling of minimum fluxes improved at the expense of peak load prediction. Also, fluctuation in daily variation became less pronounced. If FULL was raised above 1200 mg, amplitude of short-term sediment load fluctuations increased since larger capacity cells were flushed producing a greater standard deviation in the predicted data set.

By increasing RECH and keeping other parameters constant, daily load levels were increased with a reduction in variability at this time-scale since erosion at the bed became more pronounced and cells became full more quickly than before. If RECH was decreased to less than 200 mg, both daily flux magnitudes and daily variability decreased in response to reduced erosion activity at the bed. Increasing the erosion rate in the conduit (RECHX) produced increased amplitude of simulated sediment flux data on a day to day basis. By reducing RECHX to values less than 800 mg, daily variations became smoothed during the main section of data producing large residuals between predicted and observed sediment load values. This was because contribution of sediments to the outwash channel from the main conduit was reduced and peripheral cells became the dominant source.

6.3.2 Batura River

The best-fit prediction of the index of sediment load in the Bualtar River is shown in Figure 6.4. Unfortunately, the paucity of suspended-sediment concentration data does not permit satisfactory calibration of the model using a smaller sub-set of stage and sediment observations from within the main data set. Hence, this data set is treated as a calibration run to establish what might be appropriate parameters to use to predict the index of fluvially transported sediment from the Batura Glacier during middle to late ablation seasons. Since discharge data are not available, stage is used to drive the model and new parameter values have to be employed which are different from those used in simulation of the Bualtar data.

The number of cells chosen to comprise the cross-profile was 2000 since the Batura Glacier is larger than the Bualtar. Again, modelling was undertaken for data collected late in the ablation season so INIT and INITX values are small. Since WIDTH is large, the sediment capacity of individual cells (FULL) is reduced compared with those used in prediction of Bualtar data. By decreasing the value used for FULL, total sediment storage at the bed is not decreased because the total number of cells in the profile is increased. Furthermore, few continually active cells near the river channel became full since daily discharge increased during the time period preventing hourly accumulated sediment to completely fill cells located in the central region of the profile. RECH and RECHX are also smaller because the WASH function used is more powerful for stage data than that used for Bualtar simulations. The relative magnitude of these parameters is more important than absolute sizes; for optimum results, RECHX is five times greater than RECH suggesting that erosion of sediments and bedrock by

Figure 6.4 Predicted (dashed line) and observed (solid line) index of suspended-sediment load in the Batura River, 1988: the inset shows calabration parameter values.

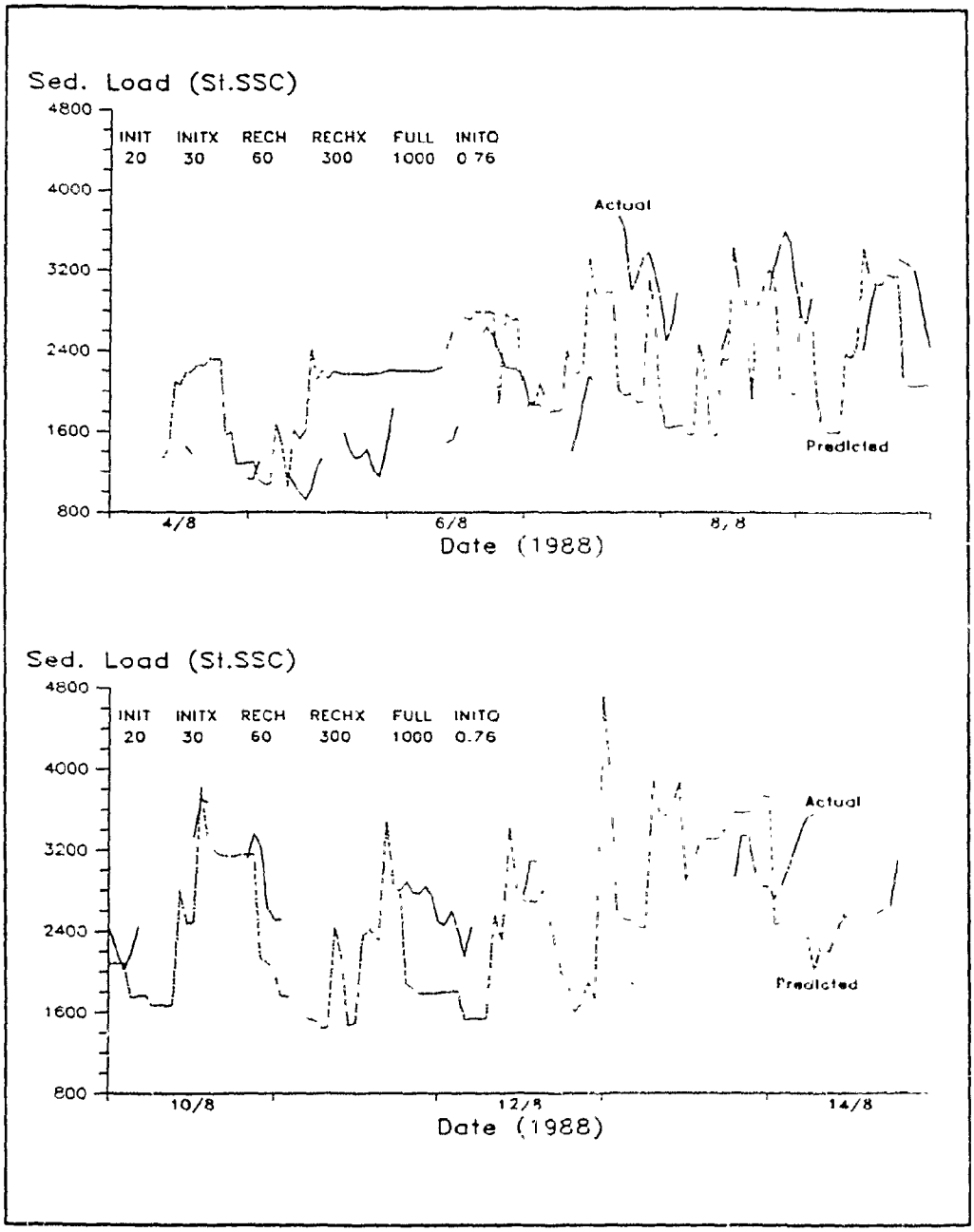

the glacier is more important beneath the Batura than beneath the Bualtar Glacier where RECHX is eight times greater than RECH.

Validation of predicted suspended-sediment load in Figure 6.4 is not easily achieved due to a lack of observed sediment flux data. However, the daily record appears to be proportional to observed data and the diurnally varying nature of sediment delivery from the glacier is accurately modelled.

On 10 August, the peak sediment load for observations during the day are simulated well by the model since timing and magnitude of the first peak at 12:00hrs is accurately predicted. In addition, timing of the second maximum sediment load on a rising flow limb is accurately predicted although magnitude is underestimated because cell sediment flushed during a period of increasing discharge was not recharged in time for the second flow maximum. On 9 August, the magnitude of maximum sediment load is accurately predicted although its timing is too soon. One problem with the simulated data is that missing stage data on 12 August causes overprediction of the next sediment load value. The reason for this is because sediment is recharged to each cell during this period, AVQ is derived from INITQ when simulation resumes rather than AVQ. Consequently, if the break is towards the end of a rising flow limb, excess water volumes produced by the WASH function are great since lateral spreading is derived from current flows and flows at the start of the monitoring period.

The daily variation in predicted load in Figure 6.4 appears to vary proportionally with observed flux levels. However, the exact nature of this characteristic is difficult to validate due to lacking observed data. A scatter plot of paired predicted and observed sediment load data, shown in Figure 6.5, suggests that there is little relationship between simulated and measured sediment load. The mean predicted flux

Figure 6.5 Scatter-plot of predicted and observed suspended-sediment load indicies in the Batura River, 1988: inset shows calibration parameter values.

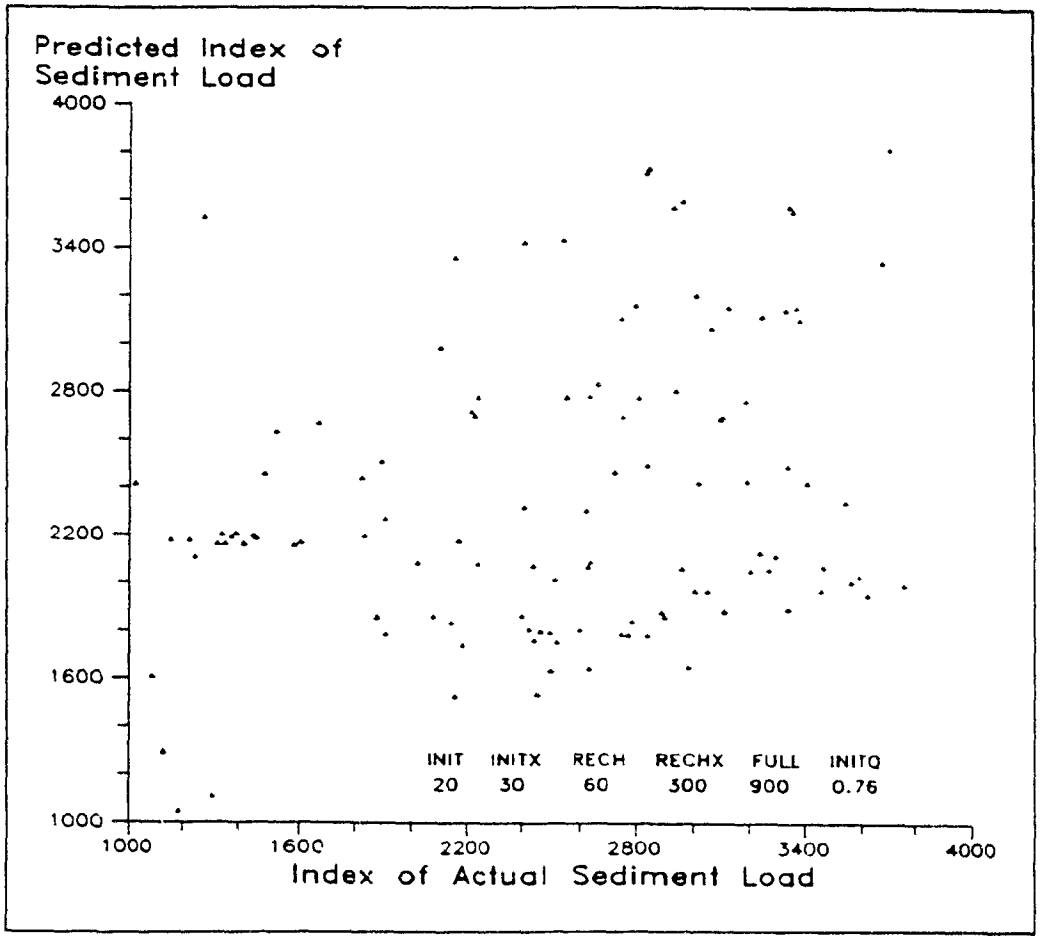

index for all simulated data is 2339 (for observed data it is 1858) with a standard deviation of 670 (for observed data it is 473). Histograms plotted for simulated and observed show that data set distributions which are not normal. Predicted data appear to be more randomly distributed over a wider range of values than observed data which are positively skewed. However, statistical tests are inconclusive because comparison between observed and predicted sediment load index data is biased due to unequal population sizes.

Parameters were varied during model calibration and a variety of predicted sediment flux records were generated. The main problem encountered during parameter optimisation was that for each combination of parameter used, comparison of model output with observed data was fraught with difficulty due to the lack of measured sediment flux data. Nevertheless, values of input parameters were altered in a similar manner to that used during calibration of the model for the Bualtar data. Although on a different scale, resulting variations in predicted sediment flux data were similar to those observed for the Bualtar data.

6.3.3 Summary of Subglacial Modelling Results

The model generated suspended-sediment flux data with varying levels of success. Coincidence of sediment load over 24 hour periods for both simulated and observed values in the Bualtar series was apparent on several occasions with good prediction in magnitude and timing of measured flux data. However, the maximum recorded sediment load was not predicted by the model since highest sediment loads

were generated two days after the measured peak. Frequent fluctuations of simulated data over 1-4 hours corresponded well with fluctuations in the observed series although through most of the predicted record after the calibration period, underestimation was a dominant feature. Underprediction of magnitude of observed data was also exhibited by low absolute values in the predicted daily sediment load record. However, relative variations in daily load were simulated with success. This was demonstrated in the time series by similar changes in timing and magnitude of observed and predicted sediment loads.

The Batura sediment load record was more problematical for prediction purposes because calibration was not possible due to the short duration and broken set of measured sediment record. Consequently, the sediment data set was not easily modelled since validation of simulation results depends on frequently monitored and precise discharge and suspended-sediment data. However, agreement between observed and predicted data was demonstrated on occasions during three days and a general rising trend in observed sediment flux was predicted.

Direct comparison of model performance for Bualtar and Batura River sediment load data is not possible because the model is driven by discharge at one site and stage at the other. The most important reason for this is because the WASH function is adapted specifically to suit available flow type. However, if comparison of modelling between sites is a primary objective, intrinsic constants which are not functionally related to stage or discharge (for example, width of glacier must be set with respect to other glaciers.

Chapter Seven

Discussion and Conclusion

7.1 Comparison Between Empirical and Causal Model Performances

It is shown that the nature of sediment delivery to fluvioglacial channels is highly complex involving several different processes in the glacier environment. Consequently, results from prediction of suspended-sediment loads in two glacial meltwater streams using simple empirical and causal models are inconclusive. In Chapter Five, linear regression analysis applied to runoff and suspended-sediment concentration data from both Bualtar and Batura Rivers proved to be incapable of simulating observed values. One reason for this lack of description is that account was not taken of sediment transfer processes operating within the glacier. Hysteresis in the relationship between sediment transport and discharge in glacier-fed streams is another factor preventing the success of empirical techniques (Bogen, 1980; Gurnell, 1987). Even when different time-scales were used within data series to calibrate sediment-discharge rating curves, predictions were poor. Hence, an alternative strategy was taken in an attempt to improve forecasting of sediment delivery to glacial rivers. However, implementation of a process-orientated approach to the same data did not significantly improve prediction of sediment transport at either sites.

Figures 7.1A and B show variations in residual values between observed and predicted data for subglacial modelling and regression analysis of Bualtar data. Best prediction of the long-term, three to four week variation in the sediment record is achieved using a subglacial modelling approach (Figure 7.1A). This is demonstrated by comparison of the average prediction of sediment flux (-116 Kgs^{-1}) which is closer to observed values than those generated by regression analysis calibrated over the same period (-203 Kgs^{-1}). The reason for an improved predicted value is due to the model's capability to account for changing channel size which influences the magnitude of flushed sediment at the bed. However, standard deviation is greater for residuals between subglacially-modelled and observed data than for results of regression analysis indicating that short-term fluctuations are not accounted for by the model. The problem with simulating short-term sediment load variations is that the Bualtar River time series is characterised by high frequency and magnitude fluctuations which are related to mechanisms of debris removal rather than subglacial sediment production. Simplification of the glacier to a one-dimensional profile at the bed does not account for the possible existence of several major subglacial channels and englacial waterways. Sudden re-working of stored sediments by these conduits probably produces the short-duration pulse events in the Bualtar River which are not incorporated into the model design.

Plotted time series of residuals from modelling and regression analysis of sediment data in the Batura River are shown in Figures 7.2A and B respectively. Despite the paucity of sediment flux index data with which to adequately verify both techniques, regression analysis results in less error of data prediction over the whole period than subglacial modelling (Figure 7.2A); standard deviation, mean and standard error of residuals are all less for the rating curve simulation than for those resulting

Figure 7.1 Time series plot of residuals generated by the model of subglacial erosion (A) and a rating curve (B) for Bualtar data, 1987. The flux rating curve in (B) is derived from linear regression analysis between sediment concentration and observed discharge ($Ssc=aQ^b$). Prediction of load is the product of predicted concentration and discharge.

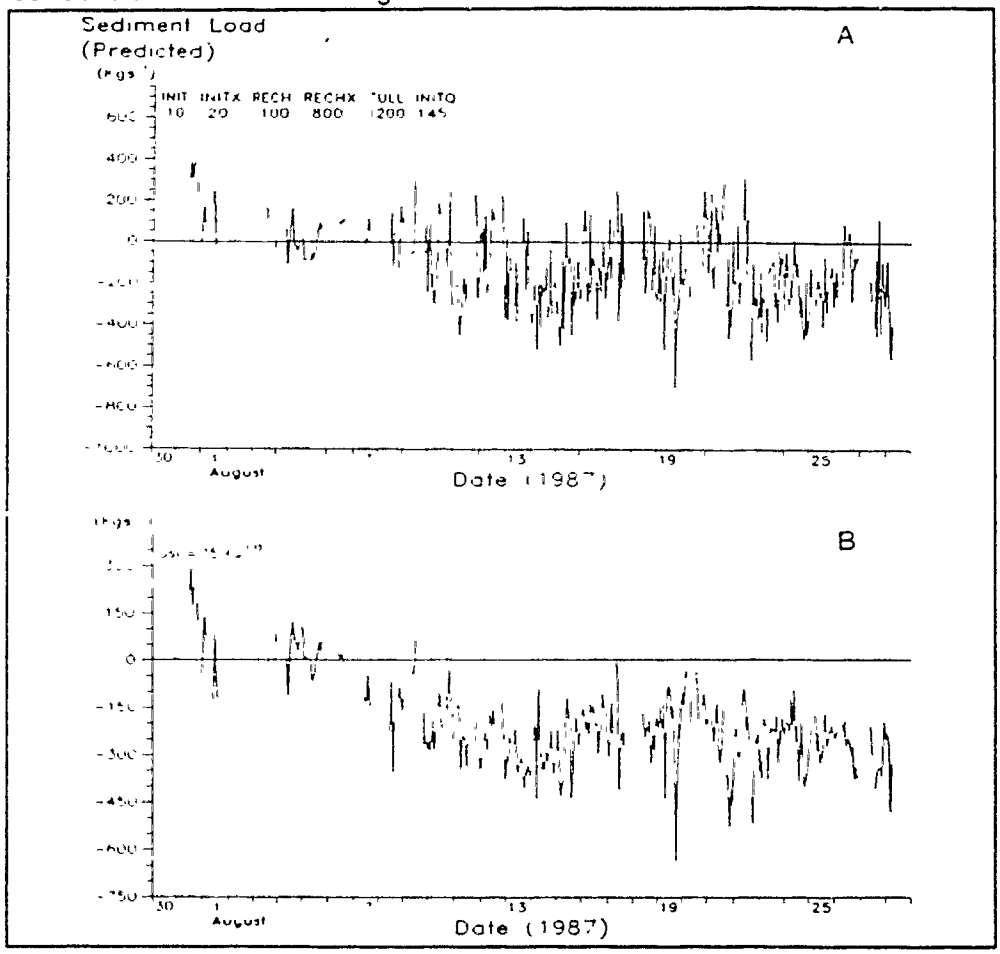

Figure 7.2 Time series plot of residuals generated by the model of subglacial erosion (A) and a rating curve (B) for Batura data, 1988. The flux rating curve in (B) is derived from linear regression analysis between sediment concentration and observed stage ($Ssc=aSt^b$). Predicted index of load is the product of predicted concentration and stage.

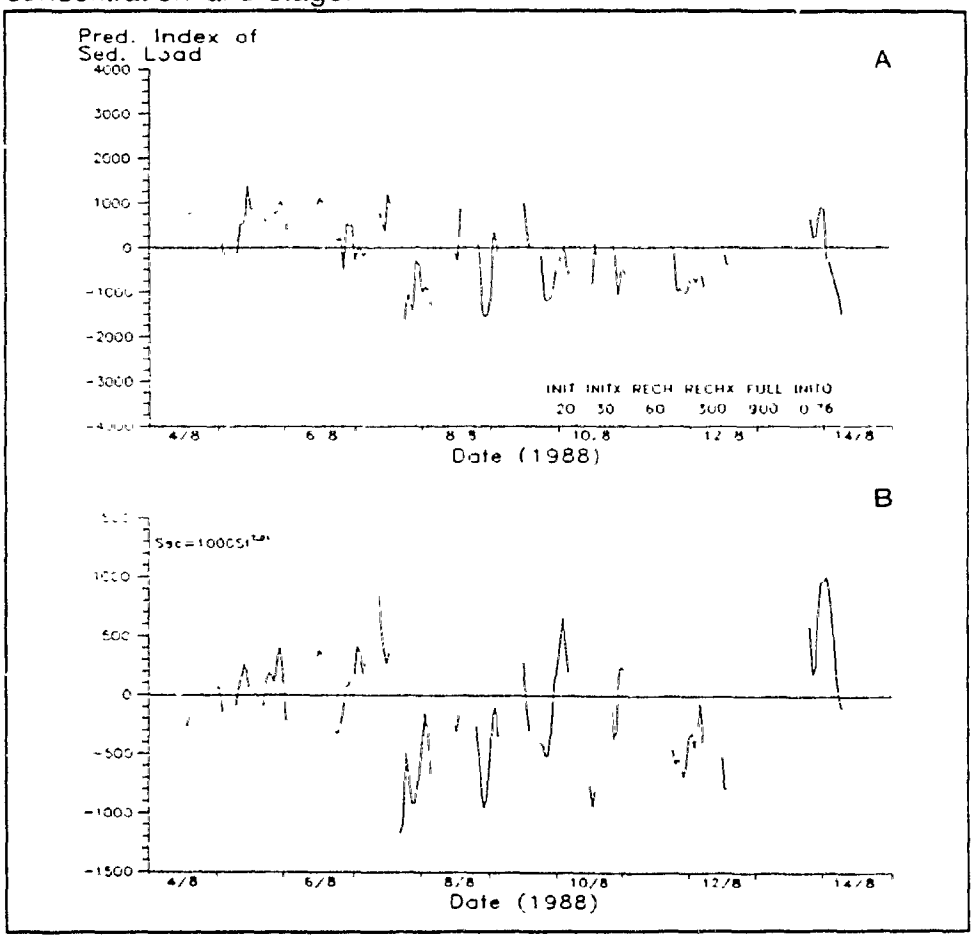

from subglacial modelling. However, the coefficient of determination of the rating curve is poor (51%) so predictions of sediment flux outside the time series are inappropriate and would lead to large prediction errors. The subglacial model does not perform well at this site because successful calibration of parameters is not achieved due to the lack of observed data with which to verify the model.

7.2 Discussion

Empirical, linear regression analysis demonstrates that time series statistics alone are not sufficient to describe or explain the relationship between suspended-sediment concentration and discharge. Although fitted curves are comparatively successful in their predictive abilities, true predictions[1] of temporally varying sediment characteristics from discharge are not founded on subglacial sedimentary and fluvial processes. This was shown by the great variety of derived rating curves which attempted to describe sediment-discharge relationships for different timescales. Thus, prediction of data outside calibrated time series have limited application due to the changing nature of relationships between basal erosion, sedimentation and water supply which produce sediment fluxes in outwash rivers.

Results of deterministic prediction of sediment transport-discharge relationships are successful only at a limited time-scale. Although certain realistic subglacial processes are incorporated into model design, simplification of the glacier into a one

[1]True prediction here is defined as forecasting of data outside the calibration period or subperiod.

dimensional form ignores important sedimentary and fluvial processes which have been associated with debris removal from glacier environments (e.g. Collins, 1989). In the Karakoram mountains, suspended loads in subglacial streams are probably related not only to erosion at the glacier bed, but also to accessibility of sediment supplies within the glacier to subglacial, englacial and supraglacial channels. Weathered material in the Bualtar and Batura rivers are derived from frequent, valley-side rock avalanching on the glacier surface in addition to subglacially eroded debris. Sudden, almost random flush events in the observed outwash channel sediment record may be caused by inclusion of such deposits into the drainage system either from slumping into conduits or as a result of sections in the drainage network becoming re-organised and incorporating untapped sediment stores into meltwater flow (Collins, 1979a). Also, longer-term sediment flushing and exhaustion events of several days' duration are not accounted for by the model. These variations in the time series are characterised by daily increasing concentrations to a peak concentration and load (e.g. on 18 August in the Bualtar record) followed by exhaustion of sediment supply during proceeding days in the series. Although diurnal "clockwise" hysteresis relationships are incorporated, the model is unable to compare rates of increasing or decreasing flow levels on one day with those from two or more days prior to simulation.

Intrinsic assumptions in the model design are another reason why predictive success is limited. For example, erosion of the bed within both glaciers is not constant as implied by the RECH and INIT parameters. Studies show that the nature and rate of basal erosion of bedrock by ice varies depending on composition and velocity of ice and bedrock topography characteristics (e.g. Boulton, 1979; Drewry, 1987). Also, the nature of cell initialisation at the onset of modelling is a factor which contributes to

model performance. Although an improvement to the original design introduced the idea that subglacial flooding prior and during modelling removes decreasing volumes of sediment from the bed with increased distance from the central channel, actual spatial distribution of debris supply is even more irregular. Secondary conduits within the glacier transport and deposit sediment at variable rates in response to local channel morphology and temporally changing meltwater dynamics. Hence, relationships between these processes need to be examined at both sites to assess their representation by algorithm components.

Aside from simplifications of physical processes operating within the glacier system, one of the main problems with implementing a model based on calibration with suspended-sediment concentration and load is representativeness of observed data. Series of instantaneous, hourly point samples taken from turbulent outwash streams reflect sediment concentrations comprised of subglacially derived material and in-channel erosion. River water sampling to obtain hourly suspended-sediment concentration data progressively includes more non-subglacially eroded debris with increased distance from the terminus. This non-glacially derived portion of sediment originates from thick deposits of glacially and fluvioglacially transported materials which have accumulated in the proglacial environment. Although Bualtar and Batura sampling sites were located as near as possible to their respective portals, sediment from such outwash deposits may have become mixed with subglacially-eroded sediments in the channel. Hence, the time series of suspended-sediment concentration data may contain biases for calibration of a model which assumes that sediment fluxes in outwash channels are entirely comprised of recently flushed deposits comprised of subglacially eroded sediment and bedrock.

Another problem with used data is that discharges measured in the Bualtar River are composed not only of meltwaters draining the Bualtar Glacier but also of diurnal and seasonal flows from the Barpu system. Unless a method is devised to separate flow components of the two glaciers, relationships between suspended-sediment, discharge and subglacial erosion in the Bualtar River remain unclear due to composite hydrograph characteristics.

Despite complications to data sets from extraneous sources and simplifications to the model, it seems reasonable to conclude that the attempt to causally model sediment transport from discharge was successful. The spurious relationship between discharge and actual sediment load does not permit direct regression analysis between these variables. However, predicted load data based on empirical relationships between concentration and discharge produced results which, although successfully describe parts of suspended-load series, cannot be inferred to occasions other than those during calibrated periods. As forecasting tools, empirical approaches are limited in their predictive capabilities since no attempt is made to account for physical processes driving the relationships. Hence, a causal approach is more desirable than a statistical strategy for sediment transport "nowcasting" and forecasting in glacier-fed streams since "it is not a question of prediction of accuracy for known conditions but one of model credibility in unknown conditions" (Klemeš, 1982, p102).

7.3 Summary and Conclusion

Briefly summarised, the objectives of this thesis are: 1. to establish magnitude and temporal variability of selected water quality characteristics in two glacial meltwater streams and infer fluvioglacial and sedimentological processes acting beneath each glacier; 2. to examine empirical relationships between suspended-sediment transport and flow characteristics during each measurement period for both rivers; 3. to implement and improve the design of a model of subglacial erosion devised by Keeley (1986); 4. to assess the effectiveness of both empirical and deterministic methods for prediction of suspended-sediment transport in both meltwater streams.

The records of measured meltwater flow and suspended-sediment concentration in the Bualtar Glacier are complicated by drainage inputs from the Barpu Glacier system. Consequently, inferences made about subglacial erosion processes and fluvial action within the Bualtar glacier are distorted by spatially variable hydrometeorological and glaciological controls over the whole basin; changing meltwater runoff and sediment concentration characteristics in the Bualtar River reflect processes operating within both the Bualtar Glacier and the Barpu Glacier system. Nevertheless, discharge and suspended-sediment concentration variations are cyclic over three time-scales.

First, a long-term rising and falling sediment and discharge cycle in the series is related to a period of sustained ice melt at the surface. Increased meltwater flow through the glacier results in increased flushing of sediment deposits as waters gain access to remote, debris-rich areas of the bed which are unworked at low flow levels. Secondly, diurnal fluctuations in meltwater flow during cloud-free days relate to maximum and minimum solar energy inputs to the system while smoothing of this

cycl· ·ompcnent occurs when solar radiation is suppressed on cooler, cloudy days. Suspended-sediment concentration variations are proportional to diurnal discharge changes although the trend becomes obscured by frequent fluctuations in concentration. These fluctuations over several hours comprise the third time-scale which is also present in the discharge record. However, short duration variations in the sediment record are not related directly to discharge changes. Supply of sediment is an important component in fluvioglacial sediment transfer since processes of sediment production and deposition within a glacial environment may be independent of fluvial activity. Sudden sediment flushes observed in the Bualtar River were not always accompanied by increased flow levels. Instead, suspended-sediment stores might have become impinged upon by the drainage system as internal channels migrated over their bed. The rapid decline in outwash sediment flux after most short-term flushes is attributed to local supply exhaustion of sedime.. since flows in the main channel continued to increase.

The measured suspended-sediment concentration and stage time series in the Batura River were short. Diurnally fluctuating flows were superimposed on a longer daily increasing flow trend. Scarcity of consecutive hourly suspended-sediment concentration data does not permit detailed inferences to be made conclusively about fluvioglacial and subglacial sediment transfer processes. However, the few data present exhibit hysteresis in the relationship between stage and suspended-sediment concentration indicating that flushing and exhaustion of debris supply was present.

To a certain extent, inferences about subglacial processes acting beneath the Bualtar and Batura Glaciers must remain speculative since discharge and suspended-sediment concentration time-series are complicated by various factors at both locations. In the case of the Bualtar Glacier, outwash flows in the Bualtar River are partially

comprised of meltwaters draining the Barpu Glacier system and unless a flow separation technique is implemented, conclusive inferences cannot be made about the Bualtar subglacial system from discharge and suspended-sediment concentration alone. In the Batura record, missing suspended-sediment concentration data does not allow detailed inferences to be made about the drainage network's ability to remove weathered basal sediments since time scales over which flushing events occur are variable; subsections of missing data probably contain fluctuations in concentration similar in magnitude and frequency as the rest of the time series (e.g. 1000 mgl^{-1} over 3 to 4 hours). In addition, at both sites, the probable existence of even shorter term fluctuations in concentration (less than one hour) which were not accommodated for by the sampling programme, may be important indicators of characteristic changes in the flushing of subglacially weathered sediments from the basal regions (Gurnell, 1982). Hence, inferences about the nature of the subglacial drainage network and sediment removal mechanisms must be treated with care.

Statistically derived rating curves neither adequately described nor simulated suspended-sediment concentration in the measured outwash rivers. No account is taken of associations between physical processes within the glacier system particularly of hysteresis relationships between paired sediment and discharge data. Hence, extrapolation of predicted suspended-sediment characteristics outside time series upon which calibrations are based are inappropriate since within both data sets, rating curve expressions between paired flow and suspended-sediment concentration data vary over different timescales. Hence, development of the model of subglacial erosion was undertaken to try and improve predictive success through a process orientated approach.

Alterations to the model did not substantially improve prediction of suspended-sediment transport from glacier-fed streams. Improvements to simplifications of reality and restricting assumptions in the causal model design only slightly increased its predictive ability compared with that of empirical models. Prediction of the suspended-sediment series at both sites was better for daily data than at a diurnal level although lack of suspended-sediment load calibration data in the Batura record did not permit comprehensive verification of simulations.

In conclusion, continually eroded sediment and parent rock at the glacier bed are probably removed at rates directly proportional to discharges in arterial meltwater streams. Hence, daily variations in outwash suspended-sediment loads are directly related to erosion of the subglacial basement. However, short-term fluctuations in sediment load of several hours in duration are not strongly related to subglacial weathering rates. Accessibility of sediment supply to all parts of the drainage network in the glacier is more important in this instance. Changes in the configuration of the drainage network and distributions of sediment stores at the bed control the magnitude of short-term fluctuations in sediment load records in outwash channels. Diurnal variations of suspended-sediment flux represent processes linking mechanisms of subglacial erosion with eventual flushing of sediments from within the glacier. This component of the model is the most difficult part to quantify since it is represented by suites of variables and constants such as bed topography, relative magnitudes of subglacial erosional forces, configuration of drainage network and ice dynamics which are difficult to verify.

Future investigations in this field would benefit from more detailed studies of diurnal discharge and suspended-sediment transport regimes in meltwater streams. By

increasing flow measurement and sampling frequency, calibration of the subglacial erosion model will improve enabling increased confidence of predicted results. Subsequently, it may be possible to expand the model to two or three dimensions and attempt to account for the processes controlling diurnal variations in sediment flux rates. However, validation of model components is a major problem with any kind of modelling technique which attempts to quantify or qualify subglacial processes since it is virtually impossible, in most cases, to inspect directly subglacial erosional and fluvial environments. Nevertheless, by taking a process-orientated path grounded on established, empirically tested ideas, the possibility for improved predictive power increases. With raised levels of knowledge and understanding of subglacial processes, validation of component parts within causal models is made possible. Eventually, it may be possible not only to predict daily, seasonal and annual sediment regimes for future periods, but also simulate short-term fluctuations in sediment production and transport in glacier-fed systems.

Bibliography

Barry, R.G. (1981), Mountain Weather and Climate, Methuen and Co., New York, 313pp.

Batura Glacier Investigation Group (1979), The Batura Glacier in the Karakoram mountains and its variations, *Scientia Sinica*, **22**(8), 958-974.

Bezinge, A. (1987), Glacial Meltwater Streams, Hydrology and Sediment Transport: The Case of the Grande Dixence Hydroelectricity Scheme, in Gurnell, A.M. and Clark, M.J. (Eds.), *Glacio-fluvial Sediment Transfer*, John Wiley and Sons Ltd., Chichester, 473-498.

Binda, G.G., Johnson, P.G. and Power, J.M. (1985), Glacier control of suspended-sediment and solute loads in a Rocky Mountain basin, in *Water Quality Evolution within the Hydrological Cycle of Watersheds. Proceedings of the Canadian Hydrological Symposium, June 1984, Quebec*, **15**, Associate Committee on Hydrology, National Research Council of Canada, NRCC no. 24633, Vol. 1, 309-327.

Bindschadler, R.A. (1983), The importance of pressurised subglacial water in separation and sliding at the glacier bed, *Journal of Glaciology*, **29**(101), 3-19.

Bogen, J. (1980), The hysteresis effect of sediment transport systems, *Norsk Geografisk Tiddskrift*, **34**, 45-54.

Bogen, J. (1989), Glacial sediment production and development of hydro-electric power in glacierized areas, *Annals of Glaciology*, **13**,

Borland, W.M. (1961), Sediment transport of glacier-fed streams in Alaska, *Journal of Geophysical Research*, **66**, 3347-3350.

Boulton, G.S. (1974), Processes and Patterns of Glacial Erosion, in Coates, D.R. (Ed.), *Glacial Geomorphology*, State University of New York, New York, 41-87.

Boulton, G.S. (1979), Process of glacier erosion on different substrata, *Journal of Glaciology*, **23**(89), 15-38.

Budd, W.F., Keage, P.L. and Blundy, N.A. (1979), Empirical studies of ice sliding, *Journal of Glaciology*, **23**(89), 157-170.

Butz, D.A.O. (1989), The agricultural use of meltwater in Hopar settlement, Pakistan, *Annals of Glaciology*, **13**, 35-39.

Caine, N. (1974) The geomorphic processes of the alpine environment, in Ives, J.D. and Barry, R.G. (Eds.), *Arctic and Alpine Environments*, Methuen, London, 721-748.

Chorley, R.J., Schumm, S.A. and Sugden, D.E. (1984), Geomorphology, Methuen and Co. Ltd., London, 605pp.

Church, M. and Gilbert, W. (1975), Proglacial fluvial and lacustrine environments, in Jopling, N.V. and McDonald, B.C. (Eds.), *Glaciofluvial and Glaciolacustrine Sedimentation*, Society of Economic Palaeontologists and Mineralogists Special Publication 23, 22-100.

Clague J.J. and Mathews, W.H. (1973), The magnitude of Jökulhlaups, *Journal of Glaciology*, **12**(66), 501-504.

Clarke, G.K.C. (1982), Glacier outburst floods from Hazard Lake, Yukon Territory, and the problem of flood magnitude prediction. *Journal of Glaciology*, **28**(98), 3-21.

Collins, D.N. (1977), Hydrology of and Alpine glacier as indicated by the chemical composition of meltwater, *Zeitschrift für Gletscherkunde und Glazialgeologie*, **13**(1-2), 219-238.

Collins, D.N. (1979a), Sediment concentration in melt waters as an indicator of erosion processes beneath an Alpine glacier, *Journal of Glaciology*, **23**(89), 247-257.

Collins, D.N. (1979b), Quantitative determinations of the subglacial hydrology of two alpine glaciers, *Journal of Glaciology*, **23**(89), 347-361.

Collins, D.N. (1988), Suspended sediment and solute delivery to meltwaters beneath an Alpine glacier, *Mitteilungen der Versuchsanstalt fur Wasserbau, Hydrologie und Glaziologie*, ETH, Zürich, **94**, 147-161.

Collins, D.N. (1989), Seasonal development of subglacial drainage and suspended sediment delivery to melt waters beneath an Alpine glacier, *Annals of Glaciology*, **13**, 45-50.

Drewry, D. (1987), Glacial Geologic Processes, Edward Arnold Ltd, London, 276pp.

Duval, P. (1979), Creep and recrystallisation of polycrystalline ice, *Bulletin de Mineralogie*, **2**(2-3), 80-85.

Emmenegger, C. and Spreafico, M. (1979), La station hydrométrique fédérale de la Massa-Blatten au front du glacier d'Aletsch, *Mitteilungen der Versuchsanstalt fur Wasserbau, Hydrologie und Glaziologie*, ETH, Zürich, **41**, 23-38.

Ferguson, R.I. (1984), Sediment load of the Hunza River, in Miller, K.J. (Ed.), *The International Karakoram Project, Volume 2*, Cambridge University Press, Cambridge, 581-598.

Ferguson, R.I., Collins, D.N. and Whalley, W.B. (1984), Techniques for investigating meltwater runoff and erosion, in Miller, K.J. (Ed.), *The International Karakoram Project, Volume 2*, Cambridge University Press, Cambridge, 374-382.

Finsterwalder, R. (1960), German glaciological and geological expedition to the Batura Mustagh and Rakaposhi Range, *Journal of Glaciology*, 3(28), 787-788.

Flohn, H. (1968), Contributions to a meteorology of the Tibetan Highlands, Atmospheric Sciences Paper, Colorado State University, Fort Collins, 130pp.

Flotron, A. (1973), Photogrammetrische messung von gletscherbewegungen mit automatischer kamera, *Vermessung, Photogrammetrie und Kultertechnik*, Jahrg. **71**, Ht. 1-73, Fachblatt., 15-17.

Fountain, A.G. (1989), The storage of water in, and hydraulic characteristics of, the firn of South Cascade Glacier, Washington State, U.S.A., *Annals of Glaciology*, **13**, 69-75.

Fowler, A.C. (1987), Sliding with cavity formation, *Journal of Glaciology*, **33**(115), 255-267.

Glen, J.W. (1955), The creep of polycrystalline ice, *Proceedings of the Royal Society of London*, Series A, **228**, 519-538.

Glover, B.J. and Johnson, P. (1974), Variations in the natural chemical concentration of river water during flood flows and the lag effect, *Journal of Hydrology*, **22**, 303-316.

Goudie, A.S., Brunsden, D., Collins, D.N., Derbyshire, E., Ferguson, R.I., Hashmet, Z., Jones, D.K.C., Perrott, F.A., Said, M., Waters, R.S. and Whalley, W.B. (1984), The geomorphology of the Hunza Valley, Karakoram mountains, Pakistan, in Miller, K.J. (Ed.), *The International Karakoram Project, Volume 2*, Cambridge University Press, Cambridge, 359-410.

Gurnell, A.M. (1982), The dynamics of suspended sediment concentration in a proglacial stream, *Hydrological Aspects of Alpine and High Mountain Areas (Proceedings of the Exeter Symposium, July, 1982)*, International Association of Hydrological Sciences, **38**, 319-330.

Gurnell, A.M. (1987), Suspended Sediment, in Gurnell, A.M. and Clark, M.J. (Eds.), *Glacio-fluvial Sediment Transfer*, John Wiley and Sons. Ltd., Chichester, 305-354.

Gurnell, A.M. and Fenn, C.R. (1984a), Box-Jenkins transfer function models applied to suspended-sediment concentration-discharge relationships in a proglacial stream, *Arctic and Alpine Research*, **16**, 93-106.

Gurnell, A.M. and Fenn, C.R. (1984b), Flow separation , sediment source areas and suspended-sediment transport in a pro-glacial stream, in Schick, A.P. (Ed.), *Channel Processes: Water, Sediment, Catchment Controls*, Catena Supplement, **5**, 109-119.

Hallet, B. (1979a), A theoretical model of glacier abrasion, *Journal of Glaciology*, **23**(89), 39-50.

Hallet, B. (1979b), Subglacial regelation water film, *Journal of Glaciology*, **23**(89), 321-334.

Hallet, B. (1981), Glacial abrasion and sliding: their dependence on the debris concentration in basal ice, *Annals of Glaciology*, **2**, 23-28.

Hammer, K.M. and Smith, N.D. (1983), Sediment production and transport in a proglacial stream: Hilda Glacier, Alberta, Canada, *Boreas*, **12**, 91-106.

Hewitt, K. (1982), Natural dams and outburst floods of the Karakoram Himalaya, in *Hydrological Aspects of Alpine and High-mountain Areas (Proceedings of the Exeter Symposium, July 1982)*, International Association of Hydrological Sciences, **38**, 259-269.

Hewitt, K. (1985), Snow and ice hydrology in remote, high mountain areas: the Himmalayan sources of the River Indus, *Snow and Ice Hydrology Project, Working Paper Number 1*, Wilfrid Laurier University, Waterloo, 28pp.

Hewitt, K. (1988), Catastrophic landslide deposits in the Karakoram Himalaya, *American Association for the Advancement of Science*, **242**(9), 64-77.

Hewitt, K. (1989), The altitudinal organisation of Karakoram geomorphic processes and depositional environments, *Zeitschrift für Geomorphologie*, **76**, 9-32.

Hjulström, F. (1935), Studies of the morphological activity of rivers as illustrated by the River Fyris, *University of Uppsala Geological Institute Bulletin, 25, 221-527.*

Holmlund, P. (1988), Internal geometry and evolution of moulins, Storglaciären, Sweden, *Journal of Glaciology*, **34**(117), 242-248.

Hooke, R.LeB. (1984), On the role of mechanical energy in maintaining subglacial conduits at atmospheric pressure, *Journal of Glaciology*, **30**(105), 180-187.

Hooke, R.LeB. (1989), Englacial and subglacial hydrology: a qualitative review, *Arctic and Alpine Research*, **21**(3), 221-233.

Hooke, R.LeB., Wold, B. and Hagen, J.O (1985), Subglacial hydrology and sediment transport at Bondhusbreen, southwest Norway, *Geological Society of America Bulletin*, **96**, 388-397.

Humphrey, N., Raymond, C.F. and Harrison, W.D. (1986), Discharges of turbid water during mini-surges of Variegated Glacier, Alaska, *Journal of Glaciology*, **32**(111), 195-207.

Iken, A. (1974), Velocity fluctuations of an arctic valley glacier: a study of the White Glacier, Axel Heiberg Island, Canadian Arctic Archipelago, *McGill University, Montreal, Axel Heiberg Island Research Reports, Glaciology*, **5**, pp116.

Iken, A. (1981), The effect of subglacial water pressure on the sliding velocity of a glacier in an idealised numerical model, *Journal of Glaciology*, **27**(97), 407-421.

Iken, A., Röthlisberger, H., Flotron, A. and Haeberli, W. (1983), The uplift of the Unteraargletscher at the beginning of the melt season - a consequence of water storage at the bed ? *Journal of Glaciology*, **29**(101), 28-47.

Iken, A. and Bindschadler, R.A. (1986), Combined measurements of subglacial water pressure and surface velocity of Findelngletscher, Switzerland: conclusions about drainage system and sliding mechanism, *Journal of Glaciology*, **32**(110), 101-119.

Jóhannessen, T., Raymond, C., and Waddington, E. (1989), Time-scale for adjustment of glaciers to changes in mass balance, *Journal of Glaciology*, **35**(121), 355-369.

Kamb, B. (1970), Sliding motion of glaciers: theory and observation, *Review of Geophysics and Space Physics*, **8**(4), 673-728.

Kamb, B. (1987), Glacier surge mechanism based on linked cavity configuration of the basal water conduit system, *Journal of Geophysical Research*, **92**(B9), 9083-9100.

Kamb, B., Raymond, C.F., Harrison, W.D., Engelhardt, H.,Echelmeyer, K.A., Humphrey, N., Brugman, M.M. and Pfeffer, T. (1985), Glacier surge mechanism: 1982-1983 surge of Variegated Glacier, Alaska, *The American Association for the Advancement of Science*, **227**(4686), 469-479.

Kasser, P. (1967, 1973), *Fluctuations of Glaciers*, **1**, 1959-65; **2**, 1965-70, Permanent Service on the Fluctuations of Glaciers of the IUGG-FAGS/ICSU, International Commission of Snow and Ice of the International Association of Scientific Hydrology, (ICSI/IAHS)/UNESCO.

Keeley, J.D. (1986), A Model of Subglacial Erosion, Unpublished M.Sc. Thesis, University of Newcastle-Upon-Tyne, 99pp.

Klemeš, V. (1982), Empirical and causal models in hydrology, in *Scientific Basis of Water Resource Management*, NRC Studies in Geophysics Series, National Academy Press, Washington D.C., 95-104.

Krimmel, R.M. and Tangborn, W.V. (1974), South Cascade Glacier: the moderating effect of glaciers on runoff, *Proceedings of the Western Snow Conference*, **42**, 9-13.

Lang, H. (1973), Variations in the relation between glacier discharge and meteorological elements, in *The Hydrology of Glaciers, (Proceedings of the Cambridge Symposium, September 1969)*, International Association of Hydrological Sciences, **95**, 85-94.

Lewin, J. (1981), River Channels, in Goudie, A.S. (Ed.), *Geomorphological Techniques*, George Allen and Unwin, London, 196-212.

Lliboutry, L. (1968), General theory of subglacial cavitation and sliding of temperate glaciers, *Journal of Glaciology*, 7(49), 21-58.

Lang, H., Schädler, B., and Davidson, G. (1977), Hydrological investigations on the Ewigschneefeld-Grosser Aletschgletscher, *Zeitschrift für Gletscherkunde und Glazialgeologie*, **12**(2), 109-124.

Liestøl, O. (1967), Storbreen Glacier in Jotunheimen, Norway, *Norsk Polarinstitutt Skrifter*, **141**, p63.

Mathews, W.H. (1964a), Water pressure under a glacier, *Journal of Glaciology*, 5(38), 235-240.

Mathews, W.H. (1964b), Sediment transport from Athabasca glacier, Alberta, International Association of Scientific Hydrology Publication, **65**, 155-165.

Mathews, W.H. (1973), Record of two jökulhlaups, in *The Hydrology of Glaciers, (Proceedings of the Cambridge Symposium, September 1969)*, International Association of Hydrological Sciences, **95**, 99-110.

Mayewski, P.A., Lyons, W.B., Ahmed, N., Smith, G., and Pourchet, M. (1984), Interpretation of the chemical and physical time-series retrieved from Setik Glacier, Ladakh Himalaya, India, *Journal of Glaciology*, **30**(104), 66-76.

Meier, M.F. and Roots, E.F. (1982), Glaciers as a water resource, *Nature and Resources*, UNESCO, **18**, 7-14.

Mercer, J.H. (1975), Karakoram, in Field, W.O. (Ed.), *Mountain Glaciers of the Northern Hemisphere, Volume 1*, Cold Regions Research and Engineering Laboratory, Hanover, New Hampshire, 371-410.

Meybeck, M. (1976), Total mineral dissolved transport by world major rivers, *Hydrological Sciences Bulletin*, **21**, 265-284.

Miller, K.J. (1984, Ed.), The International Karakoram Project, 2 Volumes, Cambridge University Press, Cambridge, Vol.1, p412; Vol.2, 635pp.

Morisawa, M. (1968), Streams; Their Dynamics and Morphology, *Earth and Planetary Sciences Series*, McGraw-Hill Co., New York, p175.

Nye, J.F. (1973a), The motion of ice past obstacles, in Whalley, E., Jones, S.J. and Gold, L.W. (Eds.), *Physics and Chemistry of Ice; Symposium on the Physics and Chemistry of Ice, Ottawa, Canada, August 1972*, Royal Society of Canada, 387-394.

Nye, J.F. (1973b), Water at the bed of a glacier, in *The Hydrology of Glaciers, (Proceedings of the Cambridge Symposium, September 1969)*, International Association of Hydrological Sciences, **95**, 189-194.

Nye, J.F. (1976), Water flow in glaciers: jökulhlaups, tunnels and veins, *Journal of Glaciology*, **17**(76), 181-207.

Nye, J.F. and Frank, F.C. (1973), Hydrology of intergrannular veins in a temperate glacier, in *The Hydrology of Glaciers, (Proceedings of the Cambridge Symposium, September 1969)*, International Association of Hydrological Sciences, **95**, 157-161.

Østrem, G. (1972), Runoff forecasts for highly glacierised basins, in *The Role of Snow and Ice in Hydrology, (Proceedings of the Banff Symposium, 1972)*, International Association of Hydrological Sciences, **107**(2 Volumes), 1111-1132.

Østrem, G. (1975), Sediment transport in glacial meltwater streams, in Jopling, N.V. and McDonald, B.C. (Eds.), *Glaciofluvial and Glaciolacustrine Sedimentation*, Society of Economic Palaeontologists and Mineralogists Special Publication 23, 101-122.

Østrem, G., Bridge, C.W. and Rannie, W.F. (1967), Glacio-hydrology, discharge and sediment transport in the Decade Glacier area, Baffin Island, N.W.T., *Geografiska Annaler, Series A*, **49**(2-4), 268-282.

Østrem, G., Zeigler, T., Ekman, S.R., Olsen, H., Andersson, J.E. and Lundén, B. (1971), *Slamtransportstudier i Norska Glaciärälvar 1970*, Stockholms Universitet Naturgeografiska Institutionen, 133pp.

Paterson, W.S.B. (1981), The Physics of Glaciers, Pergamon Press Ltd., Oxford, 380pp.

Paterson, W.S.B. and Savage, J.C. (1970), Excess pressure observed in a water filled cavity in Athabasca glacier, Canada, *Journal of Glaciology*, **9**(55), 103-107.

Raiswell, R. (1984), Chemical models of solute acquisition in glacial meltwaters, *Journal of Glaciology*, **30**(104), 49-57.

Raymond, C.F. and Harrison, W.D. (1975), Some observations on the behaviour of liquid and gas phases in temperate glacier ice, *Journal of Glaciology*, **14**(71), 213-234.

Richards, K. (1984), Some observations on suspended sediment dynamics in Storbregrova, Jotenheimen, *Earth Surface Processes and Landforms*, **9**, 101-112.

Raiswell, R. (1984), Chemical models of solute acquisition in glacial melt waters, *Journal of Glaciology*, **30**(104), 49-57.

Robin, G. de Q. (1976), Is the basal ice of a temperate glacier at the pressure-melting point? *Journal of Glaciology*, **16**(74), 183-196.

Röthlisberger, H. (1972), Water pressure in intra- and subglacial channels, *Journal of Glaciology*, **11**(62), 177-203.

Röthlisberger, H., Iken, A. and Spring, U. (1979), Piezometric observations of water pressure at the bed of Swiss glaciers, *Journal of Glaciology*, **23**(89), 429-430. (Abstract).

Röthlisberger, H. and Iken, A. (1981), Plucking as an effect of water pressure variations at the glacier bed, *Annals of Glaciology*, **2**, 57-62.

Röthlisberger, H. and Lang, H. (1987), Glacial Hydrology, in Gurnell, A.M. and Clark, M.J. (Eds.), *Glacio-fluvial Sediment Transfer*, John Wiley and Sons Ltd., Chichester, 207-284.

Rudolph, R. (1962), *Abflusstudien an Gletscherbächen*, Veröffentlichung des Museum Ferdinandeum, Innsbruck, **41**, 118-266.

Shaw, E.M. (1984), Hydrology in Practice, Van Nostrand Reinhold (U.K.) Co. Ltd., 569pp.

Shreve, R. L. (1972), Movement of waters in glaciers, *Journal of Glaciology*, **8**(62), 205-214.

Søgaard, H. and Thomsen, T. (1988), Application of satellite data to monitoring snow cover and runoff in Greenland, *Nordic Hydrology*, **19**, 225-236.

Stacey, F.D. (1977), Physics of the Earth, Wiley, New York, 324pp.

Stenborg, T. (1970), Delay of runoff from a glacier basin, *Geografiska Annaler*, **52A**(1), 1-30.

Sugden, D.E. and John, B.S. (1984), Glaciers and Landscape, Edward Arnold Ltd, London, 376pp.

Tahirkheli, R.A.K. and Jan, Q.M. (1984), The geographical and geological domains of the Karakoram, in Miller, K.J. (Ed.), *The International Karakoram Project, Volume 2*, Cambridge University Press, Cambridge, 57-70.

Tangborn, W.V. (1984), Prediction of glacier derived runoff for hydroelectric development, *Geografiska Annaler*, **66A**(3), 257-265.

Tangborn, W.V., Krimmel, R.M., and Meier, M.F (1975), A comparison of mass balance by glaciological, hydrological and mapping methods, South Cascade glacier, Washington, in *Snow and Ice (Proceedings of the Moscow Symposium, August 1971)*, International Association of Hydrological Sciences, **104**, 185-196.

Tarar, R.N. (1982), Water resources investigation in Pakistan with the help of Landsat imagery-snow surveys 1975-1978, in *Hydrological Aspects of Alpine and High-mountain Areas (Proceedings of the Exeter Symposium, July 1982)*, International Association of Hydrological Sciences, **38**, 177-190.

Theakestone, W.F. (1988), Temporal variations of isotopic composition of glacier-river water during summer: observations at Austre Okstindbreen, Okstinden, Norway, *Journal of Glaciology*, **34**(118), 310-317.

Tŭrcan, J. (1975), Snow storage distribution in mountain watersheds, in *Snow and Ice (Proceedings of the Moscow Symposium, August 1971)*, International Association of Hydrological Sciences, **104**, 335-340.

Vivian, R. (1980), The nature of the ice-rock interface: the results of investigation on 20 000 m^2 of the rock bed of temperate glaciers, *Journal of Glaciology*, **25**(92), 267-277.

Wake, C.P. (1987), Spatial and temporal variation of snow accumulation in the central Karakoram, northern Pakistan, Unpublished M.A. Thesis, Wilfrid Laurier University, Waterloo, 121pp.

Walder, J. S. (1982), Stability of sheet flow of water beneath temperate glaciers and implications for glacier surging, *Journal of Glaciology*, **28**(99), 273-293.

Walder, J.S. (1986), Hydraulics of subglacial cavities, *Journal of Glaciology*, **32**(112), 439-445.

Walder, J.S. and Hallet, B. (1979), Geometry of former subglacial water channels and cavities, *Journal of Glaciology*, **23**(89), 335-346.

Walling, D.E. (1977), Assessing the accuracy of suspended sediment rating curves for a small basin, *Water Resources Research*, **13**(3), 531-538.

WAPDA (1976), Sediment appraisal of West Pakistan rivers 1966-1975, Pakistan Water and Power Development Authority, Lahore.

Weertman, J. (1957), On the sliding of glaciers *Journal of Glaciology*, **3**(21), 33-38.

Weertman, J. (1964), The theory of glacier sliding, *Journal of Glaciology*, **5**(39), 287-303

Weertman, J. (1972), General theory of water flow at the base of a glacier or ice sheet, *Reviews of Geophysics and Space Physics*, **10**(1), 287-333.

Weertman, J. (1979), The unsolved general glacier sliding problem, *Journal of Glaciology*, **23**(89), 97-115.

Weertman, J. and Birchfield, G. E. (1983), Stability of sheet flow under a glacier, *Journal of Glaciology*, **29**(103), 374-382.

Whiteman, P. (1985), Mountain oases: a technical report of agricultural studies (1982-1984) in Gilgit district, Northern Areas, Pakistan. Gilgit, Integrated Rural Development/Pakistan Department of Agriculture (Gilgit). (FAO/UNDP. PAK/80/009).

Wood, F. B. (1988), Global Alpine glacier trends, *Arctic and Alpine Research*, **20**(4), 404-413.

Young, G.J. (1980), Streamflow formation in a glacierised watershed in the Rocky Mountains, Canada, in Materialy Gliatsiologicheskii Issledovanii, Khronika, Obsuzhdeniia, Mezhduvedomstvennyi Geofizicheskii Komitet, Sektsiia Glatsiologii, Institut Geografii, Academy Nauk SSSR/*Data of Glaciological Studies, Chronicle, Discussion, Section of Glaciology of the Soviet Geophysical Committee and Institute of Geography*, Academy of Sciences of the U.S.S.R., Symposium of Computation and Prediction of Runoff from Glaciers and Glacierised areas, September 1978, Moscow, **39**, in Russian 55-62, in English 134-139.

Young, G.J. (1981), Glacier contribution to stream flow in the Himalayan region, Report submitted to the International Development and Research Centre, Ottawa, 40pp.

Zhi-Bin, D., Ferrari, R.L., Francis, M.R., Musil, G., Oswald, G.K.A. and Xiangsong, Z. (1984), Impulse radar ice-depth sounding on the Hispar glacier, in Miller, K.J. (Ed.), *The International Karakoram Project, Volume 2*, Cambridge University Press, Cambridge, 100-110.

Appendix I

Figure A.1 Scatter plot of all paired discharge and suspended-sediment concentration data in Bualtar River, 1987.

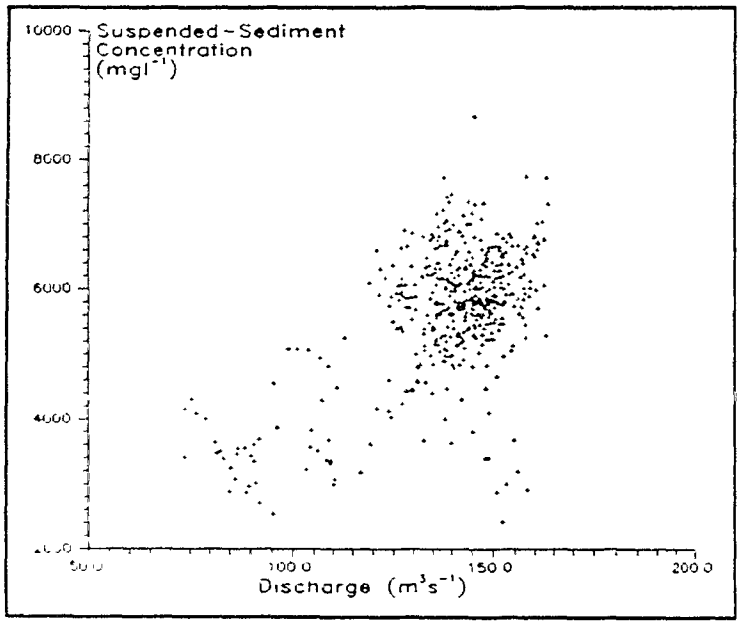

Figure A.2 Scatter plot of all paired log-transformed discharge and suspended-sediment concentration data in Bualtar River, 1987.

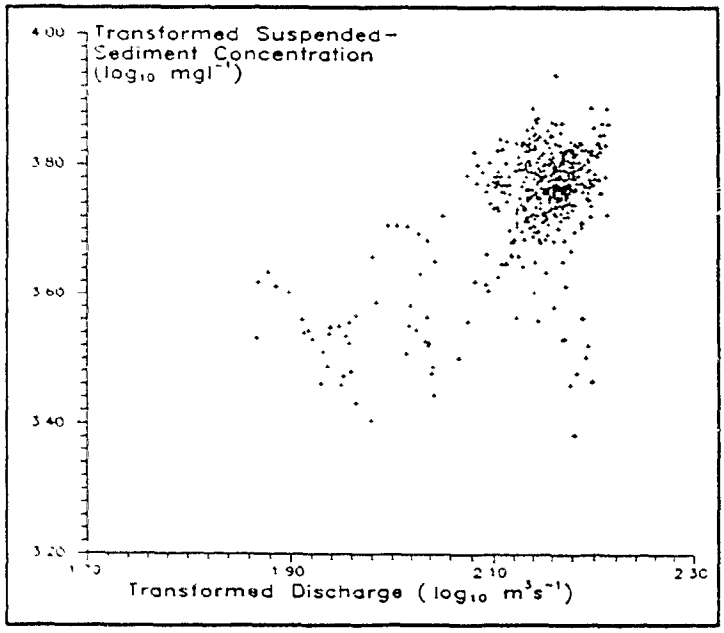

Table A.1 Linear regression statistics of the form $S=aQ^b$ for transformed discharge (Q) and suspended-sediment concentration (SSC) data in the Bualtar River, 1987: a and b are constants.

Period	Character	Corr.	R^2%	a	b
30/7-27/8	Entire Series	0.62	38	63.10	0.91
2-3/8	Falling Limb	0.81	65	2.90×10^{7}	3.41
3/8	Rising Limb	0.26	6	6.60×10^{5}	-2.58
7-8/8	Falling	0.76	57	5.75×10^{10}	4.69
8/8	Rising	0.66	39	3.80×10^{-8}	3.79
8-9/8	Falling	0.28	7	0.06	0.28
9-10/8	Falling	0.64	38	3467.00	-1.31
12/8	Rising	0.48	23	0.09	0.86
13-14/8	Falling	0.44	20	1288.00	-1.07
14-15/8	Falling	0.21	5	0.13	0.76
19/8	Rising	0.28	8	457.00	-0.90
21-22/8	Falling	0.26	7	7.24	0.76
15-15/8	Rising	0.21	5	0.13	0.75
24-26/8	Rising	0.33	11	0.71	0.44

Appendix II

Table A.2 Linear regression statistics of the form $SSC=aSt^b$ for transformed stage (St) and suspended-sediment concentration (SSC) data in the Batura River, 1988: a and b are constants.

Period	Character	Corr.	R^2%	a	b
4/8-14/8	Entire Series	0.71	51	1000.00	2.01
6-7/8	Rising/Falling	0.25	6	436.52	4.88
8-9/8	Rising/Falling	0.23	5	1096.48	2.24
13-14/8	Rising/Falling	-0.84	70	7.08×10^4	-8.27

Appendix III

Model of Subglacial Erosion

```
program Batura_Subglacial_Drainage_Model;
uses crt;

const KKMAX =  24;
      WIDTH = 2000;
      CHAN  = 1000;
      R     =  2;

var   FileQ,FileinSS,FileoutSS                    :string;
      dis,outss,ssc                               :text;
      cell                                        :array[1..3000,1..2] of real;
      Q                                           :array[1..1500] of real;
      Ssmod,Ti,Ssact                              :array[1..1000] of real;
      Init,D1,D2,Sumq,Avq,Rech,Minq,Initq,
      Susp1,Susp2,Susp3,Sstot,Initx,Rechx,Full,
      Ndate,F                                     :real;
      Wash,Limit1,Limit2,no,K,KK,KKK,I,Data,Date,
      Dc                                          :integer;
{-------------------------
PROCEDURE FLUSH
-------------------------}
procedure FLUSH;
  begin
    if I<CHAN then
      begin
        Susp1:=Susp1+cell[I,R-1]/(CHAN-I);
        cell[I,R-1]:=cell[I,R-1]/(F-(CHAN-I)+1);
      end;
    if I>CHAN then
          begin
        Susp2:=Susp2+cell[I,R-1]/(I-CHAN);
        cell[I,R-1]:=cell[I,R-1]/(F-(I-CHAN)+1);
      end;
  end;
begin
clrscr;
```

Appendix III (Cont.)

```
{----------------------------------------------------------------------
PART ONE - READ IN DATA SETS AND PARAMETERS
----------------------------------------------------------------------}

{write('Enter filename (including path) containing discharge ');
readln(FileQ);
assign(dis,Fileq);reset(dis);
write('Enter filename (including path) containing suspended-sediment ');



readln(FileinSS);
assign(ssc,FileinSS);reset(ssc);}
write('Enter filename (including path) to contain simulated
   suspended-sediment ');
readln(FileoutSS);
assign(outss,FileoutSS);rewrite(outss);
writeln;
write('Enter start date in Julian days ');
readln(Date);
writeln;

assign(dis,'d:\rejk\model\avqbu87.dat');reset(dis);
assign(ssc,'d:\rejk\model\avldbu87.dat');reset(ssc);
{assign(outss,'f:\tp\rejk\simss2.dat');rewrite(outss);}

write('Enter initial suspended-sediment concentration value (mg/L) for each
 small cell...INIT ==>  ');
read(Init);
write('Enter initial suspended-sediment concentration value (mg/L) for main
  cell...INITX ==>  ');
read(Initx);
write('Enter rate of sediment supply to each cell (mg/L)...RECH==>  ');
read(Rech);
write('Enter rate of sediment supply to main cell (mg/L)...RECHX==>  ');
read(Rechx);
write('Enter maximum sediment capacity for each cell (mg/L)...FULL==>  ');
read(Full);
write('Enter initial discharge value (cummecs)...INITQ==>  ');
read(Initq);
write('Enter minimum discharge value (cummecs) ..MINQ==>  ');
read(Minq);
```

```
{READ DATA INTO ARRAYS}

k:=1;
clrscr;
while not eof(dis) do
begin
  readln(dis,Q[K]);
  readln(ssc,Ssact[K]);
  if Q[K]>500 then Q[K]:=0;
  if Q[K]<>0 then
  begin
    if Q[K]<Minq then Minq:=Q[K];
  end;
  if Ssact[K]=999.99 then Ssact[K]:=0;
  gotoxy(1,5);write(q[k]:8:2,ssact[K]:8:2,k:3);
  Data:=K;
  K:=K+1;
end;

{-----------------------------------------
PART TWO - INITIALISE CELLS
-----------------------------------------}

K:=1;
I:=1;
while I<WIDTH+1 do
begin
  if I<CHAN then cell[I,K]:=Init/(CHAN-I);
  if I>CHAN then cell[I,K]:=Init/(I-CHAN);
  I:=I+1;
  gotoxy(1,7);writeln(cell[I,K]:6:3,I:5);
end;
cell[CHAN,1]:=Initx;  {Initial cells set up}
{-----------------------------------------
 START MAIN PART OF PROGRAM
 -----------------------------------------}


K:=1;
KK:=0;
KKK:=0;
Dc:=0;
repeat
```

```
{-----------------------------------------------------------------------------
PART THREE - CALCULATE AVERAGE DISCHARGE FOR THE PREVIOUS
             PERIOD
-----------------------------------------------------------------------------}
begin
  if Q[K]=0 then KKK:=0;
  if Q[K]=0 then Avq:=0;
  if Q[K]>0 then
  begin
    KKK:=KKK+1;
    if KKK<(KKMAX+1) then Avq:=Initq/2;
    if KKK>KKMAX then
    begin
      KK:=0;
      Sumq:=0;
      repeat
        Sumq:=Sumq+Q[K-KKMAX+KK];
        KK:=KK+1;
      until KK=KKMAX;
    Avq:=(Sumq/KKMAX)/2;
  end;
end;
end;

{-----------------------------------------------------------------------
PART FOUR - CALCULATE THE MAGNITUDE OF WASH
-----------------------------------------------------------------------}
if Q[K]>0 then
begin
  if K<KKMAX then Wash:=abs(round(((Q[K])-(Avq))/2))
  else
  begin
    if Q[K]>Q[K-1] then
    begin
      if Q[K]>Q[K-KKMAX] then Wash:=abs(round(((Q[K])-(Avq))/1.4))
      else Wash:=abs(round(((Q[K])-(Avq))/1.8))
    end;
    if Q[K]<Q[K-1] then
    begin
      if Q[K]<Q[K-KKMAX] then Wash:=abs(round(((Q[K])-(Avq))/2.6))
      else Wash:=abs(round(((Q[K])-(Avq))/2.2))
    end;
  end
end;
```

```
  Limit1:=CHAN-Wash;   {---------Calculate limits of wash----------}
  Limit2:=CHAN+Wash;
  Susp1:=0;
  Susp2:=0;
  Susp3:=0;
  F:=Wash;

{-------------------------------------------------
 PART FIVE - RECHARGE EACH CELL
 -------------------------------------------------}

if K>1 then
begin
  if Q[K]>0 then
  begin
    for I:=1 to WIDTH do
    begin
      if (I=CHAN)
        then cell[I,R]:=cell[I,R-1]+(Rechx*WASH/10)
        else
        begin
          if (cell[I,R-1]<Full)
            then cell[I,R]:=cell[I,R-1]+Rech;
          if (cell[I,R-1]>Full)
            then cell[I,R]:=Full;
        end;
      end;
    for I:=1 to WIDTH do cell[I,R-1]:=cell[I,R];
  end;
end;
```

Appendix III (Cont.)

```
{-------------------------------------------------------------------------------
PART SIX - CALCULATE THE QUANTITY OF SEDIMENT FLUSHED OUT
-------------------------------------------------------------------------------}

  For I:=Limit1 to Limit2 do
  begin
    if I=CHAN then
      begin
        Susp3:=(Susp3+cell[I,R-1]);
        cell[I,R-1]:=0;
      end
      else
        FLUSH;
  end;
  if Q[K]=0
  then Ssmod[K]:=0
  else
  begin
    Sstot:=Susp1+Susp2+Susp3;
    Ssmod[K]:=(Sstot*Q[K])/1000;
    gotoxy(1,9);writeln(ssmod[K]:8:2,k:5);
end;

{-------------------------------------------------------------------------------
PART SEVEN - OUTPUT OF PREDICTED SUSPENDED SEDIMENT
-------------------------------------------------------------------------------}


Ndate:=Date+(Dc/24);
writeln(outss,Ndate:8:3,Ssmod[K]:10:2,Ssact[K]:8:2);

Dc:=Dc+1;              {CALCULATES JULIAN ANNOTATION}
if Dc=24 then Dc:=0;
if Dc=0 then Date:=Date+1;

K:=K+1;       {REPEAT PROGRAM}
until K>Data;
close(outss);
close(dis);
close(ssc);
end.
```